# Ph.D. thesis
# Development and Applications of Methods for Correlated Relativistic Calculations of Molecular Properties

Jørn Thyssen

**Department of Chemistry**
**University of Southern Denmark –**
**Odense University**
**April 22, 2001.**

# Preface

You are about to start reading my dissertation which is the result of four years work at the Department of Chemistry, University of Southern Denmark.

I wish to thank all the present and former members of the Theoretical Chemistry Group, in particular Hans Jørgen Aagaard Jensen for supervising my project and for many fruitful and interesting discussions.

I also wish to thank Peter Schwerdtfeger, Department of Chemistry, University of Auckland, New Zealand, for allowing me to visit and work with him for 8 months. It was a very interesting stay — scientifically as well as non-scientifically.

Also, thanks to the Faculty of Science for financially supporting me.

Finally, I wish to thank my family. First my parents for encouraging me to study, and second my wife for her love and patience – the latter, when I start twaddling about quantum chemistry, computers etc.

Odense, April 22, 2001

Jørn Thyssen

Typeset with LaTeX 2$_\varepsilon$. Source code, PostScript or PDF can be downloaded from my homepage (currently `<URL:"http://assens.chem.sdu.dk/~jth">`).

# Contents

**1 Introduction** **1**
1.1 Relativistic Effects . . . . . 1
1.2 Why 4-component Calculations . . . . . 3
1.3 Electron Correlation . . . . . 5
1.4 Outline of Thesis . . . . . 6

**I Relativistic Quantum Mechanics and Electron Correlation** **13**

**2 Relativistic Quantum Mechanics** **15**
2.1 The Dirac Equation . . . . . 15
2.2 The Relativistic Molecular Hamiltonian . . . . . 17
2.3 Time Reversal Symmetry, Double Group Symmetry, and Quaternions . . . . . 21

**3 Average-of-configuration Open-shell Hartree-Fock** **27**
3.1 Introduction . . . . . 27
3.2 Theory . . . . . 28
3.2.1 The Energy . . . . . 28
3.2.2 Orbital Variations, the Gradient, and the Hessian . . . 31
3.2.3 Eigenvalue Equation for the Orbitals . . . . . 33
3.2.4 The Fock Matrix in AO Basis . . . . . 37
3.2.5 Open-shell and DIIS . . . . . 37
3.3 Applications . . . . . 39
3.3.1 Average-of-configuration Orbitals as Start Orbitals for MCSCF . . . . . 42
3.4 Conclusion . . . . . 45

**4 Relativistic Four-Component MCSCF Theory** **51**
4.1 Introduction . . . . . 51

4.2 Operators and Symmetry . . . . . 52
4.3 Parameterization and Orbital Classes . . . . . 54
4.4 Second Order Expansion of the Energy . . . . . 58
4.5 The Restricted-Step Second-Order Optimization . . . . . 60
4.6 Direct KR-MCSCF . . . . . 62
4.7 Orbital Gradients . . . . . 65
4.8 Quaternion Orbital Gradients . . . . . 68
4.9 Configurational Sigma Vectors and Density Matrices . . . . . 69
4.10 Implementation . . . . . 74

**5 Improvements and Approximations for KR-MCSCF 79**
5.1 NEO algorithm . . . . . 79
5.2 CI Sigma Vectors and Density Matrices . . . . . 80
5.3 Properties . . . . . 80
5.4 Debugging . . . . . 81
5.5 Molecular Integral Transformation . . . . . 81
5.5.1 Transform Only $(gg|aa)$ and $(ga|ga)$ Integrals . . . . . 81
5.5.2 Direct Implementation of Auxiliary $\mathbf{F}^Q$ Fock Matrices . 82
5.5.3 Semi-Direct Implementation of Auxiliary $\mathbf{F}^Q$ Fock Matrices . . . . . 82
5.5.4 Frozen Orbitals (I) . . . . . 83
5.5.5 Frozen Orbitals (II) . . . . . 83
5.5.6 Frozen Orbitals (III) . . . . . 85
5.5.7 Neglect Positronic Part of $\tilde{\mathbf{F}}^Q$ . . . . . 85
5.5.8 Diagonalization or Cholesky Decomposition of the Two-Electron Density Matrix . . . . . 87
5.5.9 Partial Neglect of $(LL|SS)$ or $(SS|SS)$ Integrals . . . . 87
5.6 Approximate Hamiltonians . . . . . 88
5.7 Neglect of $e-p$ Rotations . . . . . 88
5.8 Separate Convergence Thresholds for $e-e$ and $e-p$ Rotations 88
5.9 Transformation to Natural and Fock Type Orbitals . . . . . 89
5.10 Parallelization . . . . . 90
5.11 Hessian Update Methods . . . . . 90
5.12 Start Orbitals . . . . . 90

**6 Preliminary Applications 93**
6.1 The Ionization Potential of Zn and Hg . . . . . 93
6.2 The Effect of Relativity and Correlation on the Dipole Moments, Electric Field Gradients, and Electric Field Third Derivatives for LiX, X=F, Cl, Br, I . . . . . 98
6.2.1 Introduction . . . . . 98

6.2.2 Computational Details . . . . . 99
6.2.3 Results . . . . . 99
6.2.4 Discussion . . . . . 102

**7 Final summary and Future Research** **105**

**8 Dansk Resumé** **109**

**II Papers** **111**

**III Appendices** **151**

**A Evaluation of Matrix Exponentials** **153**

**B Quaternion MO integrals and Fock matrices** **157**
B.1 ${}^{Q}\mathbf{F}^{C}$ and ${}^{Q}\mathbf{F}^{V}$ . . . . . 157
B.2 One index transformed Fock matrices . . . . . 159
B.3 Two-electron integrals . . . . . 161
B.4 The two-electron density matrix $P$ . . . . . 165
B.5 The auxiliary Fock matrix ${}^{Q}\mathbf{F}^{Q}$ . . . . . 166
B.6 The auxiliary Fock matrix with transition density matrix . . . 173
B.7 The auxiliary Fock matrix with one-index transformed integrals 173

# List of Tables


2.1 Relationship between time-reversal symmetry, Hermiticity and Kramers basis operators $X^{\pm}_{pq}$. . . . . 23

3.1 Energies and properties for CH in different open-shell calculations. . . . . 40
3.2 Shell specification for the ground state of Cs . . . . . 40
3.3 Shell specification for the $4d_{5/2}$ core hole state of Cs . . . . . 41
3.4 Relativistic and non-relativistic core hole ionization energies for Cesium . . . . . 41
3.5 Convergence (the norm of the gradient) and the final energy for MCSCF calculations on LiI with different start orbitals. . . 44
3.6 MCSCF and MP2 natural orbital occupation numbers and character of correlating orbitals for LiI . . . . . 45
3.7 Convergence (the norm of the gradient) and the final energy for MCSCF calculations on Zn with different start orbitals. . . 46
3.8 MCSCF orbital occupation numbers and character of correlating orbitals for Zn . . . . . 46

6.1 Exponents for Zn large component basis set . . . . . 94
6.2 Exponents for Hg large component basis set . . . . . 95
6.3 Definition of active spaces for relativistic and non-relativistic MCSCF calculations on Zn, $Zn^+$, Hg, and $Hg^+$. . . . . 95
6.4 SCF and MCSCF energies for ground-state Zn and $Zn^+$ , and first ionization potential for Zn. . . . . 96
6.5 SCF and MCSCF energies for ground-state Hg and $Hg^+$ , and first ionization potential for Hg. . . . . 96
6.6 CI Coefficients for ground state Zn ($n = 4$) and Hg ($n = 6$) MCSCF calculations. . . . . 96
6.7 Natural orbital occupation numbers for ground state Zn ($n = 4$) and Hg ($n = 6$) MCSCF calculations. . . . . 97
6.8 Energy and properties for LiF . . . . . 100
6.9 Energy and properties for LiCl . . . . . 100

6.10 Energy and properties for LiBr . . . . . 101
6.11 Energy and properties for LiI . . . . . 101

# List of Figures

4.1 Overview of the division of orbital spaces for the complete active space (CAS), restricted active space (RAS), and the generalized active space (GAS) wave functions. . . . . 56
4.2 Pentadiagonal block structure of the CI Hamiltonian matrix for an even number of electrons, given for a system with six electrons. . . . . 71
4.3 Indication of the non-redundant part of the Hamiltonian for an even number of electrons, given for a system with six electrons. 72

# Chapter 1

# Introduction

## 1.1 Relativistic Effects

Although Dirac himself at the time he published his famous equations for the relativistic wave equation wrote that [1] (our emphasis),

> "The general theory of quantum mechanics is now almost complete, the imperfections that still remain being in connection with the exact fitting in of the theory with relativity ideas. This give rise to difficulties only when high-speed particles are involved, and are *therefore of no importance in the consideration of atomic and molecular structure and ordinary chemical reactions*, in which it is, indeed, usually sufficiently accurate if one neglects relativity variation of mass with velocity and assumes only Coulomb forces between the various electrons and atomic nuclei."

it is now a well established fact [2–6] that we often need to account for relativistic effects in theoretical calculations on atoms and molecules. For molecules containing heavy atoms non-relativistic calculations will not even give qualitatively correct results (*e.g.*, see [2–6]), and even for molecules containing only light atoms relativity is needed for very precise calculations [7]. With the term "*relativistic effects*" we mean the difference between the approximative physical description using a non-relativistic model and the more correct relativistic physical description. This difference is just the result of applying different physical models, and has no connection to reality — there is no such thing as an non-relativistic molecule, but there are molecules with can be described sufficiently accurate with a non-relativistic model.

However, as the majority of theoretical chemistry calculations are performed on organic molecules containing only light atoms, it is often a very

good approximation to neglect relativistic effects. But there is also considerable interest in molecules containing heavy atoms, for example molecules appearing in nuclear waste processing, such as actinide oxides: uranyl ($UO_2^{2+}$) is one of the most studied molecules containing heavy atoms, and the literature is huge: a search on *Web of Science* [8] resulted in 2298 papers where uranyl had been studied! Also molecules containing plutonium appear in nuclear waste processing. Plutonium is both radioactive and toxic, so it is very difficult to perform experiments, and there is currently only *very* few laboratories in Europe that are allowed to do experiments with plutonium. In this area calculations may both guide the experimentalists to design and help them interprete their experiments but, in time, also even replace dangerous and difficult experiments.

It may also be appropriate to use relativistic methods on molecules containing light atoms when calculating spin-dependent or magnetic properties. Examples include:

- Parity weak interactions where the relativistic operator is exceedingly simple (*e.g.*, see [9]) and it is only necessary to calculate an expectation value, whereas in non-relativistic theory it is an infinite series where the first term is a complicated linear response function [10] (see below).

- NMR parameters, where four non-relativistic operators (Fermi-contact, spin-dipole, paramagnetic spin-orbit and diamagnetic spin-orbit) are replaced by one single relativistic operator [11].

- ESR parameters, which in the relativistic realm are simple expectation values [12] become complicated linear response terms in non-relativistic theory [13].

- Spin-forbidden transitions. The relativistic wave function does not have a specific spin multiplet symmetry but is rather, in the case of a even number of electrons, a linear combination of singlets, triplets, etc. Hence, it is possible to calculate singlet – triplet transition moments directly, such as phosphorescence, using the polarization propagator (PP) method [14], whereas it is necessary to invoke double perturbation theory and calculate quadratic response functions in order to get transition moments in a non-relativistic framework [15].

The common theme for many of these properties is that spin-dependent relativistic expectation values become more complicated response functions involving the spin-orbit operator. For example, the matrix elements needed for the parity violating energy shifts within a 4-component relativistic framework

are (*e.g.*, see [9])

$$\langle 0 | \varrho_A(\mathbf{r}) \gamma_5 | 0 \rangle \,, \tag{1.1}$$

where $\varrho_A(\mathbf{r})$ is the nuclear charge distribution and $\gamma_5$ is the matrix

$$\gamma_5 = \begin{bmatrix} \mathbf{0}_2 & \mathbf{1}_2 \\ \mathbf{1}_2 & \mathbf{0}_2 \end{bmatrix} . \tag{1.2}$$

The corresponding non-relativistic expression involves the linear response function [16]

$$\ll H^{\mathrm{SO}}; H_p^s \gg, \tag{1.3}$$

where $H^{\mathrm{SO}}$ is the spin-orbit operator and $H_p^s$ the anti-commutator $\{\boldsymbol{\sigma} \cdot \mathbf{p}, \varrho_A\}_+$.

## 1.2 Why 4-component Calculations

There are several approaches to include relativistic effects. Most of them, if not all, are approximative in nature. Note that even the rigorous 4-component approach is already approximative in nature as we use the Dirac-Coulomb(-Breit) Hamiltonian which is an approximation to the full QED Hamiltonian — if it exists!

Most approaches start by eliminating the small component. Using the Foldy-Wouthuysen transformation [17] one may transform the 4-component Dirac-Coulomb-Breit operator into a 2-component Hamiltonian [18]. This requires an infinite expansion which is typically terminated after 1st order yielding the Breit-Pauli Hamiltonian [18]. The Foldy-Wouthuysen transformation can be performed analytically in absence of an external potential. Unfortunately the Breit-Pauli Hamiltonian includes many complicated terms of which many are singular, making any variational approach doomed. Instead, the operators are almost exclusively used perturbatively. This has the advantage of treating relativistic effects as perturbations to the well-known non-relativistic problem. However, the perturbative approach will only work for light atoms where the relativistic effects are small. The higher-order terms of the Foldy-Wouthuysen transformation are even more complicated and singular.

There are several other approaches based on elimination of the small component or perturbative approaches:

- Direct Perturbation Theory (DPT) developed by Kutzelnigg and coworkers [19–22], which is based on a change of the metric, and a perturbative

expansion in $c^{-2}$. Some classes of relativistic effects are treated to infinite orders in this approach. Kutzelnigg, Liu, and van Wüllen have reported a DPT MCSCF program [23, 24].

- Dyall uses a similar approach to obtain a modified Dirac equation [19, 25], which can be separated into a spin-free and a spin-dependent part [25]. At this point approximations can be invoked. For example, one may solve the spin-free modified Dirac equation and add the spin-orbit effect perturbatively.

- One may also reduce the Dirac-Coulomb-Breit operator by expansion in powers of the external field as in the second-order Douglas-Kroll-Hess method [26–29]. The operators in this approach are non-singular but involve integrals which cannot be solved analytically even for Gaussian basis set functions. The transformation can, however, be performed analytically for the free electron.

- Another alternative is the ZORA method (Zeroth Order Regular Approximation) [30, 31] where $1 + \frac{E}{2mc^2 - \hat{V}}$ is expanded in a power-series. The problem here is the potential in the denominator which will be difficult to evaluate for the electron–electron interactions in molecules. The approach is more suited for DFT where it has found its main applications, although it has been implemented for *ab initio* methods as well.

Many of these methods has troublesome features. For example, in the Douglas-Kroll-Hess method the property operators as well as the energy operators should also be transformed. Neglecting to do so will introduce *picture change effects* [32], which may be negligible for valence properties such as dipole moments, but is certainly not negligible for core properties [33, 34] and the size of the picture change error may, in fact, be as large as the relativistic effect itself [35]. The DPT MCSCF formalism by Kutzelnigg *et al.* [23, 24], in which quasi-degenerate perturbation theory has to be applied, also leads to very complicated expressions. So far only first-order DPT MCSCF has been implemented [24].

Although technically not restricted to one- or two-component methods we also mention one further approximation often used in conjunction with the above methods: Effective core potentials (ECP) or pseudo-potentials (PP). Both methods represents the core by some model potential. This reduces the number of integrals to be calculated as only the valence is treated explicitly. There also exists relativistic ECPs or PPs that can be used in non-relativistic 1-component programs to model a relativistic core.

The conclusion is that the 4-component methods provide the least complicated formalism, but due to the expensive nature of the calculations, many people have developed approximate methods where the simplicity of the 4-component calculations are sacrificed in order to obtain faster calculations. Many molecular 4-component programs such as BERTHA [36, 37] or DIRAC [38] have very efficient integral generators giving large speed-ups. For example, a relativistic DHF calculation with DIRAC requires theoretically approximately 50 times as much CPU time as an identical non-relativistic HF calculation. However, due to efficient integral screening and other techniques the factor is reduced to typically 2–10. Another example is the calculation of molecular gradients needed for first or higher order geometry optimizations. Depending on the accuracy needed in the calculation, integral screening reduces the relativistic CPU time to non-relativistic CPU time factor for the molecular gradient in CsAu from 26 to 1.5 – 3 [39]. It is also important to note that 4-component calculations are needed to calibrate the approximative methods. Another advantage is that variational inclusion of spin-orbit effects, although also included in some of the two-component methods. Yet another advantage is the simple appearance of especially magnetic operators, which are inherently relativistic. Their simple form is even kept with the non-relativistic 4-component Lévy-Leblond Hamiltonian [40, 41]. So it may even be advantageous to use 4-component non-relativistic Hamiltonian instead of the usual 1-component non-relativistic Schrödinger Hamiltonian!

Quiney, Skaane, and Grant expressed it very provocatively [37]:

> "*Ab initio* relativistic quantum chemistry: four-components good, two-components bad!"

## 1.3 Electron Correlation

After we have established that treatment of relativistic effects are needed we turn to the next problem. It is well known that we need to go beyond the independent particle model in order to calculate most atomic and molecular properties qualitatively or quantitatively correct.

As for non-relativistic theory there are many ways to include the many-body effects. Most four-component relativistic programs developed so far treat only dynamical correlation using second-order Møller-Plesset perturbation theory (MP2) [42, 43], restricted active space configuration interaction theory (RASCI) [44], or coupled-cluster methods [45–47].

An alternative route to including dynamical electron correlation is density functional theory (DFT) [48].

Most of these are based on a single configuration as reference, which is a reasonable approximation for closed shell systems. But for reactive states, excited states, states with more than one open shell, or systems with near degeneracies of states this gives rise to a manifold of configurations that will mix. In relativistic systems there are additional near degeneracies due to spin-orbit coupling. The conclusion is that in many cases you need the multi-configurational approach. MCSCF is better than CI in the sense that, due to the orbital relaxation, a shorter CI expansion can be used compared to CI. Another advantage of MCSCF is that it is fully variational.

However, in order to treat both dynamical and static correlation it is necessary to go beyond MCSCF and use, for example, the CASPT$n$ method [49, 50] or multi-configurational CC methods. The former method has not been implemented for molecular 4-component methods yet[1][2]. The latter methods are in the development phase (*e.g.*, the Fock-space CC or intermediate Hamiltonian Fock-space CC[3], or GAS CC [60]).

## 1.4 Outline of Thesis

We start by giving a short general introduction to relativistic quantum mechanics in Chapter 2. We discuss the single particle Dirac Hamiltonian and move on to the molecular relativistic Hamiltonian.

In Chapter 3 we discuss the average-of-configuration open-shell method for obtaining start orbitals for correlation methods.

Chapter 4 is dedicated to Kramers restricted MCSCF. The formalism was already published by Jensen *et al.* in 1996 [61] so we only review the formalism introducing the quaternion formalism and discuss the implementation.

In Chapter 5 we discuss numerous approximations and auxiliary algorithms for speeding up KR-MCSCF calculations.

In Chapter 6 we show a few preliminary applications of the newly developed KR-MCSCF code.

Chapter 7 summarizes the work presented in this thesis and give suggestions for further research.

The second part of the thesis is some papers and manuscripts. See Part II for a summary of these.

[1] Although there exists an 1-component CASPT2 method with relativistic effective core potentials where spin-orbit effects can be added using an effective one-electron spin-orbit Hamiltonian in MOLCAS [51–53]

[2] There has also been reported an *atomic* CASPT2 program by Vilkas *et al.* [54]

[3] For reviews see [55, 56] and references therein; for relativistic four-component Fock-space CC see [57–59].

The last part is a number of appendices with the explicit details about how to calculate $\exp(-\kappa)$ for quaternion matrices $\kappa$ and how to calculate various quaternion Fock matrices needed in the KR-MCSCF program.

# Bibliography

[1] P. A. M. Dirac, Proc. Roy. Soc. Lond. **A123**, 714 (1929).

[2] P. Pyykkö, Adv. Quant. Chem. **2**, 353 (1978).

[3] K. S. Pitzer, Acc. Chem. Res. **12**, 271 (1979).

[4] P. Pyykkö, Acc. Chem. Res. **12**, 276 (1979).

[5] P. Pyykkö, Chem. Rev. **88**, 563 (1988).

[6] P. Pyykkö, in *The effects of relativity in atoms, molecules, and the solid state*, edited by S. Wilson, I. P. Grant, and B. L. Gyorffy (Plenum Press, New York, 1991), p. 1.

[7] C. F. Fischer, Physica Scripta **T83**, 49 (1999).

[8] Institute of Scientific Information, *The Web of Science*, `<URL:"http://wos.isiglobalnet.com/CIW.cgi">`.

[9] S. A. Blundell, J. Sapirstein, and W. R. Johnson, Phys. Rev. D **45**, 1602 (1992).

[10] R. A. Hegstrom, D. W. Rein, and P. G. J. Sandars, J. Chem. Phys. **73**, 2329 (1980).

[11] W. Kutzelnigg, Theo. Chim. Acta **73**, 173 (1988).

[12] A. Nørager, *Udvikling af en relativistisk model til beregning af ESR-parametre*, Master's thesis, University of Southern Denmark (2000).

[13] O. Vahtras, B. Minaev, and H. Ågren, Chem. Phys. Lett. **281**, 186 (1997).

[14] H. J. Aa. Jensen, *Relativistic polarization propagator excitation energies* (2001), unpublished.

[15] O. Vahtras, H. Ågren, P. Jørgensen, H. J. Aa. Jensen, T. Helgaker, and J. Olsen, J. Chem. Phys. **97**, 9178 (1992).

[16] P. Lazzeretti and R. Zanasi, Chem. Phys. Lett. **279**, 349 (1997).

[17] L. L. Foldy and S. A. Wouthuysen, Phys. Rev. **78**, 29 (1950).

[18] H. A. Bethe and E. E. Salpeter, *Quantum Mechanics of One and Two Electron Atoms* (Academic, New York, 1957).

[19] W. Kutzelnigg, Z. Phys. D. **11**, 15 (1989).

[20] W. Kutzelnigg, Z. Phys. D. **15**, 27 (1990).

[21] W. Cencek and W. Kutzelnigg, J. Chem. Phys. **105**, 5878 (1996).

[22] E. Ottschofski and W. Kutzelnigg, J. Chem. Phys. **106**, 6634 (1997).

[23] W. Kutzelnigg and W. Liu, J. Chem. Phys. **112**, 3540 (2000).

[24] W. Liu, W. Kutzelnigg, and C. van Wüllen, J. Chem. Phys. **112**, 3559 (2000).

[25] K. G. Dyall, J. Chem. Phys. **100**, 2118 (1994).

[26] M. Douglas and N. M. Kroll, Annln. Phys. **82**, 89 (1974).

[27] B. A. Hess, Phys. Rev. A **32**, 756 (1985).

[28] B. A. Hess, Phys. Rev. A **33**, 3742 (1986).

[29] G. Jansen and B. A. Hess, Phys. Rev. A **39**, 6016 (1989).

[30] E. van Lenthe, E. J. Baerends, and J. G. Snijders, J. Chem. Phys. **99**, 4597 (1993).

[31] E. van Lenthe, E. J. Baerends, and J. G. Snijders, J. Chem. Phys. **101**, 9783 (1994).

[32] E. J. Baerends, W. H. E. Schwartz, P. Schwerdtfeger, and J. G. Snijders, J. Phys. B **23**, 3325 (1990).

[33] M. Barysz and A. J. Sadlej, Theo. Chim. Acta **97**, 260 (1997).

[34] V. Kelloe and A. J. Sadlej, Int. J. Quant. Chem. **68**, 159 (1998).

[35] M. Pernpointner and P. Schwerdfeger, Chem. Phys. Lett. **295**, 347 (1998).

[36] H. M. Quiney, H. Skaane, and I. P. Grant, J. Phys. B **30**, L829 (1997).

[37] H. M. Quiney, H. Skaane, and I. P. Grant, Adv. Quant. Chem. **32**, 1 (1998).

[38] T. Saue, T. Enevoldsen, T. Helgaker, H. J. A. Jensen, J. Laerdahl, K. Ruud, J. Thyssen, and L. Visscher, *"DIRAC, a relativistic ab initio electronic structure program , Release 3.1 (1998)"*.

[39] J. Thyssen and H. J. Aa. Jensen, *Integral screening in calculations of molecular gradients* (2001), unpublished.

[40] J. M. Lévy-Leblond, Comm. Math. Phys. **6**, 286 (1967).

[41] J. M. Lévy-Leblond, Annln. Phys. **57**, 481 (1970).

[42] K. G. Dyall, Chem. Phys. Lett. **224**, 186 (1994).

[43] J. K. Laerdahl, J. K. Fægri, L. Visscher, and T. Saue, J. Chem. Phys. **109**, 10806 (1998).

[44] L. Visscher, *Relativity and Electron Correlation in Chemistry*, Ph.D. thesis, University of Groningen (1993).

[45] L. Visscher, K. G. Dyall, and T. J. Lee, Int. J. Quant. Chem. Symp. **29**, 411 (1995).

[46] E. Eliav, U. Kaldor, and Y. Ishikawa, Phys. Rev. A **50**, 1121 (1994).

[47] E. Eliav, U. Kaldor, and Y. Ishikawa, Phys. Rev. A **49**, 1724 (1994).

[48] W. Liu, G. Y. Hong, D. D. Dai, L. M. Li, and M. Dolg, Theo. Chim. Acta **96**, 75 (1997).

[49] K. Andersson, P.-Å. Malmquist, B. O. Roos, A. J. Sadlej, and K. Wolinski, J. Phys. Chem. **94**, 5483 (1990).

[50] K. Andersson, P.-Å. Malmquist, and B. O. Roos, J. Chem. Phys. **96**, 1218 (1992).

[51] L. Gagliardi and B. O. Roos, Chem. Phys. Lett. **331**, 229 (2000).

[52] B. O. Roos, P.-Å. Malmquist, Y. Carrisan, and L. Gagliardi, *CASSCF/CASPT2 Studies of Uranium Compounds* (2000), presented by B. O. Roos at The Very Heavy Metal meeting.

[53] K. Andersson, A. B. M. Barysz, M. R. A. Blomberg, D. L. Cooper, T. Fleig, M. P. Fülscher, C. de Graaf, B. A. Hess, G. Karlström, R. Lindh, P.-Å. Malmquist, P. Neogrády, *et al.*, *MOLCAS Version 5* (2000), Lund University, Sweden.

[54] M. J. Vilkas, K. Koc, and Y. Ishikawa, Chem. Phys. Lett. **296**, 68 (1998).

[55] D. Mukherjee and S. Pal, Adv. Quant. Chem. **20**, 292 (1989).

[56] U. Kaldor, in *Recent Progress in Many-Body Theories*, edited by E. Schackinger, H. Mitter, and M. Sormann (Plenum, New York, 1995), vol. 4, p. 135.

[57] U. Kaldor and E. Eliav, Adv. Quant. Chem. **31**, 313 (1998).

[58] E. Ilyabaev and U. Kaldor, J. Chem. Phys. **97**, 8455 (1992).

[59] A. Shukla, B. P. Das, and D. Mukherjee, Phys. Rev. A **50**, 2096 (1994).

[60] J. Olsen, J. Chem. Phys. **113**, 7140 (2000).

[61] H. J. Aa.. Jensen, K. G. Dyall, T. Saue, and K. Faegri, Jr., J. Chem. Phys. **104**, 4083 (1996).

# Part I

# Relativistic Quantum Mechanics and Electron Correlation

# Chapter 2

# Relativistic Quantum Mechanics

In this chapter some of the many aspects of relativistic quantum mechanics is discussed. We briefly discuss the relativistic single particle wave equation; the Dirac equation. Since this thesis concerns *molecular* relativistic quantum mechanics we also discuss the molecular Hamiltonian. We end this chapter discussing how to obtain computational gains by using time-reversal symmetry and double group symmetry, and how this is easily implemented using a quaternion formalism.

Throughout this thesis we use atomic units, *i.e.*, $\hbar = m_e = 1$. Within this unit system the speed of light is $c = 137.0359895\ldots$. Although $m_e = 1$ we may write it explicitly for clarity.

## 2.1 The Dirac Equation

The starting point for all this is Dirac's famous relativistic single particle wave equation from 1928 [1], here written in Dirac's original form

$$\left(\frac{i}{c}\frac{\partial}{\partial t} + \boldsymbol{\alpha}\cdot\mathbf{p} + \beta mc\right)\psi = 0, \tag{2.1}$$

where $\mathbf{p} = -i\left[\frac{d}{dx}, \frac{d}{dy}, \frac{d}{dz}\right]$ is the momentum, and $\boldsymbol{\alpha}$ is a vector with $4\times 4$ matrices $\alpha_x$, $\alpha_y$, and $\alpha_z$ as its components. The $\alpha_u$ matrices and the $\beta$ matrix

are given by [1]

$$\begin{aligned} \alpha_u &= \begin{bmatrix} \mathbf{0}_2 & \sigma_u \\ \sigma_u & \mathbf{0}_2 \end{bmatrix}, \quad u = x, y, z, \\ \beta &= \begin{bmatrix} \mathbf{I}_2 & \mathbf{0}_2 \\ \mathbf{0}_2 & -\mathbf{I}_2 \end{bmatrix}, \end{aligned} \tag{2.2}$$

where $\sigma_u, u = x, y, z$ are the Pauli spin matrices

$$\sigma_x = \begin{bmatrix} 0 & 1 \\ 1 & 0 \end{bmatrix}, \quad \sigma_y = \begin{bmatrix} 0 & -i \\ i & 0 \end{bmatrix}, \quad \sigma_z = \begin{bmatrix} 1 & 0 \\ 0 & -1 \end{bmatrix}. \tag{2.3}$$

In order to align the non-relativistic and relativistic energy scales $\beta$ is often replaced with

$$\beta' = \begin{bmatrix} \mathbf{0}_2 & \mathbf{0}_2 \\ \mathbf{0}_2 & -2\mathbf{I}_2 \end{bmatrix}. \tag{2.4}$$

For calculation of wave functions and energies we restrict ourselves to time-independent potentials. Thus, we can remove the time-dependency. This gives us the time-independent Dirac equation

$$(\boldsymbol{\alpha} \cdot \mathbf{p} + \beta' mc)\, \psi = \frac{E}{c} \psi. \tag{2.5}$$

We will not go into great details about the structure and properties of the operator, spectrum, or eigenvalues. This can be found in many standard textbooks on the topic, for example, Moss [2] or Rose [3]. We will, however, discuss a few aspects. First, as the $\alpha$ and $\beta$ matrices are $4 \times 4$ matrices the wave function is a 4-component vector, or a 4-component spinor. Second, the spectrum is not bounded from below as the non-relativistic spectrum. For the free-particle case, Eq. (2.5), two kind of solutions occur: negative energy solutions with eigenvalues less than $-mc^2$ and positive energy solutions with eigenvalues greater than $+mc^2$ (assuming we have used $\beta$ from Eq. (2.2)). This is a consequence of the fact that the Dirac equation can be used to describe both electrons and positrons. In the presence of a nuclear potential or electronic potential there are bound positive energy states with eigenvalues slightly less $+mc^2$.

The existence of a negative energy continuum creates problems in the formulation of variational theory, since, if the negative continuum is empty, electrons will fall into it under emission of photons with energies $\approx -2mc^2$.

Dirac solved this by postulating that the negative energy states are filled [4], hence the Pauli principle will prevent the collapse into the negative energy

states. Excitations of an electron from a negative energy states will introduce a positively charged hole in the negative energy continuum: a positron. However, this introduces new problems as the vacuum is now infinitely charged with infinite energy, as the expectation value $\langle \text{vac}|\hat{H}|\text{vac}\rangle = -\infty$. This problem is solved in the QED reinterpretation by using so-called *normal ordered* operators, where $\langle \text{vac}|\hat{H}|\text{vac}\rangle = 0$.

So the question arises on what to do about the negative energy states in DHF or MCSCF calculations: should we consider the negative energy states empty (the empty Dirac approach), filled (the filled Dirac approach), or use the QED interpretation? In principle all three approaches can be used. However, the filled Dirac approach is troublesome because of the infinities involved, hence we are left with either the empty Dirac approach or the QED approach. Since we use finite basis sets we will not have infinities but rather a large number of large numbers, which is equally troublesome considering that we use finite-precision computers performing the calculations.

In most DHF procedures the empty Dirac approach is used, and the desired electronic state is an excited state to which we converge using vector selection by implicitly projecting out negative energy states [5]. This is equivalent to employing a mini-max principle [6] where the energy is minimized with respect to positive energy parameters and maximized with respect to negative energy parameters. There is also an computational aspect as it is often more expensive to treat orbitals as occupied rather than empty.

## 2.2 The Relativistic Molecular Hamiltonian

Our main interest is to perform molecular calculations for which we need a molecular Hamiltonian. In order to obtain this we first need the Dirac one-electron Hamiltonian in presence of a general static potential, namely the one generated by the nuclei in the Born-Oppenheimer reference frame. The Dirac Hamiltonian in presence of such a field is given by [1]

$$\hat{h}_D = \boldsymbol{\alpha} \cdot \mathbf{p} + \beta mc + \phi. \tag{2.6}$$

The scalar potential arising from a charge distribution is given by

$$\phi(\mathbf{r}_i) = \int d\mathbf{r}' \frac{\varrho(\mathbf{r}')}{|\mathbf{r}_i - \mathbf{r}'|} \tag{2.7}$$

where $\varrho$ is the charge distribution. In non-relativistic theory the charge distribution is often chosen to be a delta function corresponding to a treatment of the nuclei as a point charges:

$$\varrho_A(\mathbf{r}_i) = Z_A \delta(\mathbf{r}_i). \tag{2.8}$$

This leads to the usual Coulombic potential

$$\phi_A(\mathbf{r}_i) = \frac{Z_A}{r_{iA}}. \tag{2.9}$$

The Coulomb potential can also be used in relativistic calculations but in order to avoid having to reproduce singularities at the origin for the $1s_{1/2}$ and $2p_{1/2}$ orbitals, which would require very good basis sets, a finite nucleus potential is often used. The use of Gaussian basis set functions in molecular calculations favors the use of a Gaussian charge distribution [7]

$$\phi_A(\mathbf{r}_i) = Z_A \left(\frac{\eta_A}{\pi}\right)^{3/2} \exp\left(\eta_A r_{iA}^2\right) \tag{2.10}$$

where $\eta_A$ is a nuclei dependent parameter, in order to calculate integrals $\langle\chi_\mu|\phi_A|\chi_\nu\rangle$ over the potential analytically. Other forms of the charge distribution such as the two-parameter Fermi distribution [8] or the uniformly charged sphere distribution [9–12] may also be used, but they require numerical integrations. Since the differences between the different finite nucleus charge distributions are not large[1] the Gaussian charge distribution is preferred [7]. There are, however, observable differences between the *point charge* and the finite nuclei distributions (*e.g.*, see [7,9–14]). For an *extensive* review of finite nucleus distributions see Ref. [13]. As a final note we add that the nuclear potential $\phi_A$ is Lorentz invariant in the Born-Oppenheimer frame as the velocity of the nuclei is zero.

We now turn to the electron-electron interaction which obviously has to be different from the non-relativistic Coulomb operator that is not Lorentz invariant. The covariant electron-electron interaction derived from QED is

$$v_{ij,\alpha\gamma}^T = \frac{1}{r_{ij}} - \left(\frac{\boldsymbol{\alpha}_i \cdot \boldsymbol{\alpha}_j}{r_{ij}} \exp\left(i\omega_{\alpha\gamma} r_{ij}\right) + \left(\boldsymbol{\alpha}_i \cdot \nabla_i\right)\left(\boldsymbol{\alpha}_j \cdot \nabla_j\right) \frac{\exp\left(i\omega_{\alpha\gamma} r_{ij}\right) - 1}{\omega_{\alpha\gamma}^2 r_{ij}}\right). \tag{2.11}$$

The operator is derived in the Coulomb gauge ($\nabla \cdot \mathbf{A} = 0$), assuming the electrons are in stationary states in some effective static potential [15] and including only the single-photon exchange with a frequency of $\omega_{\alpha\gamma}$. In the limit of $\omega \to 0$ the electron-electron interaction, Eq. (2.11), reduces to the Coulomb-Breit interaction [16]

$$\hat{g}^{\text{Coulomb-Breit}}(\mathbf{r}_{ij}) = \hat{g}^{\text{Coulomb}}(\mathbf{r}_{ij}) + \hat{g}^{\text{Breit}}(\mathbf{r}_{ij}) \tag{2.12}$$

[1] One should be careful, however, since some properties may be *very* dependent upon the choice of nuclear charge distribution. One such property could be the parity violation energy as pointed out by Andrae [13], although there have not been reported any investigations on this subject.

where $\hat{g}^{\text{Coulomb}}$ is the usual Coulomb interaction

$$\hat{g}^{\text{Coulomb}}(\mathbf{r}_{ij}) = \frac{1}{r_{ij}}, \tag{2.13}$$

and $\hat{g}^{\text{Breit}}$ is the Breit term [16]

$$\hat{g}^{\text{Breit}}(\mathbf{r}_{ij}) = -\left(\frac{\boldsymbol{\alpha}_i \cdot \boldsymbol{\alpha}_j}{2r_{ij}} + \frac{(\boldsymbol{\alpha}_i \cdot \mathbf{r}_{ij}) \cdot (\boldsymbol{\alpha}_j \cdot \mathbf{r}_{ij})}{2r_{ij}^3}\right), \tag{2.14}$$

which also can be written as a sum

$$\hat{g}^{\text{Breit}}(\mathbf{r}_{ij}) = \hat{g}^{\text{Gaunt}}(\mathbf{r}_{ij}) + \hat{g}^{\text{gauge}}(\mathbf{r}_{ij}), \tag{2.15}$$

of the Gaunt term [17]

$$\hat{g}^{\text{Gaunt}}(\mathbf{r}_{ij}) = -\frac{\boldsymbol{\alpha}_i \cdot \boldsymbol{\alpha}_j}{r_{ij}}, \tag{2.16}$$

and the gauge term

$$\hat{g}^{\text{gauge}}(\mathbf{r}_{ij}) = \frac{(\boldsymbol{\alpha}_i \times \mathbf{r}_{ij}) \cdot (\boldsymbol{\alpha}_j \times \mathbf{r}_{ij})}{2r_{ij}^3}. \tag{2.17}$$

The Coulomb-Breit interaction (Eq. (2.12)) can be shown to be Lorentz invariant to $O(\alpha^2)$ [5, 18–22] where $\alpha$ is the fine structure constant.

The gauge term involves integrals other than $1/r_{ij}$ and is often neglected. The Gaunt term is also often omitted in order to reduce the number of integrals. The use of the $g^{\text{Coulomb}}$ interaction will in the non-relativistic limit [23] correspond to only including the spin-own-orbit and one of the Darwin-like terms of the Breit-Pauli Hamiltonian. Other terms such as the spin-other-orbit, spin-spin and others are not included. The effect of the Gaunt and gauge terms are most profound near the nucleus [24] and can be neglected for many valence properties (such as bond lengths [25] or dissociation energy [26]) whereas it may be needed for correct description of some core properties.

Analogous to non-relativistic theory the molecular Hamiltonian is now written as [18, 27]

$$\hat{H} = \sum_i \hat{h}_{D;i} + \frac{1}{2}\sum_{i \neq j} \hat{g}_{ij} + \hat{V}_{NN}, \tag{2.18}$$

where $h_{D;i}$ is the Dirac one-electron Hamiltonian for electron $i$ (Eq. (2.6)), $g_{ij}$ is the electron-electron interaction, and $V_{NN}$ is the nucleus-nucleus interaction which is treated non-relativistically in the Born-Oppenheimer frame, *i.e.*:

$$\hat{V}_{NN} = \sum_{A<B} \frac{Z_A Z_B}{R_{AB}}. \tag{2.19}$$

In the rest of this thesis we will restrict ourselves to the Dirac-Coulomb Hamiltonian

$$\hat{H}^{\text{Dirac-Coulomb}} = \sum_i \hat{h}_{D;i} + \frac{1}{2}\sum_{i\neq j} \hat{g}_{ij}^{\text{Coulomb}} + \hat{V}_{NN}, \tag{2.20}$$

We will almost exclusively use the Hamiltonian in the second quantized form rather than in the first quantized form above (Eq. (2.20)). The second quantized form of an operator is obtained from the first quantized form by evaluating [28]

$$\begin{aligned} \hat{h} &= \int d\mathbf{r}\ \Psi(\mathbf{r})^\dagger \mathbf{h}(\mathbf{r})\Psi(\mathbf{r}), \\ \hat{g} &= \iint d\mathbf{r}_1\ d\mathbf{r}_2\ \Psi(\mathbf{r}_1)^\dagger \Psi(\mathbf{r}_2)^\dagger \mathbf{g}(\mathbf{r}_1,\mathbf{r}_2)\Psi(\mathbf{r}_2)\Psi(\mathbf{r}_1), \end{aligned} \tag{2.21}$$

where $\Psi$ is the field operator given by

$$\Psi = \sum_p \phi_p p, \tag{2.22}$$

where $\phi_p$ is orbital no. $p$ and the operator $p$ is the annihilation operator. $p$ will remove an electron in orbital $\phi_p$ in a Slater determinant. The conjugate $p^\dagger$ is the creation operator that creates an electron in orbital $p$. It follows that the Dirac-Coulomb(-Breit) Hamiltonian, Eq. (2.20), in a complex spinor basis can be written as

$$\hat{H} = \sum_{pq} h_{pq} p^\dagger q + \frac{1}{2}\sum_{pqrs} g_{pq,rs} p^\dagger r^\dagger s q, \tag{2.23}$$

where the matrix elements are given by

$$\begin{aligned} h_{pq} &= (\phi_p|\hat{h}_D|\phi_q) \equiv (p|\hat{h}_D|q)\,, \\ g_{pq,rs} &= (\phi_p\phi_q|\hat{g}|\phi_r\phi_s) \equiv (pq|\hat{g}|rs)\,. \end{aligned} \tag{2.24}$$

The first and second quantization operators are equivalent in the limit of a complete basis set. For non-complete basis set the second quantization operator can be regarded as a projection onto the full first quantization operator. The advantage of working with second quantization operators is that it is possible to do simplifications at the operator level. Also, the formulae will appear as they will be implemented, and there is furtermore no explicit reference to the number of electrons.

## 2.3 Time Reversal Symmetry, Double Group Symmetry, and Quaternions

In non-relativistic quantum chemistry the use of both spin-symmetry and point group symmetry is widely used, since it reduces the computational effort considerably. As the Hamiltonian has no explicit dependence on spin, the orbitals can in the absence of an external magnetic field be split into the product of a spatial part and a spin part. The spin part can be integrated analytically which leads to large computational savings, for example, in the evaluation of two-electron integrals where sixteen integrals reduce to one[2] and four one-electron integrals reduce to one. The spatial part left after the spin integration is a boson function and can thus be adapted to point group symmetry, which can be exploited for additional computational gains.

However, in four-component relativistic quantum chemistry the Hamiltonian is spin-dependent and it is no longer possible to factorize an spinor into a separate spatial and spin part. Instead it is possible to use time-reversal symmetry which will partially recover some of the lost spin-symmetry. The anti-unitary 4-component time-reversal operator, $\mathcal{K}$, is defined by [29]

$$\hat{\mathcal{K}} = \hat{\mathcal{K}}'\hat{\mathcal{K}}_0 \tag{2.25}$$

where $\hat{\mathcal{K}}_0$ is complex conjugation operator and

$$\hat{\mathcal{K}}' = -i \begin{bmatrix} \sigma_y & \mathbf{0}_2 \\ \mathbf{0}_2 & \sigma_y \end{bmatrix}. \tag{2.26}$$

Alternatively, $\hat{\mathcal{K}}$ can be defined by its action on a fermion function (a spinor) $\phi$

$$\hat{\mathcal{K}} a\phi = a^*\hat{\mathcal{K}}\phi, \qquad \hat{\mathcal{K}}^2\phi = -\phi \qquad a \in \mathbf{C}. \tag{2.27}$$

The function

$$\bar{\phi} \equiv \hat{\mathcal{K}}\phi \tag{2.28}$$

[2]Four identical integrals:

$$(p_\alpha q_\alpha | r_\alpha s_\alpha) = (p_\alpha q_\alpha | r_\beta s_\beta) = (p_\beta q_\beta | r_\alpha s_\alpha) = (p_\beta q_\beta | r_\beta s_\beta)\,,$$

and 12 integrals vanish

$$\begin{aligned}(p_\beta q_\alpha | r_\alpha s_\alpha) = (p_\alpha q_\beta | r_\alpha s_\alpha) &= (p_\alpha q_\alpha | r_\beta s_\alpha) = (p_\alpha q_\alpha | r_\alpha s_\beta) = \\ (p_\beta q_\alpha | r_\beta s_\alpha) = (p_\beta q_\alpha | r_\alpha s_\beta) &= (p_\alpha q_\beta | r_\beta s_\alpha) = (p_\alpha q_\beta | r_\alpha s_\beta) = \\ (p_\beta q_\beta | r_\beta s_\alpha) = (p_\beta q_\beta | r_\alpha s_\beta) &= (p_\beta q_\alpha | r_\beta s_\beta) = (p_\alpha q_\beta | r_\beta s_\beta) = 0.\end{aligned}$$

and $\phi$ are denoted a Kramers pair. Throughout this thesis we will work in a *Kramers restricted* basis, *i.e.*, in the union basis $\{\{\phi\} \cup \{\bar{\phi}\}\}$. In this basis the matrix representation of an one-electron operator, $\hat{\Omega}$ (*e.g.*, the Fock operator), which is symmetric under time-reversal

$$\hat{\mathcal{K}}\hat{\Omega}\hat{\mathcal{K}}^{-1} = \hat{\Omega}, \tag{2.29}$$

will have the following properties [30]:

$$\begin{aligned} \Omega_{pq} &= \Omega_{\bar{q}\bar{p}}, \\ \Omega_{p\bar{q}} &= -\Omega_{q\bar{p}}. \end{aligned} \tag{2.30}$$

If we now define $A_{pq} = \Omega_{pq}$ and $B_{pq} = \Omega_{p\bar{q}}$ we get the following structure of $\mathbf{\Omega}$

$$\mathbf{\Omega} = \begin{bmatrix} \mathbf{A} & \mathbf{B} \\ -\mathbf{B}^* & \mathbf{A}^* \end{bmatrix}, \tag{2.31}$$

where $\mathbf{A} = \mathbf{A}^\dagger$ is a Hermitian matrix and $\mathbf{B} = -\mathbf{B}^\dagger$ is an anti-Hermitian matrix. $\mathbf{\Omega}$ can be block diagonalized with a quaternion unitary transformation, $\mathbf{U}$, defined by [31–33]

$$\mathbf{U} = \frac{1}{\sqrt{2}} \begin{bmatrix} \mathbf{I} & \check{\jmath}\mathbf{I} \\ \check{\jmath}\mathbf{I} & \mathbf{I} \end{bmatrix}. \tag{2.32}$$

The transformed $\mathbf{\Omega}$ is given by

$$\mathbf{U}^\dagger\mathbf{\Omega}\mathbf{U} = \begin{bmatrix} \mathbf{A} + \mathbf{B}\check{\jmath} & 0 \\ 0 & -\check{k}(\mathbf{A} + \mathbf{B}\check{\jmath})\check{k} \end{bmatrix} \tag{2.33}$$

which is clearly doubly degenerate[3] — this is also known as Kramers' Theorem [34]. We now define the quaternion matrix for the operator $\hat{\Omega}$ as [32, 33]

$${}^{Q}\Omega_{pq} = A_{pq} + B_{pq}\check{\jmath} = \Omega_{pq} + \Omega_{p\bar{q}}\check{\jmath} \tag{2.34}$$

which reduce the memory requirements and operation count by a factor of two (a complex $N \times N$ matrix reduced to a quaternion $\frac{N}{2} \times \frac{N}{2}$ matrix). Further symmetry reductions can be obtained as the quaternion matrix, Eq. (2.34), may reduce to a real or complex matrix depending on the point group symmetry (here shown for $D_{2h}$ and subgroups):

- $C_{2v}$, $D_{2h}$, and $D_2$: $\mathbf{B} = \mathbf{0}$, and $\mathbf{A}$ is a *real* symmetric matrix,

[3] $\mathbf{A} + \mathbf{B}\check{\jmath}$ and $-\check{k}(\mathbf{A} + \mathbf{B}\check{\jmath})\check{k}$ are Hermitian matrices related by a unitary transformation, and thus have the same eigenvalues.

Table 2.1: Relationship between time-reversal symmetry, Hermiticity and Kramers basis operators $X^{\pm}_{pq}$.

| | Hermitian operator | Anti-Hermitian operator |
|---|---|---|
| time-reversal invariant | $X^{+}_{pq}$ | $X^{-}_{pq}$ |
| time-reversal variant | $X^{-}_{pq}$ | $X^{+}_{pq}$ |

- $C_2$, $C_s$, and $C_{2h}$: $\mathbf{B} = \mathbf{0}$, but $\mathbf{A}$ is generally a complex Hermitian matrix,
- $C_1$ and $C_i$: both $\mathbf{A}$ and $\mathbf{B}$ are generally complex,

assuming a totally symmetric operator, for example, the Fock operator.

When a scalar basis set is used, *i.e.*,

$$\chi^{L\alpha}_{\mu} = \begin{pmatrix} \chi^{L}_{\mu} \\ 0 \\ 0 \\ 0 \end{pmatrix}, \quad \chi^{L\beta}_{\mu} = \begin{pmatrix} 0 \\ \chi^{L}_{\mu} \\ 0 \\ 0 \end{pmatrix}, \quad \chi^{S\alpha}_{\mu} = \begin{pmatrix} 0 \\ 0 \\ \chi^{S}_{\mu} \\ 0 \end{pmatrix}, \quad \chi^{S\beta}_{\mu} = \begin{pmatrix} 0 \\ 0 \\ 0 \\ \chi^{S}_{\mu} \end{pmatrix}, \tag{2.35}$$

such as in the DIRAC [35] program package, the atomic orbital (AO) matrices (*e.g.*, the one- and two-electron Fock matrices) may also be reduced to real or complex matrices depending on point group symmetry if single point group symmetry adapted basis functions are used [33]. The use of scalar basis set functions, Eq. (2.35), and spin-symmetry (*e.g.*, $\int \chi^{L\alpha\dagger}_{\mu} \chi^{L\beta}_{\nu} = 0$) allows the use of non-relativistic integral generators for the calculation of one- and two-electron Fock matrices and property integrals. The small component basis set functions, $\chi^{S\alpha}_{\mu}$ and $\chi^{S\beta}_{\mu}$, are constructed using kinetic balance [36] in order to ensure that the kinetic energy is properly represented in the non-relativistic limit.

It is also possible to put the Kramers restriction directly into the Hamiltonian using the relations between matrix elements from Eq. (2.30). Kramers restricted one-electron operators can be expanded in Kramers basis operators [30]

$$\begin{aligned} \hat{X}^{\pm}_{pq} &= p^{\dagger} q \pm \bar{q}^{\dagger} \bar{p}, \\ \hat{X}^{\pm}_{\bar{p}\bar{q}} &= \bar{p}^{\dagger} \bar{q} \pm q^{\dagger} p, \\ \hat{X}^{\pm}_{\bar{p}q} &= \bar{p}^{\dagger} q \mp \bar{q}^{\dagger} p, \\ \hat{X}^{\pm}_{p\bar{q}} &= p^{\dagger} \bar{q} \mp q^{\dagger} \bar{p}. \end{aligned} \tag{2.36}$$

The sign $\pm$ depend on the time-reversal symmetry and Hermiticity of the operators (see Table 2.1, reproduced from Aucar *et al.* [30]). For example, the one-electron part of the Dirac-Coulomb Hamiltonian, Eq. (2.23), is an Hermitian time-reversal invariant operator, hence it is expanded in $X^{+}_{pq}$ operators, as [30]:

$$\sum_{pq} h_{pq}\hat{X}^{+}_{pq} + \frac{1}{2}\left(h_{\bar{p}q}\hat{X}^{+}_{\bar{p}q} + h_{p\bar{q}}\hat{X}^{+}_{p\bar{q}}\right). \tag{2.37}$$

Note that the summation is over Kramers pairs. Similarly, two-electron operators can be expanded in

$$\hat{x}^{s_1,s_2}_{pq,rs} = \left(1 + s_1\hat{T}_{pq}\right)\left(1 + s_2\hat{T}_{rs}\right)p^{\dagger}r^{\dagger}sq \qquad s_1, s_2 = \pm 1 \tag{2.38}$$

where the Kramers permutation operators $\hat{T}_{pq}$ are given by

$$\hat{T}_{pq}\left(p^{\dagger}q\right) = \bar{q}^{\dagger}\bar{p}; \quad \hat{T}_{pq}\left(\bar{p}^{\dagger}q\right) = -\bar{q}^{\dagger}p \tag{2.39}$$

In the Kramers restricted basis we write the Hamiltonian, Eq. (2.23), as

$$\begin{aligned}\hat{H} = &\sum_{pq}\left[h_{pq}\hat{X}^{+}_{pq} + \frac{1}{2}\left(h_{\bar{p}q}\hat{X}^{+}_{\bar{p}q} + h_{p\bar{q}}\hat{X}^{+}_{p\bar{q}}\right)\right] \\ &+ \frac{1}{2}\sum_{pqrs}\left[(pq|rs)\,\hat{x}^{++}_{pq,rs} + (\bar{p}qr,rs)\,\hat{x}^{++}_{\bar{p}q,rs} + (p\bar{q}|rs)\,\hat{x}^{++}_{p\bar{q}|rs}\right] \\ &+ \frac{1}{4}\sum_{pqrs}(\bar{p}q|r\bar{s})\,\hat{x}^{++}_{\bar{p}q,r\bar{s}} + \frac{1}{8}\left[(\bar{p}q|\bar{r}s)\,\hat{x}^{++}_{\bar{p}q,\bar{r}s} + (p\bar{q}|r\bar{s})\,\hat{x}^{++}_{p\bar{q},r\bar{s}}\right]\end{aligned} \tag{2.40}$$

where the summation is over Kramers pairs, and *not* over four-spinors as in Eq. (2.23).

# Bibliography

[1] P. A. M. Dirac, Proc. Roy. Soc. Lond. **A117**, 610 (1928).

[2] R. E. Moss, *Advanced Molecular Qauntum Mechanics* (W. A. Benjamin, Inc., London, 1968).

[3] M. E. Rose, *Relativistic Electron Theory* (Wiley & Sons, New York, 1961).

[4] P. A. M. Dirac, Proc. Roy. Soc. Lond. **A126**, 360 (1929).

[5] M. H. Mittleman, Phys. Rev. A **24**, 1167 (1981).

[6] J. D. Talman, Phys. Rev. Lett. **57**, 1091 (1986).

[7] O. Visser, P. J. C. Aerts, D. Hegarty, and W. C. Nieuwport, Chem. Phys. Lett. **134**, 34 (1987).

[8] D. R. Yennie, D. G. Ravenhall, and R. N. Wilson, Phys. Rev. **95**, 500 (1954).

[9] A. Bohr and V. F. Weisskopf, Phys. Rev. **77**, 94 (1950).

[10] F. G. Werner and J. A. Wheeler, Phys. Rev. **109**, 126 (1958).

[11] Y. Ishikawa, R. Baretty, and J. R. C. Binning, Chem. Phys. Lett. **121**, 130 (1985).

[12] Y. Ishikawa and H. M. Quiney, Int. J. Quant. Chem. Symp. **21**, 523 (1987).

[13] D. Andrae, Phys. Rep.-Rev. Sec. Phys. Lett. **336**, 414 (2000).

[14] K. G. Dyall and J. K. Fægri, Chem. Phys. Lett. **201**, 27 (1993).

[15] W. H. Furry, Phys. Rev. **81**, 115 (1951).

[16] G. Breit, Phys. Rev. **34**, 553 (1929).

[17] J. A. Gaunt, Proc. Roy. Soc. Lond. **A122**, 513 (1929).

[18] J. Sucher, Phys. Rev. A **22**, 348 (1980).

[19] J. Sucher, Physica Scripta **36**, 271 (1987).

[20] J. Sucher, J. Phys. B **21**, L585 (1988).

[21] M. H. Mittleman, Int. J. Quant. Chem. **4**, 893 (1971).

[22] M. H. Mittleman, Int. J. Quant. Chem. **5**, 2395 (1972).

[23] H. A. Bethe and E. E. Salpeter, *Quantum Mechanics of One and Two Electron Atoms* (Academic, New York, 1957).

[24] P. Indelicato, J. Phys. B **19**, 1719 (1986).

[25] O. Visser, L. Visscher, P. J. C. Aerts, and W. C. Niuewport, Theo. Chim. Acta **81**, 405 (1992).

[26] W. A. de Jong and W. C. Nieuwport, Int. J. Quant. Chem. **58**, 203 (1996).

[27] B. Swirles, Proc. Roy. Soc. Lond. **A152**, 625 (1935).

[28] A. L. Fetter and J. D. Walecka, *Qauntum Theory of Many-particle Systems* (McGraw-Hill, New York, 1971).

[29] E. Wigner, *Nachrichten der Akad. der Wissensch. zu Göttingen*, vol. II (1932).

[30] G. A. Aucar, H. J. Aa. Jensen, and J. Oddershede, Chem. Phys. Lett. **232**, 47 (1995).

[31] N. Rösch, Chem. Phys. **80**, 1 (1983).

[32] H. J. Aa.. Jensen, K. G. Dyall, T. Saue, and K. Faegri, Jr., J. Chem. Phys. **104**, 4083 (1996).

[33] T. Saue and H. J. Aa.. Jensen, J. Chem. Phys. **111**, 6211 (1999).

[34] H. A. Kramers, Proc. Acad. Amsterdam **33**, 959 (1930).

[35] T. Saue, T. Enevoldsen, T. Helgaker, H. J. A. Jensen, J. Laerdahl, K. Ruud, J. Thyssen, and L. Visscher, *"DIRAC, a relativistic ab initio electronic structure program , Release 3.1 (1998)"*.

[36] R. E. Stanton and S. Havriliak, J. Chem. Phys. **81**, 1910 (1984).

# Chapter 3

# Average-of-configuration Open-shell Hartree-Fock

In this chapter we discuss the average-of-configuration open-shell Hartree-Fock or Dirac-Hartree-Fock method, which is a useful procedure for obtaining initial orbitals for a MCSCF or CI calculation.

## 3.1 Introduction

Since Roothaan's original paper [1] on the open-shell Hartree-Fock equations, several approaches to solve the open-shell equations have been proposed. Roothaan described two methods which required one or two matrix diagonalizations, respectively. Later, McWeeny [2], Guest and Saunders [3], Fægri and Manne [4], Huzinaga [5], and Hsu *et al.* [6] all described other alternative one-Fock matrix methods, and Davidson [7] described an alternative two-Fock matrix method. Also three-Fock matrix methods have been proposed [8]. There also exists iterative gradient-based open-shell procedures without Fock matrix diagonalization (see [9] and references therein) and iterative gradient *and* Hessian based open-shell procedures (*e.g.*, see [10]).

The most general of these methods is the one by McWeeny [2] which is an *average-of-configuration* method, where the energy is averaged over all states generated by a full CI in each of the active spaces. Also Roothaan's original paper [1] and later methods [4,11] are average-of-configuration methods, but they are all restricted to either only one open shell (Ref. [1] and [4]) or to a maximum of two open shells of different symmetry (Ref. [11]). The possibility of having several shells with the same symmetry is of interest for core-hole states as we will exemplify in Sec. 3.3. Also, McWeeny's method is a one-Fock matrix approach, which is convenient as only one Fock-matrix

diagonalization is needed and the orbitals are automatically orthogonal; no arbitrary orthogonalization procedure for the orbitals has to be invoked as it is the case with two- and three-Fock matrix methods, as, for example, the two Fock matrix approach by Visser *et al.* [11].

The orbitals obtained can be used as start orbitals for CI or MCSCF, where they may be better than alternative start orbitals, as another advantage of the average-of-configuration orbitals is that they, in general, do not have a specific spin symmetry and are therefore not biased towards any specific state. Therefore, the same orbitals can be used as start orbitals for, for example, a CI calculation of both a singlet and a triplet state. Furthermore, the orbitals obtained in an average-of-configuration approach will have the proper degeneracy. For example, a traditional "one electron in one orbital" open-shell approach will for boron treat one of the $p$ orbitals as half occupied and the two others as empty, hence the converged $p$ orbitals obtained will *not* be degenerate as the $p$ orbitals are treated differently. In an average-of-configuration approach a fractional occupation of 1/3 in each of the three $p$ orbitals could be specified, and the converged $p$ orbitals would, in fact, have the proper degeneracy.

We derive explicit expressions for the energy, energy gradient, and energy Hessian, and we also derive the expressions for the Fock matrix which we believe are optimal.

Finally, we apply our method in the calculation of the energy of CH, in a core-hole calculation on Cs, and in average-of-configuration orbitals as start orbitals for MCSCF calculations on Zn and LiI.

## 3.2 Theory

### 3.2.1 The Energy

We use the electronic Hamiltonian, Eq. (2.23), given in second quantization

$$\hat{H} = \sum_{pq} h_{pq} p^\dagger q + \frac{1}{2} \sum_{pqrs} g_{pq,rs} p^\dagger r^\dagger s q, \tag{3.1}$$

where $p^\dagger$ and $q$ are the electron creation and annihilation operators, respectively. The expression we derive are valid for both relativistic and non-relativistic Hamiltonians.

We may classify the orbitals into three classes: the inactive orbitals (doubly occupied), the active orbitals (partly occupied) and the secondary (virtual) orbitals. We will use indices $pqrs\ldots$, $ijkl\ldots$, $uvxy\ldots$, and $abcd\ldots$ for general, inactive, active, and secondary orbitals, respectively. Each of the

orbitals are distributed into a number of shells. Each shell $S$ is characterized by having $N_S$ electrons in $M_S$ orbitals. Inactive shells have $N_S = M_S$, active shells have $N_S < M_S$, and secondary shells have $N_S = 0$.

The average electronic energy is given by [2]

$$E_{\text{av}} = \sum_{k=1}^{K'} \frac{1}{K'} \left\langle 0_k \middle| \hat{H} \middle| 0_k \right\rangle = \sum_{k=1}^{K} \frac{1}{K} \langle D_k | \hat{H} | D_k \rangle \tag{3.2}$$

where $\{|0_k\rangle\}$ are the normalized linear combination of configurations which are solutions to the CI problem. The average energy is the trace of the CI Hamiltonian matrix and is thus invariant to rotations in configuration space, *i.e.* no $N$-electron basis is preferred for another and we might as well choose Slater determinants as our basis. To get the energy of the individual many-electron states present in the average-of-configuration, a CI calculation in the basis of the Slater determinants can be done. In most cases the dimension of the CI matrix is small (dimension $<$ 10–100), allowing it to be kept in memory and diagonalized completely [12].

A shell, $S$, have $N_S$ electrons distributed in $M_S$ spinors, giving a total of $K_S$ states:

$$K_S = \binom{M_S}{N_S}, \tag{3.3}$$

where $\binom{M_S}{N_S}$ is the usual binomial coefficient

$$\binom{M_S}{N_S} = \frac{M_S!}{N_S!\,(M_S - N_S)!} \tag{3.4}$$

The total number of states is given by

$$K = \prod_S K_S = \prod_S \binom{M_S}{N_S}. \tag{3.5}$$

For example, in one of the simplest cases: one electron in two orbitals:

$$\left.\begin{array}{l} N_1 = 1 \\ M_1 = 2 \end{array}\right\} \Rightarrow K = K_1 = 2 \tag{3.6}$$

The one electron part of the energy

$$E^{(1)} = \frac{1}{K} \sum_{k=1}^{K} \sum_{pq} h_{pq} \left\langle D_k \middle| p^\dagger q \middle| D_k \right\rangle. \tag{3.7}$$

can be reduced to

$$E^{(1)} = \sum_S f_S \sum_{p \in S} h_{pp}, \tag{3.8}$$

where we have used that $\left\langle D_k \middle| p^\dagger q \middle| D_k \right\rangle = \delta_{pq}$ if orbital $p$ is occupied in determinant $k$, and that only

$$\left[ \prod_{R \neq S} \binom{M_R}{N_R} \right] \cdot \binom{M_S - 1}{N_S - 1} = K \cdot f_S \tag{3.9}$$

of the original $K$ determinants have $p$ occupied, assuming $p \in S$. $f_S$ is the fractional occupation in shell $S$:

$$f_S = \frac{N_S}{M_S} \tag{3.10}$$

Analogous we derive the two-electron energy as

$$\begin{aligned} E^{(2)} = & \frac{1}{2} \sum_S \left( a_S \cdot f_S^2 \right) \sum_{p,q \in S} \left[ (pp|qq) - (pq|qp) \right] \\ & + \frac{1}{2} \sum_{S_1 \neq S_2} \left( f_{S_1} \cdot f_{S_2} \right) \sum_{\substack{q \in S_1 \\ q \in S_2}} \left[ (pp|qq) - (pq|qp) \right], \end{aligned} \tag{3.11}$$

where we have introduced the coupling coefficient

$$a_S = \begin{cases} \frac{M_S(N_S-1)}{N_S(M_S-1)} & \text{for } f_S \neq 0 \\ 1 & \text{for } f_S = 0 \end{cases}. \tag{3.12}$$

This allows us to write the total energy as

$$E_{\text{av}} = E^{(1)} + E^{(2)} = \sum_S f_S \left\{ \sum_{p \in S} \left( h_{pp} + \frac{1}{2} \sum_{S'} Q_{pp}^{S'} + \frac{1}{2}(a_S - 1) Q_{pp}^S \right) \right\}, \tag{3.13}$$

with

$$Q_{pq}^S = f_S \sum_{r \in S} (pq|rr) - (pr|rq). \tag{3.14}$$

### 3.2.2 Orbital Variations, the Gradient, and the Hessian

We wish to find stationary value conditions that define the optimal orbitals. We start by choosing an exponential unitary parameterization, where the trial function is

$$\left|\tilde{0}\right\rangle = \exp(-\hat{\kappa})\left|0\right\rangle, \tag{3.15}$$

with the orbital rotation operator given by

$$\hat{\kappa} = \sum_{rs} \kappa_{rs} r^{\dagger} s. \tag{3.16}$$

This corresponds to individual orbital transformations

$$\tilde{\phi}_p = \sum_q \phi_q \left[\exp(-\boldsymbol{\kappa})\right]_{pq}. \tag{3.17}$$

As the orbitals are generally complex we expand the energy in both $\boldsymbol{\kappa}$ and $\boldsymbol{\kappa}^*$:

$$E(\boldsymbol{\kappa}, \boldsymbol{\kappa}^*) = E^{[0]} + \boldsymbol{\lambda}^{\dagger}\mathbf{E}^{[1]} + \frac{1}{2}\boldsymbol{\lambda}^{\dagger}\mathbf{E}^{[2]}\boldsymbol{\lambda} + O(\boldsymbol{\lambda}^3), \tag{3.18}$$

where $\boldsymbol{\lambda} = [\boldsymbol{\kappa}, \boldsymbol{\kappa}^*]^T$ and

$$\begin{aligned} E^{[0]} &= E_{\mathrm{av}} = \sum_{k=1}^{K} \frac{1}{K} \langle D_k | \hat{H} | D_k \rangle \\ \mathbf{E}^{[1]} &= \begin{bmatrix} \frac{\partial E}{\partial \kappa^*} \\ \frac{\partial E}{\partial \kappa} \end{bmatrix}_{\boldsymbol{\lambda}=0} \\ \mathbf{E}^{[2]} &= \begin{bmatrix} \frac{\partial^2 E}{\partial \kappa^* \partial \kappa} & \frac{\partial^2 E}{\partial \kappa^* \partial \kappa^*} \\ \frac{\partial^2 E}{\partial \kappa \partial \kappa} & \frac{\partial^2 E}{\partial \kappa \partial \kappa^*} \end{bmatrix}_{\boldsymbol{\lambda}=0} \end{aligned} \tag{3.19}$$

$E^{[0]}$, $\mathbf{E}^{[1]}$ and $\mathbf{E}^{[2]}$ is the total energy, the gradient and the Hessian, respectively, at the expansion point. The expansion is constructed such that the Hessian is Hermitian and diagonally dominant. In the following a superscript $o$ and $o^*$ indicates differentiation with respect to $\kappa$ and $\kappa^*$, respectively. Straightforward differentiation yields the gradient

$$E_{pq}^{[1]o^*} = g_{pq}^{o^*} = \left.\frac{\partial E}{\partial \kappa_{pq}^*}\right|_{\boldsymbol{\kappa}=0} = -\sum_{k=1}^{K} \frac{1}{K} \left\langle D_k \middle| \left[q^{\dagger}p, \hat{H}\right] \middle| D_k \right\rangle = \left(E_{pq}^{[1]o}\right)^* \tag{3.20}$$

and the Hessian

$$\begin{aligned} E^{[2]o^*o}_{pq,rs} &= \left.\frac{\partial^2 E}{\partial\kappa^*_{pq}\kappa_{rs}}\right|_{\boldsymbol{\kappa}=0} \\ &= -\sum_{k=1}^{K}\frac{1}{K}\left\langle D_k\middle|\left[q^\dagger p,\left[r^\dagger s,\hat{H}\right]\right]\middle|D_k\right\rangle \\ &= \left(E^{[2]oo^*}_{pq,rs}\right)^*, \\ E^{[2]oo}_{pq,rs} &= \left.\frac{\partial^2 E}{\partial\kappa_{pq}\kappa_{rs}}\right|_{\boldsymbol{\kappa}=0} \\ &= \sum_{k=1}^{K}\frac{1}{K}\left\langle D_k\middle|\left[p^\dagger q,\left[r^\dagger s,\hat{H}\right]\right]\middle|D_k\right\rangle \\ &= \left(E^{[2]o^*o^*}_{pq,rs}\right)^*. \end{aligned} \tag{3.21}$$

Explicitly, we derive the gradient as

$$\begin{aligned} g^o_{pq} &= f_P\left\{h_{qp}+\sum_{S'}Q^{S'}_{qp}+(a_P-1)Q^P_{qp}\right\}-f_Q\left\{h_{pq}+\sum_{S'}Q^{S'}_{pq}+(a_Q-1)Q^Q_{pq}\right\} \\ &= F^P_{pq}-\left(F^Q_{qp}\right)^*, \end{aligned} \tag{3.22}$$

with $p\in P$ and $q\in Q$, and where we have introduced the generalized Fock matrix

$$F^Q_{qp} = f_Q\left\{h_{pq}+\sum_{S'}Q^{S'}_{pq}+(a_Q-1)Q^Q_{pq}\right\} \tag{3.23}$$

As the generalized Fock matrix is Hermitian[1] we immediately see that intra-shell rotations are zero. The generally non-zero elements are:

- inactive-secondary rotations:

$$g^o_{ia} = h_{ai}+\sum_{S'}Q^{S'}_{ai}, \tag{3.24}$$

- active-secondary rotations:

$$g^o_{ua} = f_U\left\{h_{au}+\sum_{S'}Q^{S'}_{au}+(a_U-1)Q^U_{au}\right\} \tag{3.25}$$

for $u\in U$,

[1]Note that this is only the case for Hartree-Fock or average-of-configuration Hartree-Fock. For MCSCF the generalized Fock matrix is, in general, non-Hermitian.

- inactive-active rotations:

$$g^o_{iu} = (1 - f_U)\left\{h_{ui} + \sum_{S'} Q^{S'}_{ui} + f_U \alpha_U Q^U_{ui}\right\} \tag{3.26}$$

  for $u \in U$, and

- inter-shell active-active rotations:

$$\begin{aligned} g^o_{uv} = (f_U - f_V)&\left\{h_{vu} + \sum_{S'} Q^{S'}_{vu}\right\} \\ &- (a_U - 1) f_U Q^U_{vu} - (a_V - 1) f_V Q^V_{vu}, \end{aligned} \tag{3.27}$$

  for $u \in U$ and $v \in V$,

where we have introduced

$$\alpha_S = \frac{1 - a_S}{1 - f_S}. \tag{3.28}$$

In the same manner the Hessian can be derived, but we will only consider the diagonal

$$\begin{aligned} E^{[2]o^*o}_{pq,pq} &= \left.\frac{\partial^2 E}{\partial \kappa^*_{pq} \kappa_{pq}}\right|_{\boldsymbol{\kappa}=0} = -\sum_{k=1}^{K} \frac{1}{K} \left\langle D_k \middle| \left[q^\dagger p, \left[p^\dagger q, \hat{H}\right]\right] \middle| D_k \right\rangle \\ &= (F^Q_{qq} - F^Q_{pp}) - (F^P_{pp} - F^P_{qq}) \\ &+ \{(pp|qq) - (pq|qp)\}(1 - \delta_{PQ}) \cdot \left(f^2_P (a_P - 1) + f^2_Q (a_Q - 1)\right). \end{aligned} \tag{3.29}$$

### 3.2.3 Eigenvalue Equation for the Orbitals

As in closed-shell and open-shell SCF theory it is possible to write the conditions for a stationary value of the energy as an eigenvalue problem, *i.e.*, it is possible to find a single Fock matrix that when diagonalized gives optimal orbitals for all shells. This Fock matrix must have off-diagonal matrix elements proportional to the orbital gradient [2]. The inactive-inactive, intra-shell active-active and secondary-secondary rotations are redundant, and these blocks of the Fock matrix can be chosen arbitrarily. But as the convergence depends critically on these elements, we have to choose these carefully.

Let us consider a very simple case, with one inactive shell and one secondary shell. The Newton step, $\boldsymbol{\lambda}$, in a second-order optimization is given as the solution to the linear equations

$$\mathbf{E}^{[2]}\boldsymbol{\lambda} = -\mathbf{E}^{[1]}. \tag{3.30}$$

If we neglect the off-diagonal elements of the Hessian, and if we furthermore neglect the two-electron terms in Eq. (3.29) the linear equations assume the following simple form in our simple case:

$$\begin{bmatrix} F_{aa} - F_{ii} & 0 \\ 0 & F^*_{aa} - F^*_{ii} \end{bmatrix} \cdot \begin{bmatrix} \kappa_{ia} \\ \kappa^*_{ia} \end{bmatrix} = - \begin{bmatrix} g^*_{ia} \\ g_{ia} \end{bmatrix} \tag{3.31}$$

The solution is

$$\begin{aligned} \kappa_{ia} &= -\frac{g^*_{ia}}{F_{aa} - F_{ii}} \\ \kappa^*_{ia} &= -\frac{g_{ia}}{F^*_{aa} - F^*_{ii}} \\ &= -\frac{g_{ia}}{F_{aa} - F_{ii}} \end{aligned} \tag{3.32}$$

To first order the new orbitals are given by

$$\tilde{\varphi} = \varphi \exp(-\kappa) \approx \varphi(1 - \kappa) \tag{3.33}$$

or

$$\begin{aligned} \tilde{\varphi}_i &= \varphi_i - \kappa^*_{ia}\varphi_a \\ &= \varphi_i - \frac{g_{ia}}{F_{aa} - F_{ii}}\varphi_a \\ \tilde{\varphi}_a &= \varphi_a + \kappa_{ia}\varphi_i \\ &= \varphi_a + \frac{g^*_{ia}}{F_{aa} - F_{ii}}\varphi_i \end{aligned} \tag{3.34}$$

The Fock matrix that upon diagonalization gives optimal orbitals is given by

$$\begin{bmatrix} A & g_{ia} \\ g^*_{ia} & B \end{bmatrix}, \tag{3.35}$$

where $A$ and $B$ are some constants we want to determine. Diagonalization of this matrix gives eigenvalues

$$\lambda = \frac{A + B}{2} \pm \sqrt{\left(\frac{A - B}{2}\right)^2 - g_{ia}g^*_{ia}}, \tag{3.36}$$

*i.e.*,

$$\begin{aligned} \lambda_i &= A - \frac{g_{ia}g^*_{ia}}{A - B} \\ \lambda_a &= B + \frac{g_{ia}g^*_{ia}}{A - B} \end{aligned} \tag{3.37}$$

The new eigenvectors $\varphi^{k+1}$ as a function of the eigenvectors from the previous iteration are given by (the square root expanded to first order)

$$\begin{aligned} \tilde{\varphi}_i &= \varphi_i - \frac{g_{ia}^*}{A-B}\varphi_a, \\ \tilde{\varphi} &= \varphi_a + \frac{g_{ia}}{A-B}\varphi_i. \end{aligned} \tag{3.38}$$

From this we see that we have to choose the diagonal as the generalized Fock matrix, *i.e.*,

$$\begin{aligned} A &= F_{ii}, \\ B &= F_{aa} \end{aligned} \tag{3.39}$$

Explicitly, we define the Fock matrix by

$$\begin{aligned} \mathbb{F}_{ij} &= F_{ij}^I = h_{ij} + \sum_{S'} Q_{ij}^{S'}, \\ \mathbb{F}_{iu} &= F_{iu}^I + \alpha_U f_U Q_{iu}^U, \qquad \text{for } u \in U, \\ \mathbb{F}_{ia} &= F_{ia}^I, \\ \mathbb{F}_{uv} &= \begin{cases} F_{uv}^I + (a_U - 1)Q_{uv}^U & \text{for } u,v \in U \\ F_{uv}^I + \frac{a_U - 1}{f_U - f_V}Q_{uv}^U + \frac{a_V - 1}{f_V - f_U}Q_{uv}^V & \text{for } u \in U,\ v \in V, \text{ and } f_U \neq f_V \\ (a_U - 1)Q_{uv}^U + (a_V - 1)Q_{uv}^V & \text{else} \end{cases}, \\ \mathbb{F}_{ua} &= F_{ua}^I + (a_U - 1)Q_{ua}^U, \qquad \text{for } u \in U, \\ \mathbb{F}_{ab} &= F_{ab}^I. \end{aligned} \tag{3.40}$$

Note that elements corresponding to non-redundant rotations are proportional to the gradient. The rest of the elements are chosen such that the differences between these resembles the diagonal part of the Hessian.

There are two different ways to construct this matrix given the matrices $\mathbf{h}$ and $\mathbf{Q}^S$ in MO basis. The simplest is just to calculate the various matrices in MO basis, and use Eq. (3.40) for distributing elements into $\mathbb{F}$. However, for convergence-acceleration schemes like DIIS [13,14] it is essential that the Fock matrix is in a fixed MO basis. The construction of the Fock matrix in a fixed MO-basis can be achieved by using the normalized density matrices as projection operators, *i.e.* the projection operator $P^S$ defined by $P^S = \frac{1}{f_S}D^S$ (for $f_S \neq 0$), where $D^S$ is the density matrix for shell $S$. In the current MO basis the projection operator is just a matrix with 1's in the diagonal for shell $S$. The projection operators can be used for selecting specific blocks of matrix. For example, if $\mathbf{D}^I$ and $\mathbf{D}^U$ are the inactive and active density

matrices, then $\frac{1}{f_I}\mathbf{D}^{I\dagger}\mathbf{A}\mathbf{D}^{U}\frac{1}{f_U} = \mathbf{P}^{I\dagger}\mathbf{A}\mathbf{P}^{U}$ will give the inactive-active block of the matrix $\mathbf{A}$. The Fock matrix, Eq. (3.40), can now be constructed as

$$\mathbb{F} = \mathbf{h} + \sum_{S'} \mathbf{Q}^{S'} + \mathbf{L} + \mathbf{L}^{\dagger} \tag{3.41}$$

with $\mathbf{L}$ is given by

$$\mathbf{L} = \sum_{U} \mathbf{P}^{U}\mathbf{Q}^{U}\left[\alpha_U f_U \mathbf{P}^{\mathrm{I}} + (a_U - 1)\left(\mathbf{P}^{\mathrm{U}} + \mathbf{P}^{\mathrm{Z}}\right)\right] + \sum_{V\neq U} \mathbf{L}^{U,V}_{\text{ac-ac}} \tag{3.42}$$

where $\mathbf{P}^{\mathrm{I}}$, $\mathbf{P}^{Z}$ and $\mathbf{P}^{U}$ are the projection operators onto the inactive, secondary and active orbitals, respectively. Note that the $\sum_U$ and $\sum_{U\neq V}$ are summations over active shells only. The active-active coupling operator, $\mathbf{L}^{U,V}_{\text{ac-ac}}$, is defined by

1. $f_U \neq f_U$

$$\mathbf{L}^{U,V}_{\text{ac-ac}} = \mathbf{P}^{U}\left[\frac{a_U - 1}{f_U - f_V}\cdot f_U \cdot \mathbf{Q}^{U} - \frac{a_V - 1}{f_U - f_V}\cdot f_V \cdot \mathbf{Q}^{V}\right]\mathbf{P}^{V} \tag{3.43}$$

2. $f_U = f_V < 1$

$$\begin{aligned}\mathbf{L}^{U,V}_{\text{ac-ac}} = \mathbf{P}^{U}\Bigg[&-\left(\mathbf{h} + \sum_{S'}\mathbf{Q}^{S'}\right)\\ &+ (a_U - 1)\cdot f_U \cdot \mathbf{Q}^{U} - (a_V - 1)\cdot f_V \cdot \mathbf{Q}^{V}\Bigg]\mathbf{P}^{V}\end{aligned} \tag{3.44}$$

3. $f_U = f_V = 1$ (inactive shell defined as an active shell)

$$\mathbf{L}^{U,V}_{\text{ac-ac}} = 0 \tag{3.45}$$

The formulas presented are valid for any Hamiltonian. Changing to a restricted basis, either non-relativistic spin-restricted or relativistic Kramers restricted, is done by replacing the spinor (spin-orbital) Fock matrix, Eq. (3.23), with a restricted Fock matrix, for example, a quaternion Fock matrix in the relativistic Kramers restricted case, as in our average-of-configuration open-shell implementation in the relativistic program package DIRAC [15].

### 3.2.4 The Fock Matrix in AO Basis

The Fock matrix, Eq. (3.40), can also be constructed from the projection operator matrices and one- and two-electron Fock matrices in the atomic orbital basis (AO basis). The contravariant projection operator, $\mathbf{P}^{ao}$, in AO basis and the covariant two-electron Fock matrices, $\mathbf{Q}^{ao}$, are given by

$$\begin{aligned} \mathbf{P}^{S,\mathrm{ao}} &= \mathbf{T}\mathbf{P}^{S,mo}\mathbf{T}^{\dagger} \Leftrightarrow \mathbf{P}^{S,\mathrm{mo}} = \mathbf{T}^{-1}\mathbf{P}^{\mathrm{ao}}\mathbf{T}^{\dagger -1} \\ \mathbf{Q}^{S,\mathrm{mo}} &= \mathbf{T}^{\dagger}\mathbf{Q}^{S,\mathrm{ao}}\mathbf{T} \end{aligned} \tag{3.46}$$

where $\mathbf{T}$ is the AO–MO transformation. We are interested in products of the type

$$\begin{aligned} \mathbf{P}^{R,\mathrm{mo}}\mathbf{Q}^{S,\mathrm{mo}}\mathbf{P}^{T,\mathrm{mo}} &= \mathbf{T}^{-1}\mathbf{P}^{R,\mathrm{ao}}\mathbf{T}^{\dagger -1}\mathbf{T}^{\dagger}\mathbf{Q}^{S,\mathrm{ao}}\mathbf{T}\mathbf{T}^{-1}\mathbf{P}^{T,\mathrm{ao}}\mathbf{T}^{\dagger -1} \\ &= \mathbf{T}^{\dagger}\mathbf{S}^{\mathrm{ao}}\mathbf{P}^{R,\mathrm{ao}}\mathbf{Q}^{S,\mathrm{ao}}\mathbf{P}^{T,\mathrm{ao}}\mathbf{S}^{\mathrm{ao}}\mathbf{T} \\ &= \left(\mathbf{T}^{\dagger}\mathbf{S}^{\mathrm{ao}}\right)\mathbf{P}^{R,\mathrm{ao}}\mathbf{Q}^{S,\mathrm{ao}}\mathbf{P}^{T,\mathrm{ao}}\left(\mathbf{T}^{\dagger}\mathbf{S}^{\mathrm{ao}}\right)^{\dagger} \end{aligned} \tag{3.47}$$

where $\mathbf{S}^{\mathrm{ao}}$ is the overlap matrix in AO basis, and where we have used $\mathbf{T}^{\dagger}\mathbf{S}^{\mathrm{ao}}\mathbf{T} = \mathbf{S}^{\mathrm{mo}} \equiv \mathbf{1}$. Where $\mathbf{T}$ is a fixed AO–MO transformation the product $\mathbf{T}^{\dagger}\mathbf{S}^{\mathrm{ao}}$ can be calculated once and reused in every iteration.

The open-shell Fock matrix, Eq. (3.41), can be calculated from AO-basis Fock and density matrices as

$$\mathbb{F} = \mathbf{T}^{\dagger}\left(\mathbf{h}^{\mathrm{ao}} + \sum_{S'}\mathbf{Q}^{S'\mathrm{ao}}\right)\mathbf{T} + \mathbf{L} + \mathbf{L}^{\dagger}, \tag{3.48}$$

with

$$\begin{aligned} \mathbf{L} = &\sum_{U}\left(\mathbf{T}^{\dagger}\mathbf{S}^{\mathrm{ao}}\right)\mathbf{P}^{U,ao}\left[\alpha_U f_U \mathbf{P}^{I} + (a_U - 1)\left(\mathbf{P}^{U} + \mathbf{P}^{Z}\right)\right]\left(\mathbf{T}^{\dagger}\mathbf{S}^{\mathrm{ao}}\right)^{\dagger} \\ &+ \sum_{U\neq V}\mathbf{L}^{U,V}_{\text{ac-ac}}. \end{aligned} \tag{3.49}$$

The active-active coupling operator, $\mathbf{L}^{U,V}_{\text{ac-ac}}$ is calculated analogous to Eqs. (3.43) – (3.45) with $\mathbf{P}^{U}$ and $\mathbf{P}^{V}$ replaced with $\left(\mathbf{T}^{\dagger}\mathbf{S}^{\mathrm{ao}}\right)\mathbf{P}^{U,\mathrm{ao}}$ and $\mathbf{P}^{V,\mathrm{ao}}\left(\mathbf{T}^{\dagger}\mathbf{S}^{\mathrm{ao}}\right)^{\dagger}$, respectively.

### 3.2.5 Open-shell and DIIS

In the convergence acceleration scheme DIIS [13, 14] an extrapolated Fock matrix, $\mathbf{F}^{\mathrm{ex}(n)}$ is formed as linear combinations of Fock matrices

$$\mathbf{F}^{\mathrm{ex}(n)} = \sum_{i\leq n} c_i \mathbf{F}_i. \tag{3.50}$$

The DIIS-coefficients, $c_i$, are found from solution of a linear equation [13, 14] or an eigenvalue problem [16]. For closed shell Hartree-Fock the linear combination, Eq. (3.50), can be formed in either AO- or MO-basis, since

$$\begin{aligned}
\mathbf{F}^{\mathrm{ex}(n)} &= \sum_{i\leq n} c_i \mathbf{F}^{I,i} && (3.51)\\
&= \sum_{i\leq n} c_i \mathbf{T}_i^\dagger \mathbf{F}^{I,i,ao} \mathbf{T}_i && (3.52)\\
&= \sum_{i\leq n} c_i \mathbf{T}^\dagger \mathbf{F}^{I,i,ao} \mathbf{T} && (3.53)\\
&= \mathbf{T}^\dagger \left( \sum_{i\leq n} c_i \mathbf{F}^{I,i,ao} \right) \mathbf{T} && (3.54)\\
&= \mathbf{T}^\dagger \left( \mathbf{h}^{\mathrm{ao}} + \sum_{i\leq n} c_i \mathbf{Q}^{I,i,ao} \right) \mathbf{T} && (3.55)
\end{aligned}$$

where $\mathbf{T}$ is the fixed AO–MO transformation matrix and we have used that the DIIS coefficients are normalized to 1: $\sum_{i\leq n} c_i = 1$. From this we see that it is equivalent to form the linear combination in either the fixed MO-basis, Eq. (3.51), or in AO-basis, Eq. (3.54) or (3.55).

In the case of open shells, we diagonalize the Fock matrix $\mathbb{F}$ given in Eq. (3.40) or Eq. (3.41). Note that $\mathbb{F}$ is only defined in MO basis — it does not exist in AO-basis as the closed-shell Fock matrix does. It is *not* valid to calculate the DIIS linear combination of the two-electron Fock matrices, Eq. (3.55):

$$\mathbf{Q}^{S,ex(n)} = \sum_{i\leq n} c_i \mathbf{Q}^{S,i}, \qquad (3.56)$$

and then construct the Fock matrix, $\mathbb{F}$, from these. The reason is that the definition of the active orbitals changes from iteration to iteration. The two-electron Fock matrix, $\mathbf{Q}^{S,i}$, from iteration $i$, is calculated using the density matrix, $\mathbf{D}^{S,i}$, from iteration $i$. But we calculate $\mathbb{F}$ (Eq. (3.41)) with the projection operators (*i.e.*, the density matrices) from iteration $n$. Hence, we use one definition of the active orbitals to calculate the two-electron Fock matrices, $\mathbf{Q}^{S,i}$, and *another* definition for the calculation of the Fock matrix, $\mathbb{F}$. This is inconsistent and convergence slowdown compared to the consistent approach has been observed! It is essential to form the DIIS linear combination is the fixed MO-basis. The diagonalization part of the SCF procedure is: Calculate $\mathbb{F}$ in a *fixed* MO-basis using Eq. (3.41); calculate the DIIS coefficients; form the DIIS linear combination of the MO Fock matrices from

this and the previous iterations; diagonalize the extrapolated Fock matrix to obtain new coefficients; and finally back-transform these to the current MO basis.

At least one implementation of open-shell DIIS uses the inconsistent sum of AO Fock matrices (Eq. (3.51)) instead of the correct (and consistent) summation of MO Fock matrices. Changing their implementation would give considerably gain in convergence.

## 3.3 Applications

We present calculations performed with the relativistic program package DIRAC [15]:

- a non-relativistic open shell calculation on CH, to demonstrate that orbital degeneracies are destroyed with conventional open-shell procedures,
- and a core-hole calculation on Cesium to demonstrate the use of several open shells.
- a MCSCF calculation on Zinc where we demonstrate the use of average-of-configuration orbitals as start orbitals for electron correlation methods.

### Open-shell Calculation on CH

This is a case where the average-of-configuration open-shell procedure has some advantages over other open-shell procedures. Carbon has two electrons in the $p$-orbitals. The $p_z$ orbital will participate in the bond to the hydrogen atom assuming that the molecular bond is along the $z$-axis. The last electron can either be in the $p_x$ orbital or the $p_y$ orbital. Three different open-shell calculations are possible:

1. 1 electron in the $p_x$ orbital (1 electron in 2 spinors)
2. 1 electron in the $p_y$ orbital (1 electron in 2 spinors)
3. 1 electron in the $p_x$ and $p_y$ orbitals (1 electron in 4 spinors)

Due to spatial symmetry the $p_x$ and $p_y$ orbitals must be degenerate. Calculation 1 and 2 above will destroy this degeneration since we treat the two $p$ orbitals differently: one is occupied and the other is empty, and vice versa. In the average-of-configuration calculation (no. 3) both $p$ orbitals are

Table 3.1: Energies and properties for CH in different open-shell calculations. The basis set is *aug-cc-pVDZ* basis set, and the bond length is $r_{\mathrm{CH}} = 2.014$ Å.

| Property/Calculation | 1 electron in 2 $p_x$ spinors | 1 electron in 2 $p_y$ spinors | 1 electron in 4 $p$ spinors |
|---|---|---|---|
| Total energy | −38.143 846 617 au | −38.143 846 617 au | −38.143 804 462 au |
| Dipole moment | −10.357 118 au | −10.357 118 au | −10.357 288 au |
| Electric field gradient | | | |
| $q^{\mathrm{C}}_{xx}$ | 1.107 696 au | −0.957 941 au | 0.074 778 au |
| $q^{\mathrm{C}}_{yy}$ | −0.957 941 au | 1.107 696 au | 0.074 778 au |
| $q^{\mathrm{C}}_{zz}$ | −0.149 755 au | −0.149 755 au | −0.149 557 au |
| $q^{\mathrm{H}}_{xx}$ | 0.008 052 au | 0.002 863 au | 0.005 458 au |
| $q^{\mathrm{H}}_{yy}$ | 0.002 863 au | 0.008 052 au | 0.005 458 au |
| $q^{\mathrm{H}}_{zz}$ | −0.010 916 au | −0.010 916 au | −0.010 916 au |

Table 3.2: Shell specification for the ground state of Cs

| Shell | #electrons | # $E_{1/2g}$ spinors | # $E_{1/2u}$ spinors | $f$ | $a$ | $\alpha$ |
|---|---|---|---|---|---|---|
| Closed shell | 54 | 30 | 24 | 1 | 1 | 0 |
| Open shell 1 ($6s^1_{1/2}$) | 1 | 2 | | $\frac{1}{2}$ | 0 | 2 |

treated similarly making them degenerate. Properties are, of course, also different for the 3 calculations as seen in Table 3.1. Calculation 1 and 2 yield the same energy and have related properties due to the rotational symmetry, whereas calculation 3 have different properties. The differences are not large for energies and dipole moments, but for the electric field gradients the difference is huge. By imposing the physically incorrect shell structure in calculation 1 and 2 we have, in effect, broken symmetry. Note that calculation 3 have the correct symmetry properties for the EFG tensor, and that $q^{\mathrm{Calc\ 1}}_{xx} \approx \frac{q^{\mathrm{Calc\ 1}}_{xx} + q^{\mathrm{Calc\ 2}}_{xx}}{2}$. In conclusion, the open shell should contain all symmetry related and degenerate orbitals otherwise wrong result may occur.

Table 3.3: Shell specification for the $4d_{5/2}$ core hole state of Cs

| Shell | #electrons | # $E_{1/2g}$ spinors | # $E_{1/2u}$ spinors | $f$ | $a$ | $\alpha$ |
|---|---|---|---|---|---|---|
| Closed shell | 46 | 22 | 24 | 1 | 1 | 0 |
| Open shell 1 ($4d^5_{3/2}$) | 5 | 6 | | $\frac{9}{10}$ | $\frac{80}{81}$ | $\frac{10}{81}$ |
| Open shell 2 ($5s^2_{1/2}$) | 2 | 2 | | 1 | 1 | 0 |
| Open shell 3 ($6s^1_{1/2}$) | 1 | 2 | | $\frac{1}{2}$ | 0 | 2 |

Table 3.4: Relativistic and non-relativistic core hole ionization energies for Cesium

| State | Energy/Hartrees | Ionization energy/Hartrees | |
|---|---|---|---|
| | | Koopmans | ΔSCF |
| Relativistic calculation | | | |
| Ground state | -7,786.7535 | | |
| $4d_{5/2}$ hole | -7,783.7447 | 3.3025 | 3.0088 |
| $4d_{3/2}$ hole | -7,783.6594 | 3.2138 | 3.0941 |
| Non-relativistic calculation | | | |
| Ground state | -7,553.8212 | | |
| $4d$ hole | -7,550.6490 | 3.3796 | 3.1722 |

### $4d$ Core-hole Calculations on Cesium

As mentioned in the introduction the average-of-configuration procedure can also be used to do SCF calculations on core-hole states. Cesium has the following electron configuration

$$1s^2 2s^2 2p^6 3s^2 3p^6 3d^{10} 4s^2 4p^6 4d^{10} 5s^2 5p^6 6s^1 \tag{3.57}$$

In the program package DIRAC [15] only symmetry in $D_{2h}$ and subgroups are used. For the $D_{2h}$ double group we only have to specify whether orbital is gerade (symmetry $E_{1/2g}$) or ungerade (symmetry $E_{1/2u}$). For Cesium we have $s$ and $d$ as gerade and $p$ as ungerade. The specification of closed and open shells for the ground state and the $4d_{5/2}$ core hole state is shown in Table 3.2 and 3.3, respectively. The specification for the $4d_{3/2}$ core hole is analogous to the $4d_{5/2}$ core hole.

With the 30s25p17d Cs basis set [17] we get the relative energies shown in Table 3.4. In the table the absolute energy of the ground states and $4d$ core-hole states are shown as well as ionization energies: the ionization energy from Koopmaan's Theorem (the orbital eigenvalue from the ground state calculation) and the ionization energy as an $\Delta$SCF value: $\Delta\text{SCF} = E(\text{core hole}) - E(\text{ground state})$. For further comparison also the non-relativistic results are shown in the table. We will not discuss the results as we have not been able to find any experimental values and as this is just an demonstration of a convenient way to obtain relaxed core-hole orbitals which can be used in correlated methods, such as CI or MCSCF. Note that the relaxation which is included in average-of-configuration $\Delta SCF$ value but not in the Koopmaan's Theorem value constitutes $\approx 10\%$ of core-hole ionization energy and can therefore, in general, not be neglected.

## 3.3.1 Average-of-configuration Orbitals as Start Orbitals for MCSCF

Finally, we demonstrate the use of average-of-configuration orbitals as start orbitals for MCSCF.

An often encountered problem using Hartree-Fock orbitals as start orbitals for MCSCF calculations is that the lowest virtuals are diffuse orbitals with eigenvalues close to zero. These orbitals bear very little resemblance with the converged orbitals, and very slow convergence will often be encountered. An often used solution is to use the virtual orbitals that diagonalize the one-electron Fock matrix (so-called $h_1$-virtuals) or the core Fock matrix ($\mathbf{h}+\mathbf{Q}^C$; so-called $F^C$ virtuals) [18], as the correlating orbitals will be shifted

down in energy whereas the diffuse virtuals will not be shifted. The problem associated with this procedure is that core-correlating functions will be shifted most downwards, and consequently put in the active space instead of the valence-correlating orbitals we are after. As the correlation energy from correlating the core is larger than from correlating the valence they will not be shifted out of the active space during the MCSCF iterations. This can often be a problem with calculations on heavy atoms where large uncontracted basis set are often used.

The best start orbitals are probably MP2 natural orbitals. MP2 natural orbitals sorted after occupation will almost always ensure that the correct correlating orbitals are put in the active space. The only problem associated with this procedure is that MP2 is a $n^5$ method, and may be time-consuming for extremely large basis sets in relativistic calculations.

As we will demonstrate with a few examples the average-of-configuration orbital can also be used as an economical alternative to MP2 natural orbitals or if MP2 natural orbitals are not available[2].

The first example is the LiI calculations presented in Sec. 6.2. The basis set is the *Sadlej* polarized basis set [19–21] for both Li and I, with an inactive space of 25 orbitals and 8 active orbitals (the iodine $5p$ orbitals, the lithium $2s$ orbitals, and the correlating iodine $5d$ orbitals). Three different options for start orbitals were used: (i) canonical Hartree-Fock orbitals, (ii) $h_1$-virtuals, (iii) average-of-configuration orbitals with three shells: (1) 25 orbitals with occupation 2, (2) 8 orbitals with occupation 6/24, and (3) the rest with zero occupation, and (iv) MP2 natural orbitals. The convergence (the norm of the gradient as a function of macro iteration number) is given in Table 3.5 along with the final energy. The MCSCF natural orbital occupation numbers and the character of the correlating orbitals are given in Table 3.6. It is fairly obvious that with $h_1$-virtuals the calculation converge towards the "wrong" state. The character of the orbitals is not clear, but it appears to be $3d$ and $4d$ orbitals. The MP2 natural orbitals are better than the average-of-configuration orbitals which takes six extra macro iterations to converge.

The second example is the Zn calculations presented in Sec. 6.1 where the basis set can be found. The inactive space consists of 15 orbitals; the active space of 3 orbitals (the $4s$ and the $4p$ orbitals). Again, we give the convergence and final energy (see Table 3.7) and the MCSCF natural occupation numbers along with the character of the correlating orbitals (see

[2]MP2 natural orbitals is currently not available as start orbitals for MCSCF calculations in DIRAC, although work is in progress to implement the necesary relaxed density matrix. When finished it would be trivial to write code for the diagonalization of this in order to obtain the transformation matrix for the transformation of the Hartree-Fock orbitals to the MP2 natural orbitals.

Table 3.5: Convergence (the norm of the gradient) and the final energy for MCSCF calculations on LiI with different start orbitals. Macro it. denotes the macro iteration number in the iterative MCSCF procedure. The norm of the wave function gradient is given for each iteration for all four calculations with different start orbitals.

| Macro it. | Norm of gradient | | | |
|---|---|---|---|---|
| | canonical HF | $h_1$-virtuals | ave HF | MP2 NO |
| 1 | 0.00192366 | 0.00137246 | 0.51395088 | 0.04680032 |
| 2 | 0.04193461 | 0.22562982 | 0.11452665 | 0.00648735 |
| 3 | 0.11413820 | 0.26825093 | 0.05945663 | 0.00007483 |
| 4 | 0.05511344 | 0.18992990 | 0.02350915 | 0.00000584 |
| 5 | 0.05856350 | 0.33028791 | 0.00264172 | |
| 6 | 0.05247107 | 0.55865076 | 0.02934558 | |
| 7 | 0.07454871 | 0.52323206 | 0.03804216 | |
| 8 | 0.01525625 | 0.26976738 | 0.00368056 | |
| 9 | 0.03836895 | 0.11399215 | 0.00009210 | |
| 10 | 0.08173234 | 0.07051797 | 0.00000333 | |
| 11 | 0.16621349 | 0.10944294 | | |
| 12 | 0.07260808 | 0.00646455 | | |
| 13 | 0.05070718 | 0.02465693 | | |
| 14 | 0.01491729 | 0.00070628 | | |
| 15 | 0.01185715 | 0.00006390 | | |
| 16 | 0.01107484 | 0.00000330 | | |
| 17 | 0.00900968 | | | |
| 18 | 0.00016823 | | | |
| 19 | 0.00000744 | | | |
| | Final energy | | | |
| | −6925.39341064 | −6925.34546245 | −6925.39341063 | −6925.39341063 |

Table 3.6: MCSCF and MP2 natural orbital occupation numbers and character of correlating orbitals for LiI, given in parentheses after the occupation number.

| Orbital no. | Start orbitals | | | | | | | |
|---|---|---|---|---|---|---|---|---|
| | canonical HF | | $h_1$-virtuals | | ave HF | | MP2 NO | |
| 1 | 1.95769 | $(5p)$ | 1.99962 | ? | 1.95769 | $(5p)$ | 1.95769 | $(5p)$ |
| 2 | 1.95769 | $(5p)$ | 1.99962 | ? | 1.95769 | $(5p)$ | 1.95769 | $(5p)$ |
| 3 | 1.95838 | $(5p)$ | 1.99960 | ? | 1.95838 | $(5p)$ | 1.95838 | $(5p)$ |
| 4 | 0.02213 | $(5d)$ | 0.00039 | ? | 0.02213 | $(5d)$ | 0.02213 | $(5d)$ |
| 5 | 0.02213 | $(5d)$ | 0.00037 | ? | 0.02213 | $(5d)$ | 0.02213 | $(5d)$ |
| 6 | 0.02196 | $(5d)$ | 0.00037 | ? | 0.02196 | $(5d)$ | 0.02196 | $(5d)$ |
| 7 | 0.01962 | $(5d)$ | 0.00001 | ? | 0.01962 | $(5d)$ | 0.01962 | $(5d)$ |
| 8 | 0.01962 | $(5d)$ | 0.00001 | ? | 0.01962 | $(5d)$ | 0.01962 | $(5d)$ |
| 9 | 0.00704 | $(6p)$ | 0.00001 | ? | 0.00704 | $(6p)$ | 0.00704 | $(6p)$ |
| 10 | 0.00704 | $(6p)$ | 0.00000 | ? | 0.00704 | $(6p)$ | 0.00704 | $(6p)$ |
| 11 | 0.00672 | $(6p)$ | 0.00000 | ? | 0.00672 | $(6p)$ | 0.00672 | $(6p)$ |

Table 3.8). We have also used $F^C$-virtuals. Again, the $h_1$-virtual calculation collapses, and this time the $1s$ orbital are correlated! The other calculations converge, although with canonical HF orbitals the convergence is slow compared to average-of-configuration and MP2 natural orbitals. The $F^C$-virtuals are clearly better than $h_1$-virtuals, and even better than the average-of-configuration orbitals.

## 3.4 Conclusion

We have presented a one-Fock matrix theory for average-of-configuration calculations. Although our formulae were derived independently they turned out identical to the formulae of McWeeny [2]. The formulas derived are valid for any number of open shells with arbitrary symmetry, and the orbitals obtained can be start orbitals for correlating methods, such as CI or MCSCF. We have also demonstrated the usability of the method in normal open-shell SCF calculations; in fact, averaging is required for some open-shell calculations such as on CH. We have also demonstrated that the method can be used for obtaining core-hole orbitals and that they can successfully be used as start orbitals for MCSCF calculations when MP2 natural orbitals are not available. Furthermore, we have discussed some important issues of

Table 3.7: Convergence (the norm of the gradient) and the final energy for MCSCF calculations on Zn with different start orbitals. Macro it. denotes the macro iteration number in the iterative MCSCF procedure. The norm of the wave function gradient is given for each iteration for all four calculations with different start orbitals.

| Macro | Norm of gradient | | | | |
|---|---|---|---|---|---|
| it. | can. HF | $h_1$-virt. | $F^C$-virt. | ave. HF | MP2 NO |
| 1 | 0.011234 | 0.000034 | 0.014531 | 0.108854 | 0.011412 |
| 2 | 0.015900 | 0.141201 | 0.003568 | 0.046614 | 0.001198 |
| 3 | 0.031116 | 0.006870 | 0.000039 | 0.003698 | 0.000004 |
| 4 | 0.001527 | 0.031431 | 0.000002 | 0.000233 | |
| 5 | 0.000033 | 0.137820 | | 0.000001 | |
| 6 | 0.000003 | 0.608407 | | | |
| 7 | | 0.056468 | | | |
| 8 | | 0.011593 | | | |
| 9 | | 0.000102 | | | |
| 10 | | 0.000004 | | | |
| | | Final energy | | | |
| | −1777.872242 | −1777.861071 | −1777.872242 | −1777.872242 | −1777.872242 |

Table 3.8: MCSCF orbital occupation numbers and character of correlating orbitals for Zn, given in parentheses after the occupation number.

| Orbital no. | Start orbitals | | | | | | | | | |
|---|---|---|---|---|---|---|---|---|---|---|
| | can. HF | | $h_1$-virt. | | $F^C$-virt. | | ave HF | | MP2 NO | |
| 1 | 1.8781 | $(4s)$ | 1.9999 | $(1s)$ | 1.8781 | $(4s)$ | 1.8781 | $(4s)$ | 1.8781 | $(4s)$ |
| 2 | 0.0406 | $(4p)$ | 0.0000 | $(p)$ | 0.0406 | $(4p)$ | 0.0406 | $(4p)$ | 0.0406 | $(4p)$ |
| 3 | 0.0406 | $(4p)$ | 0.0000 | $(p)$ | 0.0406 | $(4p)$ | 0.0406 | $(4p)$ | 0.0406 | $(4p)$ |
| 4 | 0.0406 | $(4p)$ | 0.0000 | $(p)$ | 0.0406 | $(4p)$ | 0.0406 | $(4p)$ | 0.0406 | $(4p)$ |

open-shell DIIS.

# Bibliography

[1] C. C. J. Roothaan, Rev. Mod. Phys. **32**, 179 (1960).

[2] R. McWeeny, Mol. Phys. **28**, 1273 (1974).

[3] M. F. Guest and V. R. Saunders, Mol. Phys. **28**, 819 (1974).

[4] K. Fægri and R. Manne, Mol. Phys. **31**, 1037 (1976).

[5] S. Huzinaga, J. Chem. Phys. **51**, 3971 (1969).

[6] H. Hsu, E. R. Davidson, and R. M. Pitzer, J. Chem. Phys. **65**, 609 (1976).

[7] E. R. Davidson, Chem. Phys. Lett. **21**, 565 (1973).

[8] J. S. Binkley, J. A. Pople, and P. A. Dobosh, J. Chem. Phys. **28**, 1423 (1974).

[9] C. Kollmar, Int. J. Quant. Chem. **62**, 618 (1997).

[10] H. J. Aa. Jensen, H. Ågren, and J. Olsen, in *Modern Techniques in Computional Chemistry 1990*, edited by E. Clementi (Escom, Leiden, 1990).

[11] O. Visser, L. Visscher, and P. J. C. Aerts, in *The effects of relativity in atoms, molecules and the solid state*, edited by I. P. Grant, B. Gyorffy, and S. Wilson (Plenum, New York, 1991).

[12] O. Visser, L. Visscher, P. J. C. Aerts, and W. C. Nieuwpoort, J. Chem. Phys. **96**, 2910 (1992).

[13] P. Pulay, Chem. Phys. Lett. **73**, 393 (1980).

[14] P. Pulay, J. Comput. Chem. **3**, 556 (1982).

[15] T. Saue, T. Enevoldsen, T. Helgaker, H. J. A. Jensen, J. Laerdahl, K. Ruud, J. Thyssen, and L. Visscher, *"DIRAC, a relativistic ab initio electronic structure program , Release 3.1 (1998)"*.

[16] H. Sellers, Int. J. Quant. Chem. **45**, 31 (1993).

[17] S. Huzinaga and M. Klobukowski, Chem. Phys. Lett. **212**, 260 (1993).

[18] C. W. Bauschlicher, J. Chem. Phys. **72**, 880 (1980).

[19] A. J. Sadlej, Coll. Czech. Chem. Commun. **53**, 1995 (1988).

[20] A. J. Sadlej, Theo. Chim. Acta **79**, 123 (1991).

[21] A. J. Sadlej and M. Urban, J. Molec. Spec. **80**, 147 (1991).

# Chapter 4

# Relativistic Four-Component MCSCF Theory

In this chapter we review the formalism for the Kramers restricted relativistic four-component multi-configurational self-consistent-field method originally presented by Jensen *et al.* [1] and present an KR-MCSCF implementation based on the quaternion formalism by Saue and Jensen [2].

## 4.1 Introduction

We present the implementation of the KR-MCSCF method. The formalism and implementation have the following properties:

**Relativistic four-component** As we have established in Chapter 1 we need to account for relativistic effects in order to have a qualitatively correct description of compounds with heavy elements. Relativity is also needed for extremely precise calculations on compounds containing only light elements. Furthermore, a relativistic description may be preferred for description of magnetic properties. For many purposes it is preferable to use four-component methods instead of one- or two-component methods, as the four-component methods have a very simple formalism, where all the approximate one- and two-component operators — the Hamiltonian as well as property operators — have to be transformed in order to avoid picture-change effects [3].

**Kramers restriction** This is the relativistic analogue to the spin-restriction employed in most non-relativistic methods. We base the implementation of the Kramers restriction on the use of quaternions [2] and time-reversal symmetry adapted basis operators $\hat{X}^{\pm}$ [4].

**Second order restricted step optimization** The energy is expanded to second order, and the Newton-Raphson equations are solved until a stationary point has been reached. The second order expansion of the energy is only trusted with in a hyper-sphere and the Newton step is therefore restricted. With the use of the restricted step algorithm, in practice, sharp and well-controlled convergence is always obtained.

**Direct algorithm** The Newton-Raphson equations are solved in an iterative direct manner. This is essential for large-scale MCSCF calculations where the Hessian is too large to be stored or inverted. The most CPU and memory demanding step is the calculation of CI sigma vectors and the storage and calculation of molecular integrals.

The direct second order restricted step optimization is completely analogous to the non-relativistic MCSCF method in DALTON [5] developed by Jensen *et al.* [6].

## 4.2 Operators and Symmetry

The starting point is the second quantization relativistic four-component Dirac-Coulomb operator from Eq. (2.23):

$$\hat{H} = \sum_{pq} h_{pq} p^\dagger q + \frac{1}{2} \sum_{pqrs} g_{pq,rs} p^\dagger r^\dagger s q, \tag{4.1}$$

where the matrix elements are given by:

$$\begin{aligned} h_{pq} &= \left\langle p \middle| \hat{h}_D \middle| q \right\rangle, \\ g_{pq,rs} &= \langle pr | \hat{g}_{12} | qs \rangle, \end{aligned} \tag{4.2}$$

where $\hat{h}_D$ is the Dirac one-electron operator given in Eq. (2.6), and $\hat{g}_{12}$ is the Coulomb part of two-electron interaction operator, Eq. (2.12).

It is possible to build time-reversal symmetry explicitly into the formalism by changing to a Kramers basis [4]. A time invariant Hermitian or anti-Hermitian one-electron operator are purely expanded in Kramers single replacement operators $X^+_{pq}$ or $X^-_{pq}$, respectively [4]:

$$\begin{aligned} X^\pm_{pq} &= p^\dagger q \pm \bar{q}^\dagger \bar{p}, \\ X^\pm_{\bar{p}q} &= \bar{p}^\dagger q \mp \bar{q}^\dagger p, \\ X^\pm_{p\bar{q}} &= p^\dagger \bar{q} \mp q^\dagger \bar{p}. \end{aligned} \tag{4.3}$$

For example, the Hermitian Dirac one-electron Hamiltonian, Eq. (2.6), which is time-reversal invariant in the absence of magnetic interactions, is found to be

$$\hat{h}_D = \sum_{pq} \left[ h_{pq} X^+_{pq} + \frac{1}{2} \left( h_{\bar{p}q} X^+_{\bar{p}q} + h_{p\bar{q}} X^+_{p\bar{q}} \right) \right]. \tag{4.4}$$

For two-electron operators it is necessary to use Kramers double replacement operators, Eq. (2.38), and in the Kramers basis, $\{p\} \cup \{\bar{p}\}$, the Dirac-Coulomb Hamiltonian can be written as

$$\begin{aligned} \hat{H} = & \sum_{pq} \left[ h_{pq} \hat{X}^+_{pq} + \frac{1}{2} \left( h_{\bar{p}q} \hat{X}^+_{\bar{p}q} + h_{p\bar{q}} \hat{X}^+_{p\bar{q}} \right) \right] \\ & + \frac{1}{2} \sum_{pqrs} \left[ (pq|rs)\, \hat{x}^{++}_{pq,rs} + (\bar{p}qr,rs)\, \hat{x}^{++}_{\bar{p}q,rs} + (p\bar{q}|rs)\, \hat{x}^{++}_{p\bar{q}|rs} \right] \\ & + \frac{1}{4} \sum_{pqrs} (\bar{p}q|r\bar{s})\, \hat{x}^{++}_{\bar{p}q,r\bar{s}} + \frac{1}{8} \left[ (\bar{p}q|\bar{r}s)\, \hat{x}^{++}_{\bar{p}q,\bar{r}s} + (p\bar{q}|r\bar{s})\, \hat{x}^{++}_{p\bar{q},r\bar{s}} \right], \end{aligned} \tag{4.5}$$

where summations run over orbitals, and not spinors as in Eq. (4.1).

However, there is a downside to using Kramers single and double replacement operators; namely the algebraic manipulations to evaluate the single and double commutators present in the expressions for the electronic gradient and Hessian (*e.g.*, see, Section 3.2 in Ref. [7]). Instead, it is possible formulate a Kramers restricted method by using the quaternion formalism briefly mentioned in section 2.3 without ever introducing the $\hat{X}^{\pm}$ operators explicitly. We will, however, stick with the $\hat{X}^{\pm}$ operators, and introduce the quaternion formalism at a later point.

Time-reversal symmetry is also present in the structure of the matrices. For example, a Hermitian time-reversal invariant operator, $\mathbf{\Omega}$, has the following structure in a Kramers basis

$$\mathbf{\Omega} = \begin{pmatrix} \mathbf{A} & \mathbf{B} \\ -\mathbf{B}^* & \mathbf{A}^* \end{pmatrix}, \tag{4.6}$$

where $\mathbf{A}$ and $\mathbf{B}$ are Hermitian and anti-symmetric matrices, respectively. From Eq. (4.6) it is evident that some of the matrix elements are redundant. As we saw in Section 2.3 a suitable way of saving only the non-redundant elements is by introducing the quaternions, and defining

$${}^{Q}\Omega_{pq} \equiv \Omega_{pq} + \Omega_{p\bar{q}}\check{\jmath}. \tag{4.7}$$

## 4.3 Parameterization and Orbital Classes

The KR-MCSCF wave function in iteration $k$ is given by

$$\left|c^{(k)}\right\rangle = \sum_{\mu} c_{\mu}^{(k)} \left|\Phi_{\mu}\right\rangle , \tag{4.8}$$

where the sum is over all configurations included in the CI expansion. The configurations could be Slater determinants built from the molecular 4-component Kramers orbitals or they could be configuration state functions (CSFs) which are linear combinations of Slater determinants adapted to time-reversal symmetry and/or point group symmetry. It is preferable to use CSFs as the converged state will have a well-defined behavior under the time-reversal operation and under point group symmetry operations. The use of CSFs can also reduce the work needed to calculate CI sigma vectors and in some cases it can reduce the length of the expansion. This is most evident for non-relativistic or spin-free CI expansions where a spin adapted basis can be used as spin is a good quantum number. For relativistic CI expansions with an even number of electrons, it may be advantageous to form a CSF basis of plus and minus combinations of determinants (see, *e.g.*, Messiah [8]).

The orbital belongs to one of four classes: positron orbitals, inactive orbitals (doubly occupied in all determinants), active orbitals (partially occupied), and secondary orbitals (unoccupied orbitals). We treat the positron orbitals as secondary orbitals as suggested by Mittleman [9] and converge towards the desired electronic state by employing a mini-max principle [10], in which the energy is minimized with respect to electronic orbital rotations and maximized with respect to positronic orbital rotations. Note that the presented KR-MCSCF method is the most rigorous correlation method as we allow the positronic orbitals to relax, hence in each iteration the Mittleman projection operators onto the electronic states changes analogous to DHF. It is, of course, also possible to neglect the rotations of the positronic orbitals — the $e-p$ relaxation — as done in relativistic no-pair CI, MP2, and CC. However, the $e-p$ relaxation may be important for core operators, magnetic properties (spin-spin couplings [11]) or operators that depend critically on the small component density (parity violation). Unlike non-relativistic MCSCF optimizations where all orbital rotations become redundant in the limit of full CI, only the electronic orbital rotations become redundant in relativistic optimizations; positronic orbital rotations are still non-redundant.

The electronic classes (inactive, active, and secondary orbitals) are analogous to the corresponding classes found in non-relativistic MCSCF theory (see, *e.g.*, Jensen [6]).

The configuration basis functions ($|\Phi_\mu\rangle$) are defined by how the active electrons are distributed among the active orbitals. The most general is the *Generalized Active Space* expansion [12] where all possible electron distributions of the active electrons into the active orbitals, under occupation, Kramers symmetry, and double group symmetry restrictions, are considered. The active space is divided into $n$ active spaces, each having occupation constraints: a minimum and maximum number of electrons. An example of a GAS wave function is the "traditional" Restricted Active Space (RAS) [13] wave function where the active space is partitioned into three active spaces: RAS1, RAS2, and RAS3. For RAS1 and RAS3 both a minimum and a maximum number of electrons are given, where as the distribution in RAS2 is defined by conservation of the number of active electrons in the system. Another example is the Complete Active Space (CAS) wave function which is a GAS wave function with full CI in only one active space.

These different wave function types (GAS, RAS, and CAS) are completely analogous to the non-relativistic ones, except the the non-relativistic spin and single point group symmetry restrictions are replaced with Kramers symmetry and double group symmetry restrictions. For a graphic overview of the different wave functions see Figure 4.1.

The KR-MCSCF wave function is defined completely by the configuration coefficients $c_\mu^{(k)}$ and the occupied (inactive and active) orbitals. We choose a parameterization where the orbital variations are parameterized using an exponential unitary parameterization, $\exp(-\hat{\kappa})$, and the variations of configuration coefficients are parameterized using a correction vector, $\delta$, which is orthogonal to the current configuration vector $c^{(k)}$. This is analogous to the parameterization used in Ref. [14]. Thus, the parameterized KR-MCSCF wave function is:

$$\begin{aligned} |MC(\boldsymbol{\delta},\boldsymbol{\kappa})\rangle &= \exp\left(-\hat{\kappa}\right)|\delta\rangle \\ &= \exp\left(-\hat{\kappa}\right)\frac{\left|c^{(k)}\right\rangle + \mathcal{P}\,|\delta\rangle}{\sqrt{1+\langle\delta|\mathcal{P}|\delta\rangle}}. \end{aligned} \tag{4.9}$$

We have assumed that the reference configuration vector for iteration $k$ is normalized, *i.e.*,

$$\left\langle c^{(k)}\middle|c^{(k)}\right\rangle = \sum_\mu \left(c_\mu^{(k)}\right)^* c_\mu^{(k)} = 1. \tag{4.10}$$

The correction vector

$$|\delta\rangle = \sum_\mu \delta_\mu\,|\Phi_\mu\rangle \tag{4.11}$$

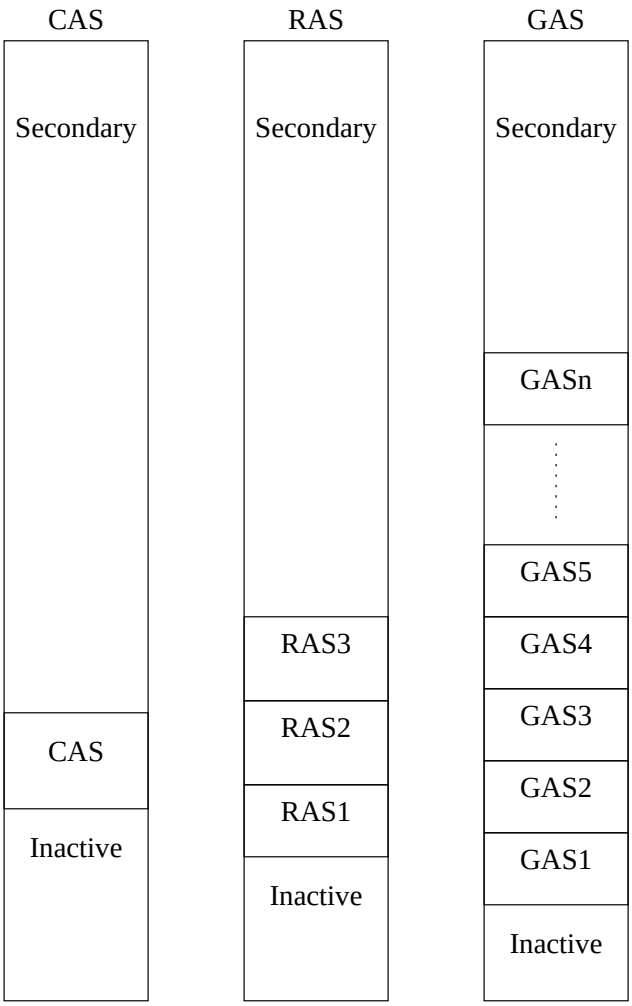


Figure 4.1: Overview of the division of orbital spaces for the complete active space (CAS), restricted active space (RAS), and the generalized active space (GAS) wave functions. The secondary space may also include the positronic orbitals.

is an arbitrary correction to the reference configuration vector, and the projection operator

$$\mathcal{P} = 1 - \left|c^{(k)}\right\rangle \left\langle c^{(k)}\right| \tag{4.12}$$

annihilates any $\left|c^{(k)}\right\rangle$ component from the correction vector. Note, that there is a redundancy in the configuration space as a correction vector $|\delta\rangle = a\left|c^{(k)}\right\rangle i, a \in \mathbf{C}$ would not change the wave function. This extra redundant parameter is related to the norm of the wave function and it can be used in the complex generalization of the norm extended optimization (NEO) algorithm [1].

The exponential unitary operator, $\exp(-\hat{\kappa})$, is the time-reversal invariant unitary operator [4]

$$\begin{aligned}\hat{\kappa} &= \sum_{rs}\left(\kappa_{rs}\hat{X}^{-}_{rs} + \frac{1}{2}\kappa_{r\bar{s}}\hat{X}^{-}_{r\bar{s}} + \frac{1}{2}\kappa_{\bar{r}s}\hat{X}^{-}_{\bar{r}s}\right)\\ &= \sum_{r<s}\left(\kappa_{rs}\hat{X}^{-}_{rs} + \kappa_{r\bar{s}}\hat{X}^{-}_{r\bar{s}} - \kappa^{*}_{rs}\hat{X}^{-}_{sr} - \kappa^{*}_{r\bar{s}}\hat{X}^{-}_{\bar{s}r}\right)\\ &+ \frac{1}{2}\sum_{r}\left(\kappa_{r\bar{r}}\hat{X}^{-}_{r\bar{r}} - \kappa^{*}_{r\bar{r}}\hat{X}^{-}_{\bar{r}r}\right).\end{aligned} \tag{4.13}$$

The variation of the complex parameters $\{\kappa_{rs}, \kappa^{*}_{rs}\}$ corresponds to all possible unitary orbital rotations as the $X^{-}_{pq}$ and $X^{-}_{qp}$ operators are generators of proper unitary rotations. As in non-relativistic theory this parameterization is chosen as it ensures that the orbitals are orthonormal and that the Kramers pairing is imposed in the variational space, allowing us to use unconstrained optimization techniques. Only non-redundant rotations, *i.e.* the rotations that does not change the energy, are included in the parameterization. Positronic–positronic, inactive–inactive, and secondary–secondary rotations are always redundant, since the energy is invariant with respect to these rotations as all their derivatives vanish. The active–active rotations are also redundant for CASSCF wave functions. For GASSCF wave functions the *intra*-shell active–active rotations are redundant, whereas the *inter*-shell active–active rotations are generally non-redundant depending on the actual specification of the calculation. It is important to include only non-redundant parameters as the Hessian otherwise will have zero eigenvalues, which may slow down convergence. For further discussions about redundant orbital rotations are how to identify them, see, *e.g.*, Jørgensen and Simons [14] or Shepard [15].

## 4.4 Second Order Expansion of the Energy

A second-order optimization is based on a second order Taylor expansion of the total energy. In relativistic theory the energy is a real function of *complex* variables, as opposed to non-relativistic theory where the energy is a real function of *real* variables. Hence our variation space is $\left[\frac{\partial}{\partial \mathbf{\Gamma}}, \frac{\partial}{\partial \mathbf{\Gamma}^*}\right]$ instead of $\left[\frac{\partial}{\partial \mathbf{\Gamma}} + \frac{\partial}{\partial \mathbf{\Gamma}^*}\right]$. $\frac{\partial}{\partial \mathbf{\Gamma}}$ and $\frac{\partial}{\partial \mathbf{\Gamma}^*}$ must be regarded as two *independent* variables. An alternative, but equivalent, parameterization is $\left[\Re(\frac{\partial}{\partial \mathbf{\Gamma}}), \Im(\frac{\partial}{\partial \mathbf{\Gamma}})\right]$. The parameter space $[\mathbf{\Gamma}, \mathbf{\Gamma}^*] = [\boldsymbol{\delta}, \boldsymbol{\kappa}, \boldsymbol{\delta}^*, \boldsymbol{\kappa}^*]$ consists of the configurational and orbital parameters. For some parameter point $\boldsymbol{\lambda} = [\mathbf{\Gamma}, \mathbf{\Gamma}^*] = [\boldsymbol{\delta}, \boldsymbol{\kappa}, \boldsymbol{\delta}^*, \boldsymbol{\kappa}^*]$ the energy can be written as

$$\begin{aligned} E(\boldsymbol{\lambda}) = E(\mathbf{\Gamma}, \mathbf{\Gamma}^*) &= \left\langle MC(\boldsymbol{\delta}, \boldsymbol{\kappa}) \middle| \hat{H} \middle| MC(\boldsymbol{\delta}, \boldsymbol{\kappa}) \right\rangle \\ &= \frac{\epsilon(\mathbf{\Gamma}, \mathbf{\Gamma}^*)}{S(\boldsymbol{\delta}, \boldsymbol{\delta}^*)} \end{aligned} \tag{4.14}$$

where the enumerator $\epsilon$ is given by

$$\begin{aligned} \epsilon(\boldsymbol{\delta}, \boldsymbol{\kappa}, \boldsymbol{\delta}^*, \boldsymbol{\kappa}^*) &= \left\langle c^{(k)} + \delta\mathcal{P} \middle| \exp(\hat{\kappa}) \hat{H} \exp\left(-\hat{\kappa}\right) \middle| c^{(k)} + \mathcal{P}\delta \right\rangle \\ &= \left\langle c^{(k)} + \delta\mathcal{P} \middle| \hat{H} + \left[\hat{\kappa}, \hat{H}\right] + \frac{1}{2}\left[\hat{\kappa}, \left[\hat{\kappa}, \hat{H}\right]\right] + \cdots \middle| c^{(k)} + \delta\mathcal{P} \right\rangle \end{aligned} \tag{4.15}$$

and the denominator by

$$\begin{aligned} S(\boldsymbol{\delta}, \boldsymbol{\delta}^*) &= \left\langle c^{(k)} + \delta\mathcal{P} \middle| \exp(\hat{\kappa}) \exp\left(-\hat{\kappa}\right) \middle| c^{(k)} + \mathcal{P}\delta \right\rangle \\ &= 1 + \langle \delta | \mathcal{P} | \delta \rangle . \end{aligned} \tag{4.16}$$

As the integrals in each iteration always are transformed to the current molecular orbitals the CEP is represented by the null vector $\boldsymbol{\lambda} = [\mathbf{0000}]^T$. The second order Taylor expansion of the energy in the independent variables $\delta$, $\delta^*$, $\kappa$, and $\kappa^*$ is given by

$$q(\boldsymbol{\lambda}) = E^{[0]} + \boldsymbol{\lambda}^\dagger \mathbf{E}^{[1]} + \boldsymbol{\lambda}^\dagger \mathbf{E}^{[2]} \boldsymbol{\lambda} \tag{4.17}$$

where $\boldsymbol{\lambda} = [\mathbf{\Gamma}, \mathbf{\Gamma}^*] = [\boldsymbol{\delta}, \boldsymbol{\kappa}, \boldsymbol{\delta}^*, \boldsymbol{\kappa}^*]$ is the step vector, $E^{[0]}$ is the total energy, $\mathbf{E}^{[1]}$ is the gradient, and $\mathbf{E}^{[2]}$ is the Hessian calculated at the current expansion

point

$$
\begin{aligned}
E^{[0]} &= \left\langle c^{(k)} \middle| \hat{H} \middle| c^{(k)} \right\rangle \\
\mathbf{E}^{[1]} &= \begin{bmatrix} \frac{\partial E}{\partial \Gamma^*} \\ \frac{\partial E}{\partial \Gamma} \end{bmatrix}_{\boldsymbol{\lambda}=\mathbf{0}} \\
\mathbf{E}^{[2]} &= \begin{bmatrix} \frac{\partial^2 E}{\partial \Gamma^* \partial \Gamma} & \frac{\partial^2 E}{\partial \Gamma^* \partial \Gamma^*} \\ \frac{\partial^2 E}{\partial \Gamma \partial \Gamma} & \frac{\partial^2 E}{\partial \Gamma \partial \Gamma^*} \end{bmatrix}_{\boldsymbol{\lambda}=\mathbf{0}}.
\end{aligned}
\tag{4.18}
$$

We use superscripts $o$, $o^*$, $c$, and $c^*$ for denoting which component of the gradient or Hessian we are evaluating; for example, $\mathbf{E}^{[1]o^*}$ denotes the first derivative of the energy with respect to $\boldsymbol{\kappa}$. Straightforward differentiation yields the gradient evaluated at $\boldsymbol{\lambda} = \mathbf{0}$

$$
\begin{aligned}
\mathbf{E}^{[1]c^*}_{\mu} &= \left.\frac{\partial E}{\partial \delta^*_\mu}\right|_{\boldsymbol{\lambda}=\mathbf{0}} = \left\langle \Phi_\mu \middle| \hat{H} \middle| c^{(k)} \right\rangle - E^{[0]} c^{(k)}_\mu = \left(\mathbf{E}^{[1]c}_{\mu}\right)^*, \\
\mathbf{E}^{[1]o^*}_{pq} &= \left.\frac{\partial E}{\partial \kappa^*_{pq}}\right|_{\boldsymbol{\lambda}=\mathbf{0}} = -\left\langle c^{(k)} \middle| \left[\hat{X}^-_{qp}, \hat{H}\right] \middle| c^{(k)} \right\rangle = \left(\mathbf{E}^{[1]o}_{pq}\right)^*, \\
\mathbf{E}^{[1]o^*}_{p\bar{q}} &= \left.\frac{\partial E}{\partial \kappa^*_{p\bar{q}}}\right|_{\boldsymbol{\lambda}=\mathbf{0}} = -\left\langle c^{(k)} \middle| \left[\hat{X}^-_{\bar{q}p}, \hat{H}\right] \middle| c^{(k)} \right\rangle = \left(\mathbf{E}^{[1]o}_{p\bar{q}}\right)^*.
\end{aligned}
\tag{4.19}
$$

The last line ($\mathbf{E}^{[1]o^*}_{r\bar{s}}$) is obtained by simply replacing $s$ with $\bar{s}$ in $\mathbf{E}^{[1]o^*}_{rs}$.

Differentiation of the energy twice yield the Hessian at the CEP

- From the $\dfrac{\partial^2 E}{\partial \Gamma^* \partial \Gamma}$ and $\dfrac{\partial^2 E}{\partial \Gamma \partial \Gamma^*}$ blocks:

$$
\begin{aligned}
\mathbf{E}^{[2]c^*c}_{\mu,\nu} &= \left.\frac{\partial^2 E}{\partial \delta^*_\mu \partial \delta_\nu}\right|_{\boldsymbol{\lambda}=\mathbf{0}} = \left\langle \Phi_\mu \middle| \hat{H} \middle| \Phi_\nu \right\rangle - E^{[0]}\delta_{\mu\nu} - \left(\mathbf{E}^{[1]c^*}_{\mu}\, c^{(k)\,*}_{\nu} + c^{(k)}_{\mu}\mathbf{E}^{[1]c}_{\nu}\right) \\
&= \left(\mathbf{E}^{[2]cc^*}_{\mu,\nu}\right)^*, \\
\mathbf{E}^{[2]c^*o}_{\mu,rs} &= \left.\frac{\partial^2 E}{\partial \delta^*_\mu \partial \kappa_{rs}}\right|_{\boldsymbol{\lambda}=\mathbf{0}} = \left\langle \Phi_\mu \middle| \left[\hat{X}^-_{rs}, \hat{H}\right] \middle| c^{(k)} \right\rangle - c^{(k)}_\mu \mathbf{E}^{[1]o}_{rs} = \left(\mathbf{E}^{[2]co^*}_{\mu,rs}\right)^*, \\
\mathbf{E}^{[2]o^*o}_{pq,rs} &= \left.\frac{\partial^2 E}{\partial \kappa^*_{pq} \partial \kappa_{rs}}\right|_{\boldsymbol{\lambda}=\mathbf{0}} = \left\langle c^{(k)} \middle| \left[\hat{X}^-_{qp}, \hat{X}^-_{rs}, \hat{H}\right] \middle| c^{(k)} \right\rangle = \left(\mathbf{E}^{[2]oo^*}_{pq,rs}\right)^*
\end{aligned}
\tag{4.20}
$$

- From the $\dfrac{\partial^2 E}{\partial\Gamma^*\partial\Gamma^*}$ and $\dfrac{\partial^2 E}{\partial\Gamma\partial\Gamma}$ blocks:

$$\begin{aligned}
\mathbf{E}^{[2]c^*c^*}_{\mu,\nu} &= \left.\frac{\partial^2 E}{\partial\delta^*_\mu\partial\delta^*_\nu}\right|_{\boldsymbol{\lambda}=\mathbf{0}} = 0 = \mathbf{E}^{[2]cc}_{\mu,\nu} \\
\mathbf{E}^{[2]c^*o^*}_{\mu,rs} &= \left.\frac{\partial^2 E}{\partial\delta^*_\mu\partial\kappa^*_{rs}}\right|_{\boldsymbol{\lambda}=\mathbf{0}} = -\left\langle\Phi_\mu\middle|\left[\hat{X}^-_{sr},\hat{H}\right]\middle|c^{(k)}\right\rangle - c^{(k)}_\mu\left(\mathbf{E}^{[1]o^*}_{rs}\right)^* = \left(\mathbf{E}^{[2]co}_{\mu,rs}\right)^*, \\
\mathbf{E}^{[2]o^*o^*}_{pq,rs} &= \left.\frac{\partial^2 E}{\partial\kappa^*_{pq}\partial\kappa^*_{rs}}\right|_{\boldsymbol{\lambda}=\mathbf{0}} = -\left\langle c^{(k)}\middle|\left[\hat{X}^-_{qp},\hat{X}^-_{sr},\hat{H}\right]\middle|c^{(k)}\right\rangle = \left(\mathbf{E}^{[2]oo}_{pq,rs}\right)^*
\end{aligned} \tag{4.21}$$

## 4.5 The Restricted-Step Second-Order Optimization

The restricted-step second-order optimization algorithm is based on the comparison between the predicted energy change based on Eq. (4.17)

$$\Delta q(\boldsymbol{\lambda}) = q(\boldsymbol{\lambda}) - E^{[0]} = \boldsymbol{\lambda}^\dagger\mathbf{g} + \frac{1}{2}\boldsymbol{\lambda}^\dagger\mathbf{H}'\boldsymbol{\lambda}, \tag{4.22}$$

where we have introduced the notation $\mathbf{g} = \mathcal{P}\mathbf{E}^{[1]} = \mathbf{E}^{[1]}$ and $\mathbf{H}' = \mathcal{P}\mathbf{E}^{[2]}\mathcal{P}$, and the actual energy change

$$\Delta E(\boldsymbol{\lambda}) = E(\boldsymbol{\lambda}) - E^{[0]} = \Delta q(\boldsymbol{\lambda}) + R^{(2)}(\boldsymbol{\lambda}). \tag{4.23}$$

When the remainder $R^{(2)}(\boldsymbol{\lambda})$ is negligible compared to the predicted energy change $\Delta q(\boldsymbol{\lambda})$, *i.e.*

$$r(\boldsymbol{\lambda}) = \frac{\Delta E(\boldsymbol{\lambda})}{\Delta q(\boldsymbol{\lambda})} = 1 + \frac{R^{(2)}(\boldsymbol{\lambda})}{\Delta q(\boldsymbol{\lambda})} \tag{4.24}$$

is close to unity, second-order expansion of the energy can be trusted to correctly describe the structure of the parameter surface. The step is therefore restricted to a region

$$\|\boldsymbol{\lambda}\| \leq r_{\text{trust}} \tag{4.25}$$

where (we hope) the second-order Taylor expansion is an acceptable approximation to the energy. $r_{\text{trust}}$ is denoted the trust radius. The task is to find the point in space such that the Hessian, $\mathbf{H}'$, has the correct structure and

Eq. (4.25) is fulfilled. If the Hessian is non-singular there always exists such a solution, and it can be written as

$$\boldsymbol{\lambda} = -\left(\mathbf{H}' - \nu\mathbf{I}\right)^{-1}\mathbf{g}, \tag{4.26}$$

with a specific, unique value of the level shift $\nu$. The optimal step can either be the Newton step,

$$\boldsymbol{\lambda} = -\mathbf{H}'^{-1}\mathbf{g}, \tag{4.27}$$

(*i.e.*, $\nu = 0$), or a point on the boundary of the region $\|\boldsymbol{\lambda}\| \leq r_{\text{trust}}$, that is, $\nu$ assumes a value which makes $\|\boldsymbol{\lambda}\| = r_{\text{trust}}$. In a non-relativistic optimization ground state optimization $\nu$ would be in the interval from $-\infty$ to the lowest eigenvalue of the Hessian. As we in relativistic ground state optimization have to maximize the energy with respect to positronic parameters and minimize the energy with respect to electronic parameters (the mini-max principle mentioned in Section 4.3) we choose $\nu$ such that the Hessian have exactly $M$ negative eigenvalues, where $M$ is the number of positronic parameters in the optimization. This point is actually a $M$th order saddle-point, and the restricted-step algorithm does not guarantee convergence towards this state as it does for non-relativistic ground-state optimizations [16], but in practice convergence is always obtained due to the big gap ($\approx -2mc^2$) between the highest positronic eigenvalue and the lowest electronic eigenvalue.

The linear equations, Eq. (4.26), are solved with an iterative algorithm such as the complex generalization of the Davidson algorithm [17] where the solution is expanded in a set of trial vectors

$$\boldsymbol{\lambda} = \sum_j e_j \mathbf{b}_j, \tag{4.28}$$

where $c_j$ are found by solving the projected linear equations

$$\left(\mathbf{H}^{\mathrm{R}} - \nu\mathbf{I}\right)\mathbf{e} = -\mathbf{g}^{\mathrm{R}}, \tag{4.29}$$

with

$$\begin{aligned} H_{ij}^{\mathrm{R}} &= \mathbf{v}_i^\dagger \mathbf{H}' \mathbf{v}_j \\ &= \mathbf{v}_i^\dagger \boldsymbol{\sigma}_j, \\ g_i^{\mathrm{R}} &= \mathbf{v}_i^\dagger \mathbf{g}. \end{aligned} \tag{4.30}$$

New trial vectors are added until sufficient convergence has been obtained. Note, than in order to implement the mini-max principle efficiently the trial

vectors, $\mathbf{b}_j$, must only have non-zero elements for either the electronic parameters or positronic parameters: To converge towards the electronic ground state we select the level shift, $\nu$, such that the reduced Hessian, Eq. (4.30), has $M$ negative eigenvalues and $N$ positive eigenvalues, where $M$ and $N$ are the number of positronic trial vectors and electronic trial vectors, respectively. Just as in the non-relativistic case it is also an computational advantage to split the electronic trial vectors into pure configurational and pure orbital trial vectors [18]. Thus, we have three kinds of trial vectors: (i) pure configurational trial vectors, $\mathbf{b}_j^c$, (ii) pure electronic orbital rotation trial vectors, $\mathbf{b}_j^e$, and (iii) pure positronic orbital rotation trial vectors, $\mathbf{b}_j^p$.

## 4.6 Direct KR-MCSCF

There are two levels in a the direct KR-MCSCF algorithm: (i) the macro iterations, where we walk towards the desired stationary point with $\mathbf{g} = \mathbf{0}$ with steps defined by Eq. (4.26), and (ii) the micro iterations for the iterative solution of the linear equations defined by Eq. (4.26) which yields the optimal step, $\boldsymbol{\lambda}$, for this macro iteration. For large scale KR-MCSCF calculations it is essential to solve Eq. (4.26) iteratively as it is not feasible to calculate the Hessian explicitly. The solution to the linear equations are found by means of linear transformations

$$\boldsymbol{\sigma}_j = \mathbf{H}'\mathbf{b}_j, \tag{4.31}$$

for a trial vector $\mathbf{b}_j$, without setting up the Hessian, $\mathbf{H}'$, explicitly. Inserting the definition of $\mathbf{H}'$ we get

$$\boldsymbol{\sigma}_j = \mathcal{P}\mathbf{E}^{[2]}\mathcal{P}\mathbf{b}_j. \tag{4.32}$$

From this we see that the projection can be achieved implicitly by selecting trial vectors orthogonal to the CEP and by explicitly projecting out the CEP from the sigma vector:

$$\boldsymbol{\sigma}_j = \mathbf{E}^{[2]}\mathbf{b}_j. \tag{4.33}$$

Each calculation of one or more linear transformations defines one micro iteration towards the desired solution of Eq. (4.26). The linear transforma-

tion, Eq. (4.33), can be written as

$$\begin{aligned}\boldsymbol{\sigma} &= \begin{pmatrix} \boldsymbol{\sigma}^{c} \\ \boldsymbol{\sigma}^{o} \\ \boldsymbol{\sigma}^{c^*} \\ \boldsymbol{\sigma}^{o^*} \end{pmatrix} \\ &= \begin{pmatrix} \mathbf{E}^{[2]c^*c} & \mathbf{E}^{[2]c^*o} & \mathbf{E}^{[2]c^*c^*} & \mathbf{E}^{[2]c^*o^*} \\ \mathbf{E}^{[2]o^*c} & \mathbf{E}^{[2]o^*o} & \mathbf{E}^{[2]o^*c^*} & \mathbf{E}^{[2]o^*o^*} \\ \mathbf{E}^{[2]cc} & \mathbf{E}^{[2]co} & \mathbf{E}^{[2]cc^*} & \mathbf{E}^{[2]co^*} \\ \mathbf{E}^{[2]oc} & \mathbf{E}^{[2]oo} & \mathbf{E}^{[2]oc^*} & \mathbf{E}^{[2]oo^*} \end{pmatrix} \times \begin{pmatrix} \mathbf{b}^{c} \\ \mathbf{b}^{o} \\ \mathbf{b}^{c^*} \\ \mathbf{b}^{o^*} \end{pmatrix}. \end{aligned} \tag{4.34}$$

We only consider the formulas for $\boldsymbol{\sigma}^c$ and $\boldsymbol{\sigma}^o$ as the remaining two blocks $\boldsymbol{\sigma}^{c^*}$ and $\boldsymbol{\sigma}^{o^*}$ are the complex conjugate of the first two. Explicitly, the blocks of the sigma vector is given by [1]:

- Configurational contribution to $\sigma^c_\mu$:

$$\begin{aligned}\sum_\nu \left[E^{[2]c^*c}_{\mu\nu} b^c_\nu + E^{[2]c^*c^*}_{\mu\nu} \left(b^c_\nu\right)^*\right] \\ = \left\langle 0 \middle| \hat{H} \middle| B \right\rangle - E^{[0]} b^c_\mu - \left(g^c_\mu\right)^* \left(c^*_\nu b^c_\nu\right) + c_\mu \left(g^c_\nu b^c_\nu\right) \\ = \left\langle 0 \middle| \hat{H} \middle| B \right\rangle - E^{[0]} b^c_\mu, \end{aligned} \tag{4.35}$$

  where we have used that $\mathbf{c}^\dagger \mathbf{b} = 0$ and that we project out $\mathbf{c}$ from the sigma vector $\boldsymbol{\sigma}^c$.

- Orbital contribution to $\sigma^c_\mu$:

$$\begin{aligned}\sum_{r>s} \left[E^{[2]c^*o}_{\nu,rs} b^o_{rs} + E^{[2]c^*o^*}_{\nu,rs} b^{o^*}_{rs} + E^{[2]c^*o}_{\nu,r\bar{s}} b^o_{r\bar{s}} + E^{[2]c^*o^*}_{\nu,r\bar{s}} b^{o^*}_{r\bar{s}}\right] \\ = \left\langle \mu \middle| \tilde{H} \middle| 0 \right\rangle - c_\mu \left(g^o_{rs} b^o_{rs} + g^o_{r\bar{s}} b^o_{r\bar{s}}\right) \\ = \left\langle \mu \middle| \tilde{H} \middle| 0 \right\rangle, \end{aligned} \tag{4.36}$$

  where we again have used that we project any $\mathbf{c}$ component out of the sigma vector $\boldsymbol{\sigma}^c$.

- Configurational contribution to $\sigma^o_{pq}$:

$$\begin{aligned}\sum_\nu \left[E^{[2]o^*c}_{\mu\nu} b^c_\nu + E^{[2]o^*c^*}_{\mu\nu} \left(b^c_\nu\right)^*\right] \\ = \left(\check{g}^o_{pq}\right)^* - \left(g^o_{pq}\right)^* \sum_\nu \left[c^*_\nu b^c_\nu + c_\nu \left(b^c_\nu\right)^*\right] \\ = \left(\check{g}^o_{pq}\right)^*, \end{aligned} \tag{4.37}$$

where we have used that $\mathbf{c}^\dagger\mathbf{b} = 0$.

- Orbital contribution to $\sigma^o_{pq}$:

$$\sum_{r>s}\left[E^{[2]o^*o}_{pq,rs}b^o_{rs} + E^{[2]o^*o^*}_{pq,rs}b^{o^*}_{rs} + E^{[2]o^*o}_{pq,r\bar{s}}b^o_{r\bar{s}} + E^{[2]o^*o^*}_{pq,r\bar{s}}b^{o^*}_{r\bar{s}}\right]$$
$$= \left(\tilde{g}^o_{pq}\right)^* + \frac{1}{2}\sum_r\left[\left(g^o_{pr}b^o_{rq}\right)^* + \left(g^o_{p\bar{r}}b^o_{\bar{r}q}\right)^* - g^o_{pr}b^o_{rq} - g^o_{p\bar{r}}b^o_{\bar{r}q}\right]. \quad (4.38)$$

Eq. (4.38) is a standard orbital gradient

$$\tilde{g}^{o^*}_{pq} = -\left\langle 0\middle|\left[\hat{X}^-_{pq},\tilde{H}\right]\middle|0\right\rangle, \quad (4.39)$$

with a one-index transformed Hamiltonian defined by

$$\begin{aligned}\hat{H} = &\sum_{pq}\left[\tilde{h}_{pq}\hat{X}^+_{pq} + \frac{1}{2}\left(\tilde{h}_{\bar{p}q}\hat{X}^+_{\bar{p}q} + \tilde{h}_{p\bar{q}}\hat{X}^+_{p\bar{q}}\right)\right]\\ &+\frac{1}{2}\sum_{pqrs}\left[\widetilde{(pq|rs)}\hat{x}^{++}_{pq,rs} + \widetilde{(\bar{p}qr,rs)}\hat{x}^{++}_{\bar{p}q,rs} + \widetilde{(p\bar{q}|rs)}\hat{x}^{++}_{p\bar{q}|rs}\right]\\ &+\frac{1}{4}\sum_{pqrs}\widetilde{(\bar{p}q|r\bar{s})}\hat{x}^{++}_{\bar{p}q,r\bar{s}} + \frac{1}{8}\left[\widetilde{(\bar{p}q|\bar{r}s)}\hat{x}^{++}_{\bar{p}q,\bar{r}s} + \widetilde{(p\bar{q}|r\bar{s})}\hat{x}^{++}_{p\bar{q},r\bar{s}}\right],\end{aligned} \quad (4.40)$$

with

$$\tilde{h}_{pq} = \sum_r\left[\left(b^o_{pr}h_{rq} - h_{pr}b^o_{rq}\right) + \left(b^o_{p\bar{r}}h_{\bar{r}q} - h_{p\bar{r}}b^o_{\bar{r}q}\right)\right] \quad (4.41)$$

and

$$\begin{aligned}\widetilde{(pq|rs)} &= (\widetilde{p}q|rs) + (pq|\widetilde{r}s)\\ &= \sum_t\left(b_{pt}\,(tq|rs) - (pt|rs)\,b_{tq} + b_{p\bar{t}}\,(\bar{t}q|rs) - (p\bar{t}|rs)\,b_{\bar{t}q}\right)\\ &+\sum_t\left(b_{rt}\,(pq|ts) - (pq|rt)\,b_{ts} + b_{r\bar{t}}\,(pq|\bar{t}s) - (pq|r\bar{t})\,b_{\bar{t}s}\right).\end{aligned} \quad (4.42)$$

Various barred and unbarred elements are obtained by simple substitutions $p \to \bar{p}$. The transition gradient $\check{\mathbf{g}}$ is also a standard orbital gradient

$$\begin{aligned}\check{g}^{o^*}_{pq} &= \left\langle 0\middle|\left[\hat{X}^-_{pq},\hat{H}\right]\middle|B\right\rangle + \left\langle B\middle|\left[\hat{X}^-_{pq},\hat{H}\right]\middle|0\right\rangle,\\ |B\rangle &= \sum_\mu b^c_\mu\,|\mu\rangle.\end{aligned} \quad (4.43)$$

evaluated using a symmetrized transition density matrix. Eq. (4.35) is a standard CI sigma vector and Eq. (4.36) is a standard CI sigma vector with the one-index transformed Hamiltonian $\tilde{H}$ also used for the one-index transformed gradient.

The sigma vector is now expressed in terms of gradient elements and CI sigma vectors. Thus, one linear transformation is equivalent to calculating one CI sigma vector and one orbital gradient — *i.e.*, equivalent to calculating one KR-MCSCF gradient, where "equivalent" means that we need the same number of CI sigma vectors and Fock matrices. However, for the KR-MCSCF gradient we will need $(ga|aa)$ MO integrals (one general and three active indices), but for the orbital part of the orbital sigma vector we will need $(gg|aa)$ and $(ga|ga)$ integrals. Hence, it will be possible to do a KR-MCSCF calculation if it is possible to do the corresponding CI calculation *and* if it is possible to calculate and store the $(gg|aa)$ and $(ga|ga)$ integrals.

## 4.7 Orbital Gradients

In this section we will evaluate the orbital gradients needed for Eqs. (4.19), (4.39), and (4.43). We start out with the electronic gradient, Eq. (4.19):

$$g_{pq} = E^{[1]o}_{pq} = \left\langle 0 \middle| \left[ X^{-}_{pq}, \hat{H} \right] \middle| 0 \right\rangle . \tag{4.44}$$

Using the identity

$$\left[ \hat{X}^{-}_{pq}, \hat{H} \right] = p^{\dagger} \left[ q, \hat{H} \right] + \left( \bar{p}^{\dagger} \left[ \bar{q}, \hat{H} \right] \right)^{\dagger} - \left( q^{\dagger} \left[ p, \hat{H} \right] + \left( \bar{q}^{\dagger} \left[ \bar{p}, \hat{H} \right] \right)^{\dagger} \right)^{\dagger} , \tag{4.45}$$

it is possible to rewrite the gradient in terms of so-called *generalized* Fock matrices or MCSCF Fock matrices

$$g_{pq} = F_{qp} - F^{*}_{pq}, \tag{4.46}$$

where $\mathbf{F}$ is the generalized Fock matrix defined by

$$F_{qp} = \left\langle 0 \middle| p^{\dagger} \left[ q, \hat{H} \right] \middle| 0 \right\rangle + \left\langle 0 \middle| \bar{p}^{\dagger} \left[ \bar{q}, \hat{H} \right] \middle| 0 \right\rangle^{*} . \tag{4.47}$$

The elements of the generalized Fock matrix can be evaluated using the commutator relations for the $\hat{X}^{\pm}$ and $\hat{x}^{++}$ operators. The result is

$$\begin{aligned} F_{qp} = & \sum_{r} \left[ D^{+}_{pr} h_{qr} + D^{+}_{p\bar{r}} h_{q\bar{r}} \right] \\ & + \sum_{rst} \left[ P^{++}_{pr,st} \left( qr|st \right) + P^{++}_{p\bar{r},st} \left( q\bar{r}|st \right) \right] \\ & + \frac{1}{2} \sum_{rst} \left[ P^{++}_{p\bar{r},\bar{s}t} \left( q\bar{r}|\bar{s}t \right) + P^{++}_{p\bar{r},s\bar{t}} \left( q\bar{r}|s\bar{t} \right) + P^{++}_{pr,\bar{s}t} \left( qr|\bar{s}t \right) + P^{++}_{pr,s\bar{t}} \left( qr|s\bar{t} \right) \right], \end{aligned} \tag{4.48}$$

where we have introduced the time-reversal invariant one- and two-electron Kramers reduced density matrices

$$\begin{aligned} D^{+}_{pq} &= \left\langle 0 \middle| \hat{X}^{+}_{pq} \middle| 0 \right\rangle, \\ P^{++}_{pq,rs} &= \left\langle 0 \middle| \hat{x}^{++}_{pq,rs} \middle| 0 \right\rangle. \end{aligned} \tag{4.49}$$

Expressions for the quaternion elements, $F_{q\bar{p}}$, can be found by substituting $p \rightarrow \bar{p}$ and $\bar{p} \rightarrow -p$.

The elements of both the one-electron and two-electron density matrices are trivially zero if any index is secondary (electronic virtuals or positronic orbitals). Hence, only density matrix elements involving inactive or active orbitals can be non-zero. The only non-zero elements involving inactive indices are

$$\begin{aligned} D^{+}_{pi} &= 2\delta_{pi}, \\ P^{++}_{iq,rs} &= 2\delta_{iq} D^{+}_{rs} - \delta_{is} D^{+}_{rq} - \delta_{i\bar{r}} D^{+}_{\bar{s}q}. \end{aligned} \tag{4.50}$$

and elements obtained by particle interchange, complex conjugation, or by operating with the time-reversal operator on the above elements. From the elements above we see that only one-electron density matrix elements with both indices active and two-electron density matrix elements with all four indices active have to be calculated and stored explicitly, since all other density matrix element are either zero or given by the formulas above (Eq. (4.50)).

Using Eq. (4.50) it is possible to calculate $F_{qp}$ for any combination of inactive, active, and secondary indices:

$$\begin{aligned} F_{pi} &= 2 \left( F^{C}_{pi} + F^{V}_{pi} \right), \\ F_{pv} &= \sum_{u} \left( D_{vu} F^{C}_{pu} + D_{v\bar{u}} F^{C}_{p\bar{u}} \right) + F^{Q}_{pv}, \\ F_{pa} &= 0, \end{aligned} \tag{4.51}$$

where we have defined the inactive, active, and auxiliary Fock matrix, respectively:

$$\begin{aligned}
F^C_{pq} &= h_{pq} + \sum_j \left[2\,(pq|jj) - (pj|jq) - (p\bar{j}|\bar{j}q)\right], \\
F^V_{pq} &= \sum_{uv} D_{uv}\left[(pq|uv) - (pv|uq)\right] + \sum_{uv} D_{\bar{u}v}\left[(pq|\bar{u}v) - (pv|\bar{u}q)\right] \\
&\quad + \sum_{uv} D_{u\bar{v}}\left[(pq|u\bar{v}) - (p\bar{v}|uq)\right] + \sum_{uv} D_{\bar{u}\bar{v}}\left[(pq|\bar{u}\bar{v}) - (p\bar{v}|\bar{u}q)\right], \\
F^Q_{pq} &= \sum_{vxy}\left[P^{++}_{pv,xy}\,(qv|xy) + P^{++}_{p\bar{v},xy}\,(q\bar{v}|xy)\right] \\
&\quad + \sum_{vxy}\left[P^{++}_{p\bar{v},\bar{x}y}\,(q\bar{v}|\bar{x}y) + P^{++}_{p\bar{v},s\bar{y}}\,(q\bar{v}|x\bar{y}) + P^{++}_{pv,\bar{x}y}\,(qv|\bar{x}y) + P^{++}_{pv,x\bar{y}}\,(qv|x\bar{y})\right].
\end{aligned} \tag{4.52}$$

The expressions with various barred and unbarred indices can as before be found using simple substitution.

The expressions for the one-index transformed gradient, Eq. (4.39), and the transition gradient, Eq. (4.43), can be derived analogously. Explicitly, the one-index transformed gradient is given by:

$$\begin{aligned}
\tilde{F}_{pi} &= 2\left(\tilde{F}^C_{pi} + \tilde{F}^V_{pi}\right), \\
\tilde{F}_{pv} &= \sum_u \left(D_{vu}\tilde{F}^C_{pu} + D_{v\bar{u}}\tilde{F}^C_{p\bar{u}}\right) + \tilde{F}^Q_{pq}, \\
\tilde{F}_{pa} &= 0,
\end{aligned} \tag{4.53}$$

where we have defined the inactive, active, and auxiliary one-index transformed Fock matrices which are identical with the normal Fock matrices except that the normal integrals are replaced with their one-index transformed analogues (Eqs. (4.41) and (4.42)). The transition gradient is given by:

$$\begin{aligned}
\check{F}_{pi} &= 2\check{F}^V_{pi}, \\
\check{F}_{pv} &= \sum_u \left(\check{D}_{vu}F^C_{pu} + \check{D}_{v\bar{u}}F^C_{p\bar{u}}\right) + \check{F}^Q_{pq}, \\
\check{F}_{pa} &= 0,
\end{aligned} \tag{4.54}$$

where we have defined the active and auxiliary transition Fock matrices, which are are identical to the normal Fock matrices except that the normal density matrices are replaced with the symmetrized transition density

matrices

$$\begin{aligned} \check{D}_{uv} &= \langle 0|\hat{X}^{+}_{uv}|B\rangle + \langle B|\hat{X}^{+}_{uv}|0\rangle\,, \\ \check{P}_{uv,xy} &= \langle 0|\hat{x}^{++}_{uv,xy}|B\rangle + \langle B|\hat{x}^{++}_{uv,xy}|0\rangle\,. \end{aligned} \tag{4.55}$$

Note that there is no $\check{F}^{C}_{pq}$ contribution to $\check{F}_{pi}$ as the CI trial vectors $\mathbf{b}^{c}$ are orthogonal to the CI reference vector $\mathbf{c}$. The expressions for with various barred and unbarred indices can be found using simple substitution.

## 4.8 Quaternion Orbital Gradients

All orbital quantities from Section 4.6 can be reformulated using the quaternion formalism. For example, the quaternion gradient, Eq. (4.46), is defined by

$$\begin{aligned} {}^{Q}g_{pq} &\equiv g_{pq} + g_{p\bar{q}}\check{j} \\ &= \left(F_{qp} - F^{*}_{pq}\right) + \left(F_{\bar{q}p} - F^{*}_{p\bar{q}}\right)\check{j} \\ &= {}^{Q}F_{qp} - {}^{Q}F^{*}_{pq}. \end{aligned} \tag{4.56}$$

Completely analogous to Eq. (4.51) for the generalized spinor Fock matrix, the quaternion generalized Fock matrix is defined by

$$\begin{aligned} {}^{Q}F_{pi} &= 2\left({}^{Q}F^{C}_{pi} + {}^{Q}F^{V}_{pi}\right), \\ {}^{Q}F_{pv} &= \sum_{u} {}^{Q}D_{vu}\,{}^{Q}F^{C}_{pu} + {}^{Q}F^{Q}_{pv}, \\ {}^{Q}F_{pa} &= 0. \end{aligned} \tag{4.57}$$

For a detailed derivation of the quaternion inactive, active, and auxiliary Fock matrices we refer to sections B.1 and B.5 in Appendix B. Similarly, analogous formulae for the one-index transformed gradient, one-index transformed generalized, inactive, active, and auxiliary Fock matrices and transition gradients, transition generalized, active, and auxiliary Fock matrices can be derived (see Appendix B for details). The orbital sigma vectors, Eqs. (4.37) and (4.38), are now given by:

- Configurational contribution to ${}^{Q}\sigma^{o}{}_{pq}$:

$$\left({}^{Q}\check{g}^{o}_{pq}\right)^{*}, \tag{4.58}$$

- Orbital contribution to ${}^{Q}\sigma^{o}{}_{pq}$:

$$\left({}^{Q}\tilde{g}^{o}_{pq}\right)^{*} - \frac{1}{2}\sum_{r}\left[{}^{Q}g^{o}_{pr}\,{}^{Q}b^{o}_{qr} - {}^{Q}b^{o}_{pr}\,{}^{Q}g^{o}_{qr}\right], \tag{4.59}$$

with all summations are over orbitals and not spinors.

The quaternion matrices may reduce to real or complex matrices depending on the point group symmetry

- for $C_{2v}$, $D_{2h}$, and $D_{2d}$ all matrices are real and the CI vectors are also real (or pure imaginary). For $D_{2h}$ the quaternion matrices will also be blocked by inversion symmetry in *gerade* and *ungerade* blocks.

- for $C_2$, $C_s$, and $C_{2h}$ all quaternion matrices reduce to complex matrices, but the CI vectors are generally complex. In $C_{2h}$ the matrices will be blocked by inversion symmetry.

- for $C_i$ and $C_1$ there are no reductions and all matrices are, in general, quaternion. For $C_i$ we may use inversion symmetry. The CI vectors are generally complex.

Note that some of the savings from symmetry comes from the reduction of quaternion matrices to real or complex matrices, and the rest of the savings comes from the blocking of matrices by inversion symmetry.

## 4.9 Configurational Sigma Vectors and Density Matrices

A more in-depth analysis of direct Kramers restricted CI can be found in Ref. [19] and Ref. [20], and we will only re-iterate the most important results here.

One of the potentially most time-consuming step is the calculation of the configurational sigma vectors, Eqs. (4.19), (4.35), and (4.36):

$$\begin{aligned}
\sigma_\mu &= \sum_\nu \left\langle \Phi_\mu \middle| \hat{H} \middle| \Phi_\nu \right\rangle c_\nu, \\
\sigma_\mu^{cc} &= \sum_\nu \left\langle \Phi_\mu \middle| \hat{H} \middle| \Phi_\nu \right\rangle b_\nu, \\
\sigma_\mu^{co} &= \sum_\nu \left\langle \Phi_\mu \middle| \tilde{H} \middle| \Phi_\nu \right\rangle c_\nu.
\end{aligned} \tag{4.60}$$

All three kinds of sigma vectors can be calculated in the same way, as the normal Hamiltonian $\hat{H}$ and the one-index transformed Hamiltonian $\tilde{H}$ have the same symmetry under time-reversal, complex conjugation, and particle interchange.

The Hamiltonian matrix elements, $\left\langle \Phi_\mu \middle| \hat{H} \middle| \Phi_\nu \right\rangle$ can be expressed in terms of integrals and coupling coefficients

$$H_{\mu\nu} = \left\langle \Phi_\mu \middle| \hat{H} \middle| \Phi_\nu \right\rangle = \sum_{uv} A^{\mu\nu}_{uv} h_{uv} + \frac{1}{2} \sum_{uvxy} A^{\mu\nu}_{uv,xy} \, (uv|xy) \,, \tag{4.61}$$

with

$$\begin{aligned} A^{\mu\nu}_{uv} &= \left\langle \Phi_\mu \middle| \hat{X}^{+}_{uv} \middle| \Phi_\nu \right\rangle , \\ A^{\mu\nu}_{uv,xy} &= \left\langle \Phi_\mu \middle| \hat{x}^{++}_{uv,xy} \middle| \Phi_\nu \right\rangle . \end{aligned} \tag{4.62}$$

The calculation of density matrices

$$\begin{aligned} D^{\pm}_{pq} &= \left\langle L \middle| \hat{X}^{\pm}_{pq} \middle| R \right\rangle = \sum_{\mu\nu} \left(c^L_\mu\right)^* A^{\mu\nu}_{pq} c^R_{nu}, \\ P^{\pm\pm}_{pq,rs} &= \left\langle L \middle| \hat{x}^{\pm\pm}_{pq,rs} \middle| R \right\rangle , \left(c^L_\mu\right)^* A^{\mu\nu}_{pq,rs} c^R_{nu}, \end{aligned} \tag{4.63}$$

is very similar to the calculation of CI sigma vectors, and we will not consider them here.

The current state of the art CI programs (*e.g.*, LUCIA by J. Olsen) use the concept of alpha and beta strings [13, 21–23], which leads to very efficient calculations of the couplings coefficients $A^{\mu\nu}_{uv}$ and $A^{\mu\nu}_{uv,xy}$. In non-relativistic theory we can write a determinant as [21]

$$\Phi_\mu = \boldsymbol{\alpha}(I, N_\alpha)\boldsymbol{\beta}(I, N_\beta) \, |0\rangle \,, \tag{4.64}$$

where $\boldsymbol{\alpha}$ ($\boldsymbol{\beta}$) are alpha (beta) strings of creation operators of length $N_\alpha$ ($N_\beta$). Completely analogous we write a relativistic Slater determinant in terms of barred and unbarred orbitals instead of alpha and beta strings:

$$\Phi_\mu = \mathbf{p}(I, N_p)\bar{\mathbf{p}}(I, N_{\bar{p}}) \, |0\rangle \,, \tag{4.65}$$

where $\mathbf{p}$ ($\bar{\mathbf{p}}$) are strings of barred spinor (unbarred spinor) creation operators of length $N_p$ ($N_{\bar{p}}$).

Similar to the non-relativistic $M_S$ quantum number defined by $M_S = \frac{1}{2}(N_\alpha - N_\beta)$ we define

$$M_K = \frac{1}{2}(N_p - N_{\bar{p}}), \tag{4.66}$$

Note that the spinors will, in general, not be pure alpha or beta functions but will have non-zero components for both spin orientations, although for spin-free calculations or calculations with the non-relativistic 4-component

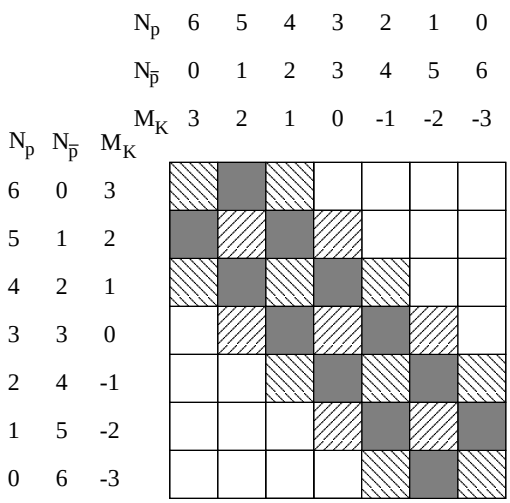


Figure 4.2: Pentadiagonal block structure of the CI Hamiltonian matrix for an even number of electrons, given for a system with six electrons. The unshaded blocks are zero for all point groups. The plain grey groups are zero for real and complex point groups. The two different backgrounds in the striped blocks highlight the partitioning of the Hamiltonian in the real and complex groups into two disjoint sections (reproduced from Ref. [19]).

Lévy-Leblond Hamiltonian the spinors will, in fact, be pure alpha or beta, but the class of unbarred spinors will contain both pure alpha and beta spinors depending on the boson symmetry of the spatial part of the orbital. For example, spinors of boson symmetry $A$ will have alpha spin (depending on the orientation of the $C_2$ axis) whereas spinors of symmetry $B$ will have beta spin. This means that for a spin-free calculation determinants with $M_S = 0$ will be scattered into the $M_K = 0, \pm 2, \pm 4, \ldots$ blocks. Note also that in non-relativistic CI expansions the CI Hamiltonian will be block-diagonal in $M_S$, *i.e.*, different determinants with different $M_S$ values will not couple, whereas in a relativistic CI expansion determinants with different $M_K$ values do, in general, couple.

As the Hamiltonian — either the normal Hamiltonian (Eq. (4.5)) or the one-index transformed Hamiltonian (Eq. (4.40)) — contains at most two-body operators, the CI Hamiltonian matrix element between two determinants that differs in more than two spinors must be zero. From this we see that $H_{\mu\nu} = 0$ for $|\Delta M_K| = |M_K^\mu - M_K^\nu| > 2$, and, assuming the determinants are ordered into subsets on $M_K$ values, the Hamiltonian is penta-diagonal. This structure is represented in Fig. 4.2 for a system with six electrons (reproduced from Ref. [19]).

The integral classes needed for the CI Hamiltonian depend on the dif-

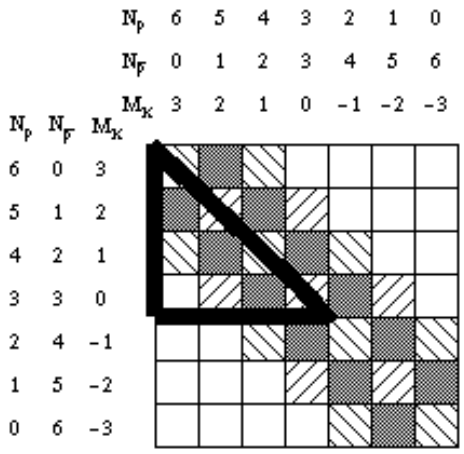


Figure 4.3: Indication of the non-redundant part of the Hamiltonian for an even number of electrons, given for a system with six electrons. The elements above the diagonal are redundant as the CI Hamiltonian is Hermitian. The elements in the lower part of the CI Hamiltonian is given by time-reversal symmetry. See text and Fig. 4.2 for detailed explanation on the shadings.

ference, $\Delta M_K$, between the two determinants. The integral classes needed are [19]:

- $\Delta M_K = 0$: $h_{uv}$, $(uv|xy)$, and $(u\bar{v}|\bar{x}y)$,
- $\Delta M_K = 1$: $h_{u\bar{v}}$ and $(uv|\bar{x}y)$,
- $\Delta M_K = 2$: $(u\bar{v}|x\bar{y})$.

From this we immediately see that the $\Delta M_K = 1$ block is zero for real and complex groups as they only involve integrals with an odd number of bars which is zero for real and complex groups. This is represented with the gray shading in Fig. 4.2. It also separates the Hamiltonian into two disjoint sections for real and complex groups as represented by the two different stripings in Fig. 4.2.

For an odd number of electrons the two sets are related by time-reversal symmetry, and the two sets of eigenvectors constitute Kramers pairs of $N$-electron states where $\Psi$ will follow one row in the fermion irrep and $\bar{\Psi}$ will follow the other.

For an even number of electrons the two sets are not related and corresponds to different boson symmetry. We note that for $N$ even

$$\hat{\mathcal{K}}\,|\Psi\rangle = |\Psi\rangle\,. \tag{4.67}$$

The wave function is a linear combination of determinants and their Kramers partners

$$|\Psi\rangle = \sum_{\mu} c_{\mu} |\Phi_{\mu}\rangle + (1 - \delta_{\mu\bar{\mu}}) c_{\bar{\mu}} |\Phi_{\bar{\mu}}\rangle \,. \tag{4.68}$$

The $(1-\delta_{\mu\bar{\mu}})$ is to avoid double-counting the closed shell determinants $|\Phi_{\mu}\rangle = |\Phi_{\bar{\mu}}\rangle$. Operating with the time-reversal operator on $|\Phi_{\mu}\rangle$ gives

$$\hat{\mathcal{K}} |\Psi\rangle = \sum_{\mu} c^*_{\mu} |\Phi_{\bar{\mu}}\rangle + (1 - \delta_{\mu\bar{\mu}}) c^*_{\bar{\mu}} |\Phi_{\mu}\rangle \,. \tag{4.69}$$

Equating Eq. (4.68) with (4.69) we see that

$$c_{\mu} = c^*_{\bar{\mu}}, \tag{4.70}$$

The set of determinants with even $M_K$ is symmetric under the principal axis (or reflection for $C_s$) whereas the set of determinants with odd $M_K$ is antisymmetric. For example, in $C_2$ the determinants with even $M_K$ will have symmetry $A$ and whereas the ones with odd $M_K$ will have symmetry $B$. For the $C_{2v}$ point group the determinants with even $M_K$ will also split into determinants with real CI coefficients ($A_1$ symmetry) and determinants with pure imaginary CI coefficients ($A_2$ symmetry). The odd $M_K$ determinants also split: $B_2$ ($B_1$) symmetry determinants will have real (imaginary) CI coefficients. For $C_{2h}$ and $D_{2h}$ the wave function will also have inversion symmetry, and can be selected as gerade or ungerade.

For $N$ even it is possible to use time-reversal symmetry adapted configuration state functions (CSF) which renders the CI Hamiltonian real [19]. The advantage of using CSFs is that the wave function is guaranteed to be time-reversal invariant. However, this can also be ensured by only saving the $M_K \geq 0$ parts of the CI vectors, as the $M_K < 0$ part can be generated by time-reversal symmetry, using Eq. (4.70) under the assumption that the determinants are sorted such that all $|\Phi_{\mu}\rangle$ has semi-positive $M_K$ values and $|\Phi_{\bar{\mu}}\rangle$ has semi-negative $M_K$ values. The non-redundant part of the CI Hamiltonian is indicated in Fig. 4.3. We suggest the following algorithm for calculating sigma vectors for $N$ even in determinant basis is

1. Loop over $M_K^{\sigma} = M_K^{\min}, \ldots, M_K^{\max}$ with step $M_K^{\text{step}}$.
   $M_K^{\min}$ will be 0 or 1 depending on boson symmetry (*e.g.*, 0 for $A$ symmetry or 1 for $B$ in $C_2$), $M_K^{\max}$ is determined by the number of electrons, and the step length $M_K^{\text{step}}$ is 2 for real or complex point groups and 1 for quaternion point groups.

(a) Loop over $M_K^c = \max\left(M_K^\sigma - 2, M_K^{\min}\right), \ldots, M_K^\sigma$ with step $M_K^{\text{step}}$. The missing $M_K^\sigma + 1$ and $M_K^\sigma + 2$ is generated using complex conjugation. The diagonal part $M_K^\sigma = M_K^c$ can be done with special triangular code.

i. Loop over determinants and calculate $H_{\mu\nu}$, and sum up $\sigma_\mu = \sigma_\mu + H_{\mu\nu} c_\nu$ and if $M_K^c \geq 0$ then $\sigma_\nu = \sigma_\nu + H_{\mu\nu}^* c_\mu$.

The algorithm for calculating sigma vectors for $N$ odd is identical to the one above, except that $M_K^{\min}$ should be equal to $-M_K^{\max}$.

## 4.10 Implementation

In this section will describe the basic steps in the implementation based on the algorithms and formulae presented in the previous sections.

1. **Setup of the calculation:** Select basis set, active space, convergence threshold, generate start guess, find non-redundant orbital rotations etc. Set macro iteration counter $k = 0$.

2. **Increment macro iteration count:** $k := k + 1$.

3. **Integral transformation:** Calculate the needed molecular orbital integrals. In general, we need $(gg|aa)$ and $(ga|ga)$ integrals (two general and two active indices) [1]. Within the current implementation this is the most time-consuming step, and in Chapter 5 we will look on various approximations.

4. **Energy & gradient:** Calculate the energy and the gradient (Sec. 4.7):

   (a) the calculation of the active density matrices ${}^Q D_{uv}$ and $P_{uv,xy}$,

   (b) the calculation of the standard Fock matrices ${}^Q F_{pq}^C$ and ${}^Q F_{pq}^V$,

   (c) reading of the molecular orbital integral file, calculate $F_{pq}^Q$ and store the $(uv|xy)$ integrals. The former for the orbital gradient and the latter for the configuration gradient and the configurational contribution to $\sigma_\mu^c$,

   (d) calculate the energy:

$$\begin{aligned} E &= \left\langle 0 \middle| \hat{H} \middle| 0 \right\rangle \\ &= \sum_i \left({}^Q h_{ii} + {}^Q F_{ii}^C\right) + \sum_{uv} {}^Q D_{uv} {}^Q F_{uv}^C + \sum_u {}^Q F_{uu}^Q, \end{aligned} \tag{4.71}$$

[1] Due to limitations in the current implementation of the direct molecular integral transformation $(gg|ga)$ integrals are actually calculated.

and the gradient from Eqs. (4.46) and (4.51),

(e) and finally calculate the configurational gradient as a CI sigma vector (the first line of Eq. (4.19)).

All the matrices calculated in this step are saved as they are all needed for the linear transformation in the micro iterations. If the norm of the gradient, $\|\mathbf{g}\| < t_{\text{gradient}}$, where $t_{\text{gradient}}$ is the threshold chosen in Step 1, the wave function is converged and we exit the macro iteration loop

5. **Step control:** Check if the step is acceptable, *i.e.*, if the ratio Eq. (4.24) is sufficiently close to unity. If not, the decrement the macro iteration counter and solve the reduced linear equations, Eq. (4.29), for a reduced trust radius $r_{\text{trust}}$, and go back to Step 2.

6. **Find Restricted Step:** Solve the linear equation, Eq. (4.26), by projecting the Hessian onto a set of trial vectors. The implementation of step 6*a* to 6*d* is based on an extension of the linear reponse program by Saue and Jensen [24].

   (a) **Initial trial vector(s):** Find the initial trial vectors using the generalized Davidson-Liu algorithm using a residual as minus the gradient. Set micro iteration count $j = 0$.

   (b) **Linear transformation(s):** Increment micro iteration count: $j := j+1$, and calculate the linear transformation(s) — the sigma vector(s) — using Eqs. (4.35) – (4.38). This requires the calculation of one-index transformed quaternion matrices (${}^{Q}\tilde{\mathbf{F}}^{C}$, ${}^{Q}\tilde{\mathbf{F}}^{V}$, and ${}^{Q}\tilde{\mathbf{F}}^{Q}$) and quaternion transition Fock matrices (${}^{Q}\check{\mathbf{F}}^{V}$ and ${}^{Q}\check{\mathbf{F}}^{Q}$) (see Appendix B for details) along with the CI sigma vectors.

   (c) **Solve the reduced linear equations:** Add the new elements to the reduced Hessian, (4.30), and solve the reduced linear equations Eq. (4.29) finding the level shift $\nu$ and the step $\boldsymbol{\lambda}$ such that the step is within the trust radius and the Hessian has the proper structure.

   (d) **Calculate new trial vector(s):** Calculate the residual

$$\mathbf{r} = (\mathbf{H}' - \nu\mathbf{I})\,\boldsymbol{\lambda} + \mathbf{g}. \tag{4.72}$$

   If the norm of the residual is sufficiently small, exit the micro iteration loop and jump to step 7. When we are close to convergence the linear equation should be solved to within $t_{\text{gradient}}$ in order to obtain quadratic convergence. When we are far away from

convergence it is sufficient to obtain the general direction, and a suitable threshold is $0.2\|\mathbf{g}\|$ [6]. If the micro iterations are not converged new trial vector(s) are generated using the generalized Davidson-Liu algorithm [17] and jump to step 6($b$).

7. **Obtain new orbitals:** Find the new orbitals

$$\begin{aligned} \mathbf{c}^{k+1} &= \frac{\mathbf{c}+\boldsymbol{\delta}}{\|\mathbf{c}+\boldsymbol{\delta}\|}, \\ {}^{Q}\boldsymbol{\varphi}^{k+1} &= {}^{Q}\boldsymbol{\varphi}^{k} \exp\left(-{}^{Q}\boldsymbol{\kappa}\right). \end{aligned} \tag{4.73}$$

For the details on how to calculate the new orbitals, ${}^{Q}\boldsymbol{\varphi}^{k+1}$, see Appendix A. Also, the orbitals may also be transformed to Fock-type and/or natural orbitals (see Sec. 5.9). Jump to step 2.

The algorithm described above has been implemented within the DIRAC program package.

# Bibliography

[1] H. J. Aa.. Jensen, K. G. Dyall, T. Saue, and K. Faegri, Jr., J. Chem. Phys. **104**, 4083 (1996).

[2] T. Saue and H. J. Aa.. Jensen, J. Chem. Phys. **111**, 6211 (1999).

[3] E. J. Baerends, W. H. E. Schwartz, P. Schwerdtfeger, and J. G. Snijders, J. Phys. B **23**, 3325 (1990).

[4] G. A. Aucar, H. J. Aa. Jensen, and J. Oddershede, Chem. Phys. Lett. **232**, 47 (1995).

[5] T. Helgaker, H. J. A. Jensen, P. Jørgensen, J. Olsen, K. Ruud, H. Ågren, T. Andersen, K. L. Bak, V. Bakken, O. Christiansen, P. Dahle, E. K. Dalskov, *et al.*, *DALTON, an electronic structure program, Release 1.0 (1997).*

[6] H. J. Aa. Jensen, H. Ågren, and J. Olsen, in *Modern Techniques in Computional Chemistry 1990*, edited by E. Clementi (Escom, Leiden, 1990).

[7] T. Fleig, C. M. Marian, and J. Olsen, Theor. Chem. Acc. **97**, 125 (1997).

[8] A. Messiah, *Quantum Mechanics* (North Holland, Amsterdam, 1967).

[9] M. H. Mittleman, Phys. Rev. A **24**, 1167 (1981).

[10] J. D. Talman, Phys. Rev. Lett. **57**, 1091 (1986).

[11] G. A. Aucar, T. Saue, L. Visscher, and H. J. Aa. Jensen, J. Chem. Phys. **110**, 6208 (1999).

[12] J. Olsen, unpublished.

[13] J. Olsen, B. O. Roos, P. Jörgensen, and H. J. Aa. Jensen, J. Chem. Phys. **89**, 2185 (1988).

[14] P. Jörgensen and J. Simons, *Second Quantization-Based Methods in Quantum Chemistry* (Academic, New York, 1981).

[15] R. Shepard, Adv. Chem. Phys. **69**, 63 (1987).

[16] P. Jørgensen, P. Swanstrøm, and D. L. Yeager, J. Chem. Phys. **78**, 347 (1983).

[17] E. Davidson, Int. J. Quant. Chem. **17**, 87 (1975).

[18] H. J. Aa. Jensen, P. Jörgensen, and H. Ågren, J. Chem. Phys. **87**, 451 (1987).

[19] H. J. Aa. Jensen, in *Relativistic and Electron Correlation Effects in Molecules and Solids*, edited by G. L. Malli (Plenum, New York, 1994), p. 179.

[20] T. Fleig, J. Olsen, and C. Marian, J. Chem. Phys. (2001), (in press).

[21] N. C. Handy, Chem. Phys. Lett. **74**, 280 (1980).

[22] P. J. Knowles and N. C. Handy, Chem. Phys. Lett. **111**, 315 (1984).

[23] S. Zarrabian, C. R. Sarma, and J. Paldus, Chem. Phys. Lett. **155**, 183 (1989).

[24] T. Saue and H. J. Aa. Jensen, *Relativistic 4-component linear response*, unpublished.

# Chapter 5

# Improvements and Approximations for KR-MCSCF

The current implementation is neither finished nor in a fully stable state. In this chapter we discuss what needs to be finished and various improvements that can be made to the code. We also discuss some approximations that can be invoked to speed up calculations.

## 5.1 NEO algorithm

The current implementation is solely based on solving the Newton-Raphson equations. It is an advantage to use the *Norm Extended Optimization* algorithm instead [1, 2]. The NEO algorithm is based on solving a eigenvalue equation instead of the Newton-Raphson linear equations. The advantage of the algorithm is that the level shift $\nu$ is automatically in the correct interval as the eigenvalues of the (reduced) Hessian is known hence $\nu$ can be chosen in the correct interval. This makes it particularly simple to implement excited state wave function optimizations.

Status: we have a working version of a direct iterative eigenvalue solver, currently used for calculating excitation energies within the polarization propagator (PP) method [3]. That part of the program has to be modified for use within the KR-MCSCF optimization.

## 5.2 CI Sigma Vectors and Density Matrices

The current CI implementation is a very simple minded determinant based approach. At the beginning of the calculation (Step 1 in the Section 4.10) a list of the determinants in the CI expansion is generated, and CI sigma vectors are generated straightforwardly:

```
Loop over MKI
   Loop over MKJ with abs(MKI-MKJ) <= 2
      Loop over determinants I with MK = MKI
         Loop over determinants J with MK = MKJ
            Calculate CI Hamiltonian element H(IJ)
            Sigma(I) = Sigma(I) + H(IJ) B(J)
         End Loop
      End Loop
   End Loop
End Loop
```

The bottleneck in this approach is that $H_{IJ}$ is zero for many determinants, but we still have to check that for each $(IJ)$. The $N^2$ complexity of this algorithm gets dominant for large CI expansions which limits the current implementation around $100,000$ – $200,000$ determinants. Also, the current implementation does not employ the reduction for an even number of electrons suggested in Sec. 4.9, although the program does use the blocking by $M_K$ value.

Status: work is in progress to interface the spin-dependent large-scale CI program LUCIAREL by Jeppe Olsen and Timo Fleig into the KR-MCSCF program. Their implementation is string-based and can handle *very* large CI expansions (see Ref. [4]).

## 5.3 Properties

Currently, only first order properties (expectation values) can be calculated. Many interesting properties are higher order, for example, spin-spin couplings, chemical shifts, and polarizabilities, all of which require linear response [5]. Also, the formalism for relativistic four-component quadratic response has been implemented for DHF [6], and it should, in principle, be straightforward extensible to KR-MCSCF.

Another interesting property is the molecular gradient. We have already implemented the molecular gradient for DHF (*ibid.*, page 133), and as the formulae for the MCSCF molecular gradient is very similar because it also is

fully variational, it should be relatively simple to implement the KR-MCSCF molecular gradient. The only new thing required, compared to DHF, is the back-transformation of the active two-electron density matrix to AO-basis. It is probably required to do this back-transformation batch-wise as the full AO two-electron density matrix can be fairly large due to the $n_{AO}^4$ scaling — $n_{AO} > 1000$ is not unusual, making the storage requirements in the tera-byte size.

Status: In principle, most of the ingredients for a Kramers restricted multi-configurational response program (KR-MCLR) is present, but needs to be put together. The same applies, in principle, for a KR-MC quadratic response program. The KR-MCSCF molecular gradient should also be relatively simple to implement. Also excitation energies within the relativistic polarization propagator method [3] should be simple to implement.

## 5.4 Debugging

At the time of the deadline for this thesis there was still a few problems left for some point groups.

Status: Unknown.

## 5.5 Molecular Integral Transformation

Some of the steps of the KR-MCSCF calculations are *very* expensive. The most expensive step for all the calculations performed in the forthcoming section was the integral transformation where the current implementation in DIRAC require us to transform the integrals $(gg|ga)$ (three general indices and one active index). As a general index is both electronic and positronic it requires substantial CPU time to generate the integrals and the disk space requirements can be large.

### 5.5.1 Transform Only $(gg|aa)$ and $(ga|ga)$ Integrals

It would therefore be of big interest to modify the integral transformation program to generate only the integrals needed ($(gg|aa)$ and $(ga|ga)$).

Status: not implemented, as it requires substantial changes to the integrals transformation program. Another possibility is the "poor mans version" where the integral transformation is called twice.

### 5.5.2 Direct Implementation of Auxiliary $\mathbf{F}^Q$ Fock Matrices

Another alternative would be an direct implementation of the auxiliary Fock matrices ${}^Q\mathbf{F}^Q$, ${}^Q\tilde{\mathbf{F}}^Q$, and ${}^Q\check{\mathbf{F}}^Q$ which would not require disk space (except for intermediate quantities in the integral transformation).

Status: not implemented. Requires a substantial amount of work.

### 5.5.3 Semi-Direct Implementation of Auxiliary $\mathbf{F}^Q$ Fock Matrices

The auxiliary one-index transformed Fock matrix is given by

$$\begin{aligned}\tilde{F}^Q_{pu} &= \sum_{vxy} \widetilde{(pv|xy)} Puv, xy \\ &= \sum_{vxy} (\tilde{p}v|xy)\, P_{uv,xy} + (p\tilde{v}|xy)\, P_{uv,xy} + (pv|\tilde{x}y)\, P_{uv,xy} + (pv|x\tilde{y})\, P_{uv,xy},\end{aligned} \tag{5.1}$$

where the first term is just the transform of the ordinary $\mathbf{F}^Q$ matrix:

$$\sum_r b_{pr} F^Q_{rv}, \tag{5.2}$$

and

$$\begin{aligned}(p\tilde{v}|xy) &= \sum_r -(pr|xy)\, b_{rv}, \\ (pv|\tilde{x}y) &= \sum_r b_{xr}\, (pv|ry)\,, \\ (pv|x\tilde{y}) &= \sum_r -(pv|xr)\, b_{ry}.\end{aligned} \tag{5.3}$$

By defining:

$$\tilde{x} = \sum_r b_{xr} r, \tag{5.4}$$

and calculating the set of $(g\{a,\tilde{a}\}|\{a,\tilde{a}\}a)$ integrals we can calculate all terms of the $\tilde{\mathbf{F}}^Q$ matrix; the first term from the ordinary $\mathbf{F}^Q$ matrix, the second term from the $(g\tilde{a}|aa)$ integrals, the third term and the fourth term from the $(ga|\tilde{a}a)$ integrals (using some of the relations for double-quaternion integrals).

We have now reduced the integral storage requirements from $2n_g^2n_a^2$ to $n_ga^3$ (for the gradient and $\check{\mathbf{F}}^Q$) plus $n_g(2n_a)^2n_a$ for each trial vector. Although we have to calculate the $(g\{a,\bar{a}\}|\{a,\bar{a}\}a)$ integrals for each trial vector there might still be a gain or status quo in CPU time as "small" integral transformations (index 3 and 4 are a small number of orbitals) are substantially faster than the $(ga|ga)$ integrals transformation otherwise needed.

Status: not implemented, requires some work, but should be relatively easy to implement within the current implementation of the molecular integral transformation program.

### 5.5.4 Frozen Orbitals (I)

In order to reduce the number of orbitals which has to be included in the molecular integral transformation one may also freeze orbitals. It is possible to freeze inactive, virtual, or positronic orbitals. As very large *uncontracted* basis sets often are employed in relativistic calculations there is a large number of high-lying virtuals that may contribute very little to correlation effects, and one may freeze the orbitals, excluding them from the integrals transformation. It is also possible to freeze the core. Frozen orbitals should be used with care as these orbitals may be important for some properties.

Status: implemented.

### 5.5.5 Frozen Orbitals (II)

The freezing of orbitals has the downside that the orbitals to be frozen must be selected beforehand. It would be desirable to dynamically select which orbitals to freeze. A very simple strategy is to freeze orbitals that have negligible gradient elements. Assuming the Hessian is diagonal,

$$\mathbf{H}' = \begin{bmatrix} H_{aa} & 0 \\ 0 & H_{bb} \end{bmatrix} \tag{5.5}$$

and that the gradient is zero for orbitals $b$:

$$\mathbf{g} = \begin{bmatrix} g_a \\ 0 \end{bmatrix} \tag{5.6}$$

the Newton step is given by

$$\begin{aligned} \boldsymbol{\lambda} &= \mathbf{H}'^{-1}\mathbf{g} \\ \begin{bmatrix} \lambda_a \\ \lambda_b \end{bmatrix} &= \begin{bmatrix} \frac{g_a}{H_{aa}} \\ 0 \end{bmatrix} \end{aligned} \tag{5.7}$$

effectively freezing the orbital.

However, this idea can be improved radically using our mathematical insight of the structure of the gradient. The gradient can be considered as having two parts: an occupied – occupied block (inactive – active and active – active rotations) and an occupied – virtual block (occupied – virtual and occupied – positronic rotations). The occupied – virtual block of this matrix will have $n_{occ}$ columns and $n_{virt} = n^e_{virt} + n^p_{virt}$ rows. From linear algebra we know that this matrix will have rank $\leq \min(n_{occ}, n_{virt}) = n_{occ}$ assuming $n_{occ} < n_{virt}$. It is now possible to perform a *singular value decomposition* (SVD) of the occupied – virtual block of the gradient, transforming the virtual orbitals to the set of virtuals that gives the most compact representation of the gradient. This is done by diagonalization of the matrix $\mathbf{g}^\dagger_{occ-virt}\mathbf{g}_{occ-virt}$, and transforming the virtual orbitals with the eigenvector solutions of this matrix. After this transformation only $n_{occ}$ virtual orbitals will have non-zero gradient elements, and one may freeze the remaining orbitals.

Step 3 in Section 4.10 is replaced with a $(ga|aa)$ integral transformation, needed to get the gradient correct. After Step 4 we perform the transformation of the virtual orbitals as described above. The virtual parts of the gradient and all the Fock matrices calculated in Step 4 must also be transformed. Before Step 6 we have to calculate the integrals needed for the micro-iterations: $(gg|aa)$ and $(ga|ga)$, but only with the reduced set excluding the orbitals with zero gradient. In effect, we have reduced the integral transformation from $n^2n^2_{active}$ to $nn^3_{active}$ (for the gradient) + $(2n_{occ})^2n^2_{active}$ (for the sigma vectors). Since, in general, $2n_{occ} \ll n$ this will give big reductions in CPU time and disk space requirements.

We have, however, assumed that the Hessian is diagonal, Eq. (5.5). If this is not the case we are effectively using a projected Hessian, and if the coupling blocks are large the quadratic convergence is destroyed. Unfortunately, preliminary test shows that this is actually the case often leading to extremely slow convergence.

The reduced set of orbital gives a correct description of the gradient. Along the same lines as above we add the orbitals that gives the most compact description of the initial orbital trial vector

$$b^o_{pq} = \frac{-g_{pq}}{H_{pq,pq}}. \tag{5.8}$$

Like before, we diagonalize $\mathbf{b}^\dagger_{occ-virt}\mathbf{b}_{occ-virt}$ and select the set of orbitals with eigenvalues larger than zero, yielding a total number of $2n_{occ}$ virtuals. These virtuals include a correct description of the gradient and the initial trial vector, and the couplings between these. Preliminary test shows that the

convergence is still very slow, but faster than only including the gradient SVD orbitals. The convergence is not quadratic but rather linear and comparable to DIIS DHF iterations.

Status: implemented, but requires more work in order to run satisfactory. This can be exploited by any MCSCF program, but will be most beneficial for the programs using direct molecular integral transformations.

### 5.5.6 Frozen Orbitals (III)

It is also possible to combine the two previous approaches including virtuals which has SVD eigenvalues larger than zero *or* $\mathbf{F}^C + \mathbf{F}^V$ Fock matrix eigenvalues smaller than some threshold, for example 100 au. With this approach we freeze all high-lying virtuals but except those of them that are important for the gradient. The advantage compared to *Frozen orbitals (I)* above, is that the full gradient is calculated, and that the high-lying virtuals is relaxed, but only macro iterations where they are important to describe the gradient.

Status: implemented, but gives slow convergence.

### 5.5.7 Neglect Positronic Part of $\tilde{\mathbf{F}}^Q$

As the positronic part of the molecular integral file is dominant it would also be of interest to approximate (or neglect) the positronic part of the auxiliary Fock matrices. A straightforward strategy would be to approximate the two-electron density matrix

$$P_{ux,xy} \approx D_{uv} D_{xy} - D_{uy} D_{xv}, \tag{5.9}$$

in which case $\mathbf{F}^Q$ reduces to (written in spinor basis)

$$\begin{aligned} F^Q_{pq} &= \sum_{vxy} (pv|xy)\, P_{qv,xy} \\ &\approx \sum_{vxy} (pv|xy)\, (D_{qv} D_{xy} - D_{qy} D_{xv}) \\ &= \sum_{v} F^V_{px} D_{qv}. \end{aligned} \tag{5.10}$$

This is exact for doubly-occupied and empty orbitals, but the exchange term is under-estimated for weakly occupied orbitals. So a better solution would be to use the better approximation

$$P_{uv,xy} \approx D_{uv} D_{xy} - \delta_{uy} D_{xv}, \tag{5.11}$$

in which case $\mathbf{F}^Q$ reduces to (written in spinor basis)

$$\begin{aligned} F^Q_{pq} &= \sum_{vxy} (pv|xy)\, P_{qv,xy} \\ &\approx \sum_{vxy} (pv|xy)\, (D_{qv} D_{xy} - \delta_{uy} D_{xv}) \\ &= \sum_{v} D_{qv} \left[ \sum_{xy} D_{xy}\, (pv|xy) \right] - \sum_{y} \delta_{qy} \left[ D_{vx}\, (pv|xy) \right] \\ &= \sum_{v} F^{\mathrm{Cou}}_{px} D_{qv} - F^{\mathrm{Exch}}_{pq} \end{aligned} \tag{5.12}$$

where $\mathbf{F}^{\mathrm{Cou}}$ and $\mathbf{F}^{\mathrm{Exch}}$ are Coulomb-only and exchange-only Fock matrices, respectively. Unlike Eq. (5.10) this approximation requires the calculation of new Fock matrices.

However, as we still need integrals with one positronic index for the gradient[1] and for the one-index transformed Hamiltonian needed for the orbital contribution to the configurational sigma vector we can not totally neglect positronic integrals. With integrals with one positronic index we will get: (i) a correct gradient, (ii) correct $e-e$ block of Hessian, (iii) correct $e-p$ block of Hessian, but (iv) *incorrect* $p-p$ block of Hessian. The latter should not, in general, matter as the $p-p$ block of the Hessian is dominated by $2mc^2$. For example, within the Sternheim approximation [7] (see also Aucar *et al.* [8]) the $p-p$ part of the Hessian is actually explicitly set to $2mc^2$.

It is possible to go even further and approximate the entire orbital–orbital part of the Hessian using Eqs. (5.10) or (5.12). In order to get the gradient correct we only need $(ga|aa)$ integrals (this also gives a correct configurational – orbital part of the Hessian).

Status: Eq. (5.10) is implemented (the calculation "only" requires $(ge|ea)$ integrals). Eq. (5.12) would be very easy to implement. The suggested approximation of the entire $e-e$ Hessian has also been implemented, but preliminary test indicates convergence problems most likely caused by the Hessian being non-Hermitian. It is apparently important to add terms to the sigma-vectors which makes the Hessian Hermitian. If it is possible to make this approximation stable it could also be applied in non-relativistic MCSCF programs.

[1] In order to control and check convergence it is necessary to calculate the gradient correctly. With a correct gradient we can do any approximation to the Hessian as this will only affect the rate of convergence. With an approximate gradient *and* an approximate Hessian we may converge to wrong orbitals!

### 5.5.8 Diagonalization or Cholesky Decomposition of the Two-Electron Density Matrix

It is also possible to diagonalize the two-electron density matrix

$$\mathbf{P}_{\cdot,\cdot} = \mathbf{V}^\dagger \mathbf{\Lambda} \mathbf{V}, \tag{5.13}$$

where $\mathbf{\Lambda}$ is a diagonal matrix. This allows us to write the auxiliary Fock matrix as a sum of Coulomb-only Fock matrices

$$\begin{aligned} F^Q_{pq} &= \sum_{xvy} (pv|xy)\, P_{qv,xy} \\ &= \sum_i \lambda_i V_{qv,i} V^*_{i,xy}\, (pv|xy) \\ &= \sum_i \lambda_i V_{qv,i} F'_{pv}, \end{aligned} \tag{5.14}$$

where $\mathbf{F}'$ is a Coulomb-only Fock matrix. Another possibility is to Cholesky decompose the residual after Eq. (5.10)

$$P_{ux,xy} - D_{uv} D_{xy} - D_{uy} D_{xv}. \tag{5.15}$$

The auxiliary Fock matrix can be calculated as Eq. (5.10) plus an additional number of Coulomb-only Fock matrices. With both of these two methods we would only need integrals with one general (electronic and positronic) index and three active indices to get both gradient and Hessian correct. The price we pay is having to calculate many Fock matrices (in the worst case scenario: $a^2$ Fock matrix where $a$ denotes the number of active orbitals.

Status: not implemented, but it requires very little work to do so.

### 5.5.9 Partial Neglect of $(LL|SS)$ or $(SS|SS)$ Integrals

The so-called *one center* approximation [9] for the small component two-electron integrals

$$\begin{aligned} (\mu^S_A \nu^S_B | \kappa^S_C \lambda^S_D) &\approx \delta_{AB} \delta_{CD}\, (\mu^S_A \nu^S_B | \kappa^S_C \lambda^S_D)\,, \\ (\mu^L_A \nu^L_B | \kappa^S_C \lambda^S_D) &\approx \delta_{CD}\, (\mu^L_A \nu^L_B | \kappa^S_C \lambda^S_D)\,, \end{aligned} \tag{5.16}$$

where $A$, $B$, $C$, and $D$ indicate on which center the atomic orbital basis function is located, can speed-up the integral transformation and Fock matrix constructions. The savings are largest for molecules with more than one heavy atom, but even for molecules such as YbH there is a saving of approx.

30% in Fock matrix constructions. It would also be advantageous to dynamically determine which integrals are needed. For example, far away from convergence it would, in general, be a waste of time to calculate all Fock matrices and integrals with all $(LL|LL)$, $(LL|SS)$, and $(SS|SS)$ integrals. Note that for consistency the KR-MCSCF calculation should start with at least the same integral classes as the DHF calculation, otherwise the KR-MCSCF optimization might "undo" some of effects of the $(LL|SS)$ and $(SS|SS)$ integrals in the first few iterations, and then "redo" the changes later when the $(LL|SS)$ and $(SS|SS)$ are introduced in the KR-MCSCF optimization.

Integral screening in the integral transformation has also been implemented [10].

Status: implemented.

## 5.6 Approximate Hamiltonians

Beside the standard Dirac-Coulomb Hamiltonian DIRAC also supports both a spin-free Dirac-Coulomb Hamiltonian based on Dyall's spin-free formalism [11] and the Lévy-Leblond non-relativistic Hamiltonian [12, 13].

Status: The program already supports the use of real or approximate boson symmetry in the CI expansion, but it could also be advantageous to use spin multiplet (singlet, triplet, etc.) adapted CSFs.

## 5.7 Neglect of $e-p$ Rotations

Finally, it is possible to neglect the $e-p$ rotations. Within this approximation the positronic solutions are not relaxed at the MCSCF step. In the limit of full CI this corresponds to the no-pair CI method. See Section 6.1, and 6.2 for the effect of $e-p$ rotations on energy and some first order properties.

Status: Implemented.

## 5.8 Separate Convergence Thresholds for $e-e$ and $e-p$ Rotations

Suppose we have a relativistic MCSCF wave function that is fully relaxed with respect to $e-e$ relaxations, *i.e.* $\|\mathbf{g}^e\| < t$, where $t$ is the wave function threshold. The pure positronic Newton step is

$$\mathbf{x}^p = -\mathbf{H'}^{-1}\mathbf{g}^p. \tag{5.17}$$

and the predicted second order energy change is

$$\begin{aligned}\Delta E^p &= -\frac{1}{2}\mathbf{g}^{p\dagger}\mathbf{H}'^{-1}\mathbf{g}^p \\ &\approx \|\mathbf{g}^p\|^2\frac{1}{2mc^2},\end{aligned} \tag{5.18}$$

as the positronic part of the Hessian is dominated by $-2mc^2$, The second order energy change from a pure electronic step is

$$\Delta E^e \approx -t^2. \tag{5.19}$$

If we require that $\Delta E^p < |\Delta E^e|$ we get:

$$\|\mathbf{g}^p\| < \sqrt{2}ct \approx 200t. \tag{5.20}$$

The step length associated with this gradient is:

$$\|\mathbf{x}^p\| \approx \frac{t}{200}. \tag{5.21}$$

That is, if we are only interested in the energy or the wave function we can choose separate threshold for the convergence of $e-e$ rotations and $e-p$ rotations! However, care should be taken if the wave function is used for properties that critically depend on the small component density such as parity violation, or if the wave function is used for linear or higher-order response where it is assumed that the wave function is converged, *i.e.* the last part of Eq. 4.59 or Eq. (4.59) is ignored leaving the Hessian Hermitian only to within $\|\mathbf{g}^p\|$, which may result in problems converging the response functions.

Status: not implemented, but it is very trivial to do so.

## 5.9 Transformation to Natural and Fock Type Orbitals

Similar to non-relativistic MCSCF optimizations (*e.g.*, see Ref. [14]) it may be advantageous to transform the orbitals obtained in Step 7 in Section 4.10 in order to improve the diagonal dominance of the Hessian. For non-relativistic calculations there is empirical evidence that the inactive and virtual orbitals that diagonalize $\mathbf{F}^C + \mathbf{F}^V$ improves diagonal dominance, and transformation of the active orbitals to natural orbitals (the orbitals that diagonalize the active part of the one-electron density matrix) also improves diagonal dominance. For GAS calculations pseudo-natural orbitals that diagonalize the

density matrix within each GAS space are used, as the energy is generally not invariant to rotations between the GAS spaces. It should be noted that the transformation to natural or pseudo-natural active orbitals also change the CI vector, which has to be counter-rotated [15, 16].

Status: Fock type orbitals are implemented, although without the counter-rotation of the CI vectors, which limits us to the transformation of only the inactive, virtual, and positronic orbitals.

## 5.10 Parallelization

Parallelization is possible (and beneficial) at the following steps:

1. integral transformation step,
2. Fock matrix calculations (for the gradient or various parts of the sigma vectors),
3. CI sigma vectors and density matrices.

Status: Partially implemented; the integral transformation step and the Fock matrix calculations are both parallelized, and, within the current implementation, it should be very simple to add parallelization of CI sigma vectors and density matrices.

## 5.11 Hessian Update Methods

As an alternative to the gradient and Hessian based optimization procedure presented, it is also possible to use gradient based optimization with an approximate Hessian. The Hessian can be updated using the previous calculated gradients (*e.g.*, see the monograph by Fletcher [17]). The use of gradient based methods requires only $(ga|aa)$ integrals.

Status: not implemented.

## 5.12 Start Orbitals

Finally, we note the importance of good start orbitals. As discussed in Ch. 3 canonical DHF orbitals are not particularly well suited, as the lowest virtuals often are very diffuse functions which we do not want to include in the active space. Other possibilities include $h_1$-virtuals or $F^C$-virtuals [18], and average-of-configuration DHF orbitals. For heavy atoms the quality (proper

degeneracies, proper occupation) of the final converged DHF orbitals depend, in general, strong on the quality of the DHF start orbitals. Currently the only option for DHF start orbitals in DIRAC is the orbitals obtained from the diagonalization of the one-electron Hamiltonian, that is, the orbitals obtained from solving a one-electron system. The lowest orbitals are then occupied according to the aufbau principle. From non-relativistic theory the orbital energies are given by

$$E = -\frac{Z^2}{2n^2}, \tag{5.22}$$

which means that the orbital energies of the start orbitals are almost degenerate for each shell. This will always give wrong start occupation for the 4th row and below in the periodic system! For example, for LiI the proper occupation for iodine is $1s2s2p3s3p3d4s4p4d5s5p$ where $5s5p$ is in the valence. However, using the orbitals from the diagonalization of the one-electron Hamiltonian will instead occupy $1s2s2p3s3p3d4s4p4d4f$ as the $4f$ will have eigenvalues much lower in energy ($\approx -88$ au.) compared to the 5-shell ($\approx -56$ au.). Besides slowing down convergence we may often end up with orbitals that do not have the proper degeneracies and in the average-of-configuration case we may have wrong orbitals among the active orbitals or shells divided between different active spaces. When these "broken" orbitals are used in the following MCSCF procedure it may be impossible or difficult to converge towards the state we are interested in.

As an alternative to using Fock orbitals (canonical, average-of-configuration, $h_1$-virtuals, or $F^C$-virtuals) natural orbitals (MP2 NO) can be used as MCSCF start orbitals. MP2 NOs is probably the best method for obtaining start orbitals even for molecules with large static correlation [19], where the MP2 natural occupation numbers are far from correct, but where the ordering of the orbitals is still correct.

However, MP2 is still more expensive than DHF in terms of CPU time, and open-shell MP2 is not entirely trivial restricting us to closed shell molecules.

Status: MP2 NO is under implementation. A better DHF start guess is, however, still needed, for example, atomic densities or relativistic Hückel.

# Bibliography

[1] H. J. Aa. Jensen, in *Relativistic and Electron Correlation Effects in Molecules and Solids*, edited by G. L. Malli (Plenum, New York, 1994), p. 179.

[2] H. J. Aa.. Jensen, K. G. Dyall, T. Saue, and K. Faegri, Jr., J. Chem. Phys. **104**, 4083 (1996).

[3] H. J. Aa. Jensen, unpublised.

[4] T. Fleig, J. Olsen, and C. Marian, J. Chem. Phys. (2001), (in press).

[5] T. Saue and H. J. Aa. Jensen, *Relativistic 4-component linear response*, unpublished.

[6] P. Norman and H. J. Aa. Jensen, *Relativistic 4-component quadratic reponse*, unpublished.

[7] M. M. Sternheim, Phys. Rev. **128**, 676 (1962).

[8] G. A. Aucar, T. Saue, L. Visscher, and H. J. Aa. Jensen, J. Chem. Phys. **110**, 6208 (1999).

[9] H. J. Aa. Jensen and L. Visscher, unpublished.

[10] T. Saue, unpublished.

[11] K. G. Dyall, J. Chem. Phys. **100**, 2118 (1994).

[12] J. M. Lévy-Leblond, Comm. Math. Phys. **6**, 286 (1967).

[13] J. M. Lévy-Leblond, Annln. Phys. **57**, 481 (1970).

[14] H. J. Aa. Jensen, H. Ågren, and J. Olsen, in *Modern Techniques in Computional Chemistry 1990*, edited by E. Clementi (Escom, Leiden, 1990).

[15] P.-Å. Malmquist, Int. J. Quant. Chem. **30**, 479 (1986).

[16] P.-Å. Malmquist and B. O. Roos, Chem. Phys. Lett. **155**, 189 (1989).

[17] R. Fletcher, *Practical methods of optimization*, vol. 1 (Wiley, New York, 1980).

[18] C. W. Bauschlicher, J. Chem. Phys. **72**, 880 (1980).

[19] H. J. Aa. Jensen, private communication.

# Chapter 6

# Preliminary Applications

Very early in the development we discovered that one of the bottlenecks in larger KR-MCSCF calculation is the calculation of molecular integrals. This is partly due to an, for our purposes, sub-optimal implementation of the molecular integral transformation, but also partly due to the large basis sets we use. Therefore we concentrated most of our efforts on developing several schemes for speeding up the integral transformation step. As a consequence we can only present a few preliminary applications. Nevertheless, these calculations show some very interesting features of relativistic MCSCF calculations.

## 6.1 The Ionization Potential of Zn and Hg

The first ionization potential, $\mathrm{IP}_1$, of Zn is defined by

$$\mathrm{IP}_1 = E(\mathrm{Zn}^+) - E(\mathrm{Zn}), \tag{6.1}$$

where $E(\mathrm{Zn}^+)$ and $E(\mathrm{Zn})$ are the energies of $\mathrm{Zn}^+$ and Zn, respectively. Zn has near-degeneracies due to the strong interaction between $4s^2_{1/2}$, $4p^2_{1/2}$, and $4p^2_{3/2}$ configurations [2]. Hg has a similiar electronic structure, and we expect strong static correlation due to the interaction between the $6s^2_{1/2}$, $6p^2_{1/2}$, and $6p^2_{3/2}$ configurations.

For Zn we used a $20s18p13d$ large component basis set (Ref. [2] or see Table 6.1), and for Hg we used a $23s19p14d9f$ large component basis set [3] to which we added two diffuse $p$ functions for the description of the $6p$ orbitals (see Table 6.2 for the basis set). The different active space we have used are defined in Table 6.3. The relativistic calculations have been performed with the Dirac-Coulomb Hamiltonian, and without $e-p$ relaxation. The effect of the Breit interaction not included in the Dirac-Coulomb Hamiltonian

Table 6.1: Exponents for $20s18p13d$ large component Zn basis set. The exponents are taken from Ref. [1] and ranges for the $s$, $p$, and $d$ functions are taken from Ref [2]. The small component basis set is generated by kinetic balance.

| Exponents | Used for |
|---|---|
| 4250042.1 | $s$ |
| 663740.70 | $s$ |
| 144800.18 | $sp$ |
| 38457.241 | $sp$ |
| 11633.475 | $sp$ |
| 3957.4984 | $sp$ |
| 1508.8936 | $sp$ |
| 624.94155 | $spd$ |
| 272.06944 | $spd$ |
| 121.77099 | $spd$ |
| 54.721784 | $spd$ |
| 24.885485 | $spd$ |
| 11.536923 | $spd$ |
| 5.2194206 | $spd$ |
| 2.34219989 | $spd$ |
| 1.0625147 | $spd$ |
| 0.46920953 | $spd$ |
| 0.18025741 | $spd$ |
| 0.08726504 | $spd$ |
| 0.04021766 | $spd$ |

Table 6.2: Exponents for $23s21p14d9f$ large component Hg basis set. The exponents are taken from Ref. [3] except for two extra $p$ exponents. The small component basis set is generated by kinetic balance.

| Exponents | Used for | Exponents | Used for |
|---|---|---|---|
| 52311095.52 | $(s)$ | 16369430.48 | $(p)$ |
| 12004904.50 | $(s)$ | 2923564.628 | $(p)$ |
| 3398412.630 | $(s)$ | 665746.2787 | $(p)$ |
| 1053466.233 | $(s)$ | 176341.9102 | $(p)$ |
| 352643.1218 | $(s)$ | 52520.02187 | $(p)$ |
| 125378.8033 | $(s)$ | 17323.66041 | $(p)$ |
| 46972.27384 | $(s)$ | 6286.133614 | $(p)$ |
| 18358.59081 | $(s)$ | 2487.310520 | $(p)$ |
| 7416.846186 | $(sd)$ | 1058.036925 | $(p)$ |
| 3086.363699 | $(sd)$ | 475.7144214 | $(pf)$ |
| 1323.964977 | $(sd)$ | 223.3130370 | $(pf)$ |
| 582.7863441 | $(sd)$ | 108.1488395 | $(pf)$ |
| 265.3934503 | $(sd)$ | 52.33974957 | $(pf)$ |
| 125.7373693 | $(sd)$ | 26.18680515 | $(pf)$ |
| 61.44748799 | $(sd)$ | 12.96730950 | $(pf)$ |
| 30.74341476 | $(sd)$ | 6.287389869 | $(pf)$ |
| 15.11217155 | $(sd)$ | 2.961603741 | $(pf)$ |
| 7.329464658 | $(sd)$ | 1.274534919 | $(pf)$ |
| 3.486387448 | $(sd)$ | 0.4920498338 | $(p)$ |
| 1.499571734 | $(sd)$ | 0.189961 | |
| 0.5971311522 | $(sd)$ | 0.073337 | |
| 0.2083253336 | $(sd)$ | | |
| 0.06626400900 | $(s)$ | | |

Table 6.3: Definition of active spaces for relativistic and non-relativistic MCSCF calculations on Zn and $Zn^+$ ($n = 4$) and Hg and $Hg^+$ ($n = 6$). Excitation level is the excitations allowed from *active space 1* into *active space 2* (S=singles; D=doubles).

| Calculation | Active space 1 | Active space 2 | Excitation level |
|---|---|---|---|
| dhf | empty | empty | n/a |
| cas1 | $nsnp$ | empty | n/a |
| ras1 | $(n-1)dnsnp$ | $nd(n+1)s$ | SD |

Table 6.4: SCF and MCSCF energies (au) for ground-state Zn ($^1S_0$) and $Zn^+$ ($^2S_{1/2}$), and first ionization potential (eV) for Zn. See text and Table 6.3 for definition of calculations.

| Calculation | $E$(Zn) (au) | $E$($Zn^+$) (au) | $IP_1$ (eV) |
|---|---|---|---|
| | Non-relativistic | | |
| hf | −1777.84077 | −1777.56021 | 7.634 |
| cas1 | −1777.87224 | −1777.56021 | 8.491 |
| ras1 | −1778.08064 | −1777.77471 | 8.572 |
| | Relativistic | | |
| dhf | −1794.61046 | −1794.32410 | 7.792 |
| cas1 | −1794.64154 | −1794.32410 | 8.638 |
| ras1 | −1794.85249 | −1794.54140 | 8.465 |
| Exp. (Ref. [4]) | | | 9.388 |

Table 6.5: SCF and MCSCF energies (au) for ground-state Hg ($^1S_0$) and $Hg^+$ ($^2S_{1/2}$), and first ionization potential (eV) for Hg.

| Calculation | $E$(Hg) (au) | $E$($Hg^+$) (au) | $IP_1$ (eV) |
|---|---|---|---|
| | Non-relativistic | | |
| hf | −18408.3278 | −18408.0779 | 6.80 |
| cas1 | −18408.3570 | −18408.0779 | 7.59 |
| | Relativistic | | |
| dhf | −19648.8777 | −19648.5632 | 8.56 |
| cas1 | −19648.9023 | −19648.5632 | 9.23 |
| Exp. (Ref. [4]) | | | 10.44 |

Table 6.6: CI Coefficients for ground state Zn ($n = 4$) and Hg ($n = 6$) MCSCF calculations.

| Configuration | Zn | | Hg | |
|---|---|---|---|---|
| | $c_I^{\rm rel}$ | $c_I^{\rm nr}$ | $c_I^{\rm rel}$ | $c_I^{\rm nr}$ |
| $(ns_{1/2})^2$ | 0.970511 | 0.969052 | 0.979622 | 0.966388 |
| $(np_{1/2})^2$ | −0.141310 | −0.142521 | −0.136079 | −0.148428 |
| $(np_{3/2})^2$ | −0.138091 | −0.142521 | −0.104457 | −0.148428 |

Table 6.7: Natural orbital occupation numbers for ground state Zn ($n = 4$) and Hg ($n = 6$) MCSCF calculations.

| Orbital | Zn | | Hg | |
|---|---|---|---|---|
| | $NO^{rel}$ | $NO^{nr}$ | $NO^{rel}$ | $NO^{nr}$ |
| $ns_{1/2}$ | 1.884 | 1.878 | 1.919 | 1.868 |
| $np_{1/2}$ | 0.040 | 0.041 | 0.037 | 0.044 |
| $np_{3/2}$ | 0.038 | 0.041 | 0.022 | 0.044 |

is localized to the core region, hence it gives similar energy shift for both X and $X^+$ (X=Zn,Hg) and should therefore have very little influence on the ionization potential [2, 5]. The effect of relaxing the positronic orbitals has also largest effect on the core region and should therefore not have any significant effect on the IP (See Sec. 5.8 for a discussion on the effect of $e - p$ relaxation on the energy). We used DALTON [6] and DIRAC [7] for the non-relativistic and relativistic calculations, respectively.

The energies and the $IP_1$ for Zn is given in Table 6.4. For Zn the energy difference between the *dhf* and *cas1* calculations (0.31 au) is the static correlation energy for the interaction between the $4p^2$ states. Note that the static correlation energy is the same at both the relativistic and the non-relativistic level. For Zn+ there are no interaction between the $4s$ and the $4p$ state due to inversion symmetry. For Hg there is a relativistic static correlation energy of 0.025 au, whereas it is 0.029 au at the non-relatistic level, that is, relatistic effects and correlation effects are non-additive. For Zn the relativistic effect on the $IP_1$ is only 0.15 eV, whereas it for Hg is 1.64 eV. For both calculations relativity is clearly needed for quantitative descriptions, and for Hg even for qualitative descriptions.

The strong static correlation for both Zn and Hg can also be seen from the large CI coefficients on the $p^2$ configurations (Table 6.6) or from the large natural orbital (NO) occupation numbers of the $p$ orbitals (Table 6.7). Also note the spin-orbit splitting of the CI coefficients and NO occupation numbers.

Based on non-relativistic MP2 natural occupation numbers for Zn it is important to correlate the $3d$ orbitals, which is why we have selected a larger active space with 12 electrons in the $3d4s4p4d5s$ orbitals. However, a CAS calculation in this space requires more than 20 million determinants, which is way beyond the limits of the current KR-MCSCF program. Instead we use the restricted active space approach and split the active space into a RAS1 space with $4d4s4p$ and a RAS2 space of $4d5s$, allowing only single

and double excitations (the *ras1* calculation). However, this calculations is not large enough to obtain the the experimental value for the Zn $IP_1$ (9.388 eV, Ref. [4]). We need to include more dynamical correlation, either in terms of relativistic CASPT2 (*e.g.*, see Ref. [2]), multi-reference CI, or even larger MCSCF calculations. It will not be sufficient to do a relativistic MP2 calculation due to the large static correlation.

Similarly, we need to retrieve dynamical correlation to obtain a $IP_1$ for Hg comparable to the experimental value.

We also note that it was very difficult to obtain suitable start orbitals for Zn for the *ras1* and *ras2* calculations. $h_1$-virtuals and $F^C$-virtuals as start orbitals did not work and the calculations converged towards a wrong state. The average-of-configuration orbitals were so far away from the converged orbitals that it required 25+ KR-MCSCF macro iterations to converge, but eventually the calculation converged towards the right state. The problem was the core-correlating orbitals present in the basis set, so we solved the problem using $F^C$-virtuals and freezing the core. When the frozen-core calculation had converged we let the core orbitals relax. This clearly emphasizes the need for a relativistic natural orbital MP2 start guess.

## 6.2 The Effect of Relativity and Correlation on the Dipole Moments, Electric Field Gradients, and Electric Field Third Derivatives for LiX, X=F, Cl, Br, I

### 6.2.1 Introduction

In this section we briefly investigate the effects of relativity and correlation on a number of first-order properties for LiX, X=F,Cl,Br,I. We calculate the properties at the several levels:

***nr*** non-relativistic,

***noep*** relativistic with bare-nucleus positronic orbitals projected out, which can be considered equivalent to an infinite order Douglas-Kroll transformation

***skipep*** relativistic with $e-p$ relaxation only at the DHF level (the no-pair approximation at the correlated level),

***full*** relativistic with $e-p$ relaxation both at the DHF and MCSCF level (the most rigous treatment)

We calculate the dipole moment, the electric field gradient (EFG), and the electric field third derivative (EFT). The dipole moment is chosen as an representative of a valence property. The EFG and EFT are chosen as presentatives of core properties. *A priori* we expect increasing relativistic effects going down the periodic table; from almost no effects in LiF to considerable effects in LiI. Also, for the relativistic MCSCF calculations we do not expect many differences between the *noep*, *skipep*, and *full* treatment, as the relaxation of the $e-p$ orbitals are not so important for these kind of properties. The importance of the $e-p$ relaxation is most evident in calculation of second-order magnetic properties, such as in-direct spin-spin couplings [8]. However as we have not yet developed at MC-RPA program we are not able to investigate this yet.

### 6.2.2 Computational Details

The bond lengths for all compounds were taken from [9]. The *Sadlej* polarized basis set [10–12] were used for all atoms. All calculations were performed with the DIRAC [7] program package using the Dirac-Coulomb Hamiltonian for the relativistic calculations and the 4-component non-relativistic Lévy-Leblond Hamiltonian for the non-relativistic calculations.

### 6.2.3 Results

For LiF we have chosen an active space consisting of the Iodine $2s2p3s3p$ orbitals. The iodine $2p$ orbitals are mixed with the Lithium 2s orbital, so the total number of active orbitals is 8 with 8 electrons (CAS 8/8). This active space is very similar to the non-relativsitic "4220" CAS space often employed for $H_2O$. As both Li and F are light atoms we do not expect any major relativistic effects for properties.

The results of the calculations on LiF are given in Table 6.8. The relavistic effects are, as expected, negligible. The effects of correlation varies very much, ranging from a negligible few percent for the dipole moment to 30%+ for the electric field gradient on F. As the relativistic effects are small there are virtually no difference at all between the different levels of $e-p$ rotations.

For LiF the most important correlating orbitals are the $3p$ orbitals. However, for LiCl and down the most important correlating orbitals are the $nd$ orbitals ($3d$ for LiCl, $4d$ for LiBr, and $5d$ for LiI). Based on non-relativistic MP2 natural occupation numbers we choose an active space of the $3p3d4p$ with 6 electrons (CAS 6/11). The correlating $3d$ orbitals include some hybridization with the Li $3s$ orbitals. The correlating $4p$ orbitals are also mixed with the $4d$ orbitals.

Table 6.8: Energy and properties for LiF. E is the total energy, $\mu$ the dipole moment, $q_{zz}^X$ is the electric field gradient at nucleus X, and $h_{zzzz}^X$ is the electric field third derivative at nucleus X.

| Wave function | E<br>au | $\mu$<br>Debye | $q_{zz}^{\mathrm{Li}}$<br>au | $q_{zz}^{\mathrm{F}}$<br>au | $h_{zzzz}^{\mathrm{Li}}$<br>au | $h_{zzzz}^{\mathrm{F}}$<br>au |
|---|---|---|---|---|---|---|
| Non-relativistic | | | | | | |
| HF | −106.976091 | 6.4831 | −0.0468 | −0.1848 | 0.0422 | 0.1135 |
| CAS (8/8) | −107.106556 | 6.3422 | −0.0412 | −0.2418 | 0.0556 | 0.1149 |
| Relativistic | | | | | | |
| DHF (*noep*) | −107.068329 | 6.4814 | −0.0468 | −0.1853 | 0.0421 | 0.1134 |
| DHF | −107.068328 | 6.4834 | −0.0468 | −0.1853 | 0.0421 | 0.1134 |
| CAS 8/8 (*noep*) | −107.200506 | 6.3375 | −0.0411 | −0.2418 | 0.0556 | 0.1151 |
| CAS 8/8 (*skipep*) | −107.200505 | 6.3375 | −0.0411 | −0.2418 | 0.0556 | 0.1151 |
| CAS 8/8 (*full*) | −107.200505 | 6.3375 | −0.0411 | −0.2418 | 0.0556 | 0.1151 |

Table 6.9: Energy and properties for LiCl. E is the total energy, $\mu$ the dipole moment, $q_{zz}^X$ is the electric field gradient at nucleus X, and $h_{zzzz}^X$ is the electric field third derivative at nucleus X.

| Wave function | E<br>au | $\mu$<br>Debye | $q_{zz}^{\mathrm{Li}}$<br>au | $q_{zz}^{\mathrm{Cl}}$<br>au | $h_{zzzz}^{\mathrm{Li}}$<br>au | $h_{zzzz}^{\mathrm{Cl}}$<br>au |
|---|---|---|---|---|---|---|
| Non-relativistic | | | | | | |
| HF | −467.041624 | 7.2917 | −0.0273 | 0.1557 | 0.0276 | 0.0256 |
| CAS (6/11) | −467.161987 | 7.2706 | −0.0270 | 0.1634 | 0.0279 | 0.0223 |
| Relativistic | | | | | | |
| DHF (*noep*) | −468.490493 | 7.2859 | −0.0273 | 0.1549 | 0.0275 | 0.0256 |
| DHF | −468.490479 | 7.2859 | −0.0273 | 0.1549 | 0.0275 | 0.0256 |
| CAS 6/11 (*noep*) | −468.617901 | 7.2521 | −0.0268 | 0.1723 | 0.0280 | 0.0258 |
| CAS 6/11 (*skipep*) | −468.617885 | 7.2521 | −0.0269 | 0.1723 | 0.0280 | 0.0258 |
| CAS 6/11 (*full*) | −468.617891 | 7.2519 | −0.0269 | 0.1728 | 0.0280 | 0.0258 |

Table 6.10: Energy and properties for LiBr. E is the total energy, $\mu$ the dipole moment, $q_{zz}^X$ is the electric field gradient at nucleus X, and $h_{zzzz}^X$ is the electric field third derivative at nucleus X.

| Wave function | E<br>au | $\mu$<br>Debye | $q_{zz}^{\mathrm{Li}}$<br>au | $q_{zz}^{\mathrm{Br}}$<br>au | $h_{zzzz}^{\mathrm{Li}}$<br>au | $h_{zzzz}^{\mathrm{Br}}$<br>au |
|---|---|---|---|---|---|---|
| Non-relativistic | | | | | | |
| HF | −2579.89999 | 7.4471 | −0.0177 | 0.3704 | 0.0302 | −0.5777 |
| CAS (6/11) | −2580.00518 | 7.3903 | −0.0172 | 0.4071 | 0.0306 | −0.4758 |
| Relativistic | | | | | | |
| DHF (*noep*) | −2610.60078 | 7.4348 | −0.0180 | 0.3884 | 0.0293 | −0.3621 |
| DHF | −2610.60025 | 7.4348 | −0.0180 | 0.3884 | 0.0293 | −0.3622 |
| CAS 6/11 (*noep*) | −2610.70538 | 7.3708 | −0.0174 | 0.4226 | 0.0298 | −0.2465 |
| CAS 6/11 (*skipep*) | −2610.70485 | 7.3708 | −0.0174 | 0.4227 | 0.0298 | −0.2465 |
| CAS 6/11 (*full*) | −2610.70489 | 7.3706 | −0.0175 | 0.4224 | 0.0298 | −0.2490 |

Table 6.11: Energy and properties for LiI. E is the total energy, $\mu$ the dipole moment, $q_{zz}^X$ is the electric field gradient at nucleus X, and $h_{zzzz}^X$ is the electric field third derivative at nucleus X.

| Wave function | E<br>au | $\mu$<br>Debye | $q_{zz}^{\mathrm{Li}}$<br>au | $q_{zz}^{\mathrm{I}}$<br>au | $h_{zzzz}^{\mathrm{Li}}$<br>au | $h_{zzzz}^{\mathrm{I}}$<br>au |
|---|---|---|---|---|---|---|
| Non-relativistic | | | | | | |
| HF | −6925.3016 | 7.6676 | −0.0170 | 0.7468 | 0.0220 | −11.6121 |
| CAS (6/8)[a] | −6925.3592 | 7.5171 | −0.0175 | 0.8768 | 0.0226 | 0.6198 |
| CAS (6/11) | −6925.3875 | 7.5958 | −0.0172 | 0.8224 | 0.0226 | −11.4476 |
| Relativistic | | | | | | |
| DHF (*noep*) | −7098.8586 | 7.6333 | −0.0172 | 0.6213 | 0.0207 | −3.1928 |
| DHF | −7098.8586 | 7.6333 | −0.0172 | 0.6213 | 0.0207 | −3.1926 |
| CAS 6/8 (*noep*) | −7098.9359 | 7.5932 | −0.0180 | 0.7005 | 0.0209 | −2.6497 |
| CAS 6/8 (*skipep*) | −7098.9328 | 7.5932 | −0.0180 | 0.7004 | 0.0209 | −2.6498 |
| CAS 6/8 (*full*) | −7098.9328 | 7.5932 | −0.0180 | 0.7004 | 0.0209 | −2.6498 |
| CAS 6/11 (*noep*) | −7098.9458 | 7.5441 | −0.0174 | 0.6928 | 0.0215 | −3.4268 |
| CAS 6/11 (*skipep*) | −7098.9427 | 7.5440 | −0.0174 | 0.6924 | 0.0215 | −3.3867 |
| CAS 6/11 (*full*) | −7098.9427 | 7.5440 | −0.0173 | 0.6924 | 0.0215 | −3.3857 |

*a* This calculation has most likely converged towards an wrong state

The results of the calculations on LiCl are given in Table 6.9. The relativistic effects are still moderate (< 1%), and consequently the difference between the different relativistic CAS calculations are completely negligible. Also, it appears that relativity and correlation are non-additative, but since both correlation and relativstic effects are quite small it is not so important.

For LiBr we choose a active space analogous to the LiCl calculation: 6 electrons in the $4p4d5p$ orbitals. The results of the calculations are given in Table 6.10. As for LiCl the effects of relativity are small for the both dipole moment and the Li electric field (EF) derivatives (relativity: 1 – 2%; correlation 1 – 4%). For the Br EF derivatives the effect of correlation is more than 10% for the Br EFG and 30%+ for the Br EFT. The relativstic effects are larger than correlation effects for the Br EFT, and the non-additivity of correlation and relativistic effects are around 1% for the Br EFT.

Again, for LiI we choose a active space analogous to the LiCl calculation: 6 electrons in the $5p5d6p$ orbitals (CAS 6/11). We have also performed the calculations with the smallest balanced active space consisting of the $5p$ and $5d$ orbitals only (CAS 6/8). The results of the calculations are given in Table 6.11. As for the previous molecules the effect of relativity is quite modest on the dipole moment, and the Li EF derivatives. For the I EF derivatives the effect of relativity is quite large ($\approx$ 20% for $q^I_{zz}$ and more than 70% for $h^I_{zzzz}$). The non-relativistic CAS (6/8) calculation shows some of the problems we have experienced obtaining good start orbitals for heavy atoms. The converged CAS (6/8) state is obviously not the right one, most likely caused by a bad KR-MCSCF start guess.

### 6.2.4 Discussion

Although we expect the LiX, X = F, Cl, Br, I, to have similar electronic structure we see a change in the choice of correlating orbitals. Due to the mathematical structure of the Schrödinger or Dirac equation there are no $2d$ orbitals to correlate the occupied $2p$ orbitals in LiF, hence the most important correlating orbitals are the $3p$ orbitals. LiCl, LiBr, and LiI all have $nd$ orbitals, and they turn out to be the most important ones for correlation. Apart from the underlying mathematical structure this can also be understod qualitatively: the fluorine atom is relatively small and the most important dynamical correlation is the "in-out" correlation which is cared for by the $3p$ orbitals. As chlorine, bromine, and iodine are larger atoms, the $3p$, $4p$, or $5p$ electrons avoid each other by staying on different sides of the atom (angular correlation). The angular correlation is cared for by the $nd$ orbitals.

As a side-remark we also note that obtaining start orbitals are not trivial for the heavier atoms (see Section 3.3.1 for more details).

For LiI we did also perform the non-relativistic HF calculations with a larger uncontracted 28s25p19d10f basis set for I and a 12s9p6d basis set for Li [13]. The values obtained are 7.46 Debye for the dipole moment, $-0.020$ au for the Li EFG, 0.791 au for the I EFG, 0.022 au for the Li EFT, and 17.28 au for the I EFT. Comparing with the values obtained in this work we see moderate effects ($< 10\%$) for all properties except the I EFT which changes sign! A relativistic DHF calculation using the larger basis set yields: 1.045 au for the I EFG and 7.27 au for the I EFT. The differences compared to the Sadlej basis set we employed are quite large. As the EFT transform as $Y_4$ (spherical harmonics with $l = 4$) the EFT is zero for orbitals with $l < 2$ (in LiI the I $1s$ orbitals can give of course give a contribution due to polarization). This means the EFT is very sensitive to the quality of the $d$ basis functions.

Finally, we conclude that both relativity and correlation are needed. For the lighter atoms it is very good approximation to neglect relativity, but for the heavier atoms the effect of relativity can be dramatic. Also, from the LiI calculations we see that relativity and correlation are non-additive, so there is no easy way out, and we have to deal with correlation at the relativistic level. Also, for these molecules that are almost no effect of $e - p$ relaxation. The difference in properties between the *noep*, *skipep*, and *full* calculations presented here are negligible. The largest effect is for the CAS 6/11 calculation of LiI, where the effect is 1% for the I EFT. As the $e-p$ part of the Hessian was the most expensive part of the calculations it is desirable to not include it.

# Bibliography

[1] S. Huzinaga and M. Klobukowski, J. Molec. Spec. **167**, 1 (1988).

[2] M. J. Vilkas, K. Koc, and Y. Ishikawa, Chem. Phys. Lett. **296**, 68 (1998).

[3] K. Fægri, unpublished.

[4] C. E. Moore, *Natl. Bur. Stand. U. S. Circ. No. 467*, vol. Vol. I(1949), Vol. II(1952), and Vol. III(1958) (U.S. GPO, Washington, D.C., 1949, 1952 and 1958).

[5] Y. Ishikawa and K. Koc, Int. J. Quant. Chem. **65**, 545 (1997).

[6] T. Helgaker, H. J. A. Jensen, P. Jørgensen, J. Olsen, K. Ruud, H. Ågren, T. Andersen, K. L. Bak, V. Bakken, O. Christiansen, P. Dahle, E. K.

Dalskov, *et al.*, *DALTON, an electronic structure program, Release 1.0 (1997).*

[7] T. Saue, T. Enevoldsen, T. Helgaker, H. J. A. Jensen, J. Laerdahl, K. Ruud, J. Thyssen, and L. Visscher, *"DIRAC, a relativistic ab initio electronic structure program , Release 3.1 (1998)"*.

[8] G. A. Aucar, T. Saue, L. Visscher, and H. J. Aa. Jensen, J. Chem. Phys. **110**, 6208 (1999).

[9] K. P. Huber and G. Herzberg, *Constants of Diatomic Molecules* (Van Nostrand, New York, 1979).

[10] A. J. Sadlej, Coll. Czech. Chem. Commun. **53**, 1995 (1988).

[11] A. J. Sadlej, Theo. Chim. Acta **79**, 123 (1991).

[12] A. J. Sadlej and M. Urban, J. Molec. Spec. **80**, 147 (1991).

[13] J. Thyssen, P. Schwerdtfeger, M. Bender, W. Nazarewicz, and P. B. Semmes, Phys. Rev. A **63**, 022505 (2001).

# Chapter 7

# Final summary and Future Research

In this thesis we have presented the implementation of a direct Kramers restricted four-component multi-configurational SCF program. The KR-MCSCF method presented is currently the most rigourous way to include relativistic effects along with correlation effects, since we, in contrary to the no-pair CI, MBPT, and CC-methods, allow the positronic orbitals to relax. We have also presented the average-of-configuration Dirac-Hartree-Fock method which can be used for generating start orbitals for the KR-MCSCF optimization.

We have chosen to work within the four-component framework due to the relatively simple appearence of operators and the often simple formalism compared to the very complicated nature of the regularized methods where the small component is eliminated. The current problem with the four-component methods is the expensive nature: (i) many electrons and (ii) the small component basis set. Problem (i) is also present in non-relativistic or approximative relativistic approaches and is as such not a four-component problem. The only way to deal with this is to use effective core potentials or pseudo-potentials. Problem (ii) is somewhat related to problem (i), but the problem is the numerous $(SS|SS)$ and $(SS|LL)$ (plus the Gaunt or Breit interaction) two-electron integrals, however through several approximations it is possible to neglect many of these. Through these approximations we remove the unneeded integrals and we approach the computational scaling of the more approximative methods keeping the simple four-component formalism. We believe this is clearly the best way to procede (approximations *within* the 4-component formalism versus approximations *to* the formalism).

With the few preliminary applications presented in this thesis we have discovered a number of interesting items:

- The difficulty of producing orbital start guess for the MCSCF procedure.
- The apparent negligible effect of relaxing the positronic orbitals for energy and some selected properties (more research on this is clearly needed).
- The non-additivity of relativistic and correlation effects, which of course is not a new discovery, but clearly indicates the need for correlated relativistic methods.

The potential applications for which the presented KR-MCSCF program can be used is numerous. We will just mention a few applications and would have liked or is planning to investigate, and a few selected improvements:

- The effect of $e-p$ rotations on properties, especially on magnetic properties such as spin-spin couplings or properties that depend critically on the small component density such as parity violating energy shifts. As the spin-spin coupling is a second-order property this requires the implementation of a KR-MCRPA program. For the parity violating properties we have to deal with molecules in complex or quaternion point groups, which, at the deadline of this thesis, did not work to our full satisfaction.
- Investigate actinide and lanthanide compounds. Due to the very complicated electronic structure of the actinides and lanthanides a multi-configurational approach is often mandatory.
- ESR properties: hyper-fine couplings and $g$ tensors. This requires the implementation of the time reversal anti-symmetric density matrix.
- Magnetic properties in general. Due to the inherent relativistic appearence of magnetic operators these are often best described in the four-component frame-work even for "non-relativistic" molecules.
- All the same kind of applications where non-relativistic MCSCF programs have been applied, which include, but are not limited to, dissociation of molecules, chemical reactions, properties for excited states, and much more.
- Improve the implementation of the program (see chapter 5 for more details). Beside the approximations mentioned above to avoid calculating many integrals, all the non-relativistic auxiliary optimization algorithms can be employed, for example, the transformation of orbitals to improve diagonal dominance of the Hessian.

- Better orbital start guess: MP2 natural orbitals are clearly preferred over $h_1$-virtuals, average-of-configuration or canonical Dirac-Hartree-Fock orbitals. The relaxed MP2 density matrix is under implementation, so MP2 natural orbital start guesses should be available soon.

- The MCSCF is particularly suited for retrieving the static correlation. It would be a very interesting project to implement post-MCSCF methods for getting dynamical correlation: CASPT2 (or other multi-reference MBPT methods) or multi-reference CI.

In conclusion, we believe the future is looking bright for four-component methods, and the presented KR-MCSCF program is the wave function module for a general toolbox for the calculation of correlated properties within a four-component relativistic framework.

# Chapter 8

# Dansk Resumé

Dette er min Ph.D. afhandling, som er resultatet er 4 års studier og forskning ved Kemisk Institut, Syddansk Universitet i Odense.

Vi starter med at argumentere for nødvendigheden af en fire-komponent relativistisk *multi-konfigurational selv-konsistent felt* (MCSCF) metode. For det første er beskrivelsen af relativistiske effekter i molekyler nødvendig for en kvalitativ og kvantitativ beskrivelse af molekyler der indeholder tunge atomer. Det kan også være nødvendig med en relativistisk beskrivelse for meget præcise beregninger på atomer med kun lette atomer. Endvidere er en relativistisk beskrivelse ofte foretrukket for bl.a. magnetiske egenskaber. For det andet er en fire-komponent beskrivelse den bedste og simpleste formalisme til at beskrive relativistiske effekter. For det tredje er en MCSCF metode nødvendig for en kvalitativ beskrivelse af den klasse af atomer og molekyler hvor der er nær-degenerede tilstande (statisk korrelation).

I Kapitel 2 gives en kort introduktion til de begreber i relativistisk kvantemekanik som vi har brug for i de efterfølgende kapitler, f.eks. enkelt-partikel Dirac-ligningen og fler-partikel Hamilton-operatoren.

I Kapitel 3 diskuteres *average-of-configuration* åben-skal Dirac-Hartree-Fock formalismen. Metoden bliver f.eks. brugt til at generere start orbitaler til MCSCF metoden.

Dem relativistiske MCSCF metode er netop emnet for kapitel 4. Selve formalismen er tidligere publiceret [H. J. Aa. Jensen, K. G. Dyall, T. Saue og K. Fægri, J. Chem. Phys, **104**, 4083 (1996)], så vi gennemgår blot teorien. Dog introducerer vi den quaternionske formalisme for alle orbitale størrelser samt diskuterer hovedpunkterne i implementationen. I kapitel 5 diskuteres en række approximationer samt en række hjælpe algortimer for KR-MCSCF bølgefunktionsoptimeringer. Herefter præsenteres i kapitel 6 et lille antal indledende beregninger hvori det beskrevne MCSCF program benyttes.

I kapitel 7 opsummerer indholdet af denne afhandling. Desuden gives der

også forslag til fremtidig forskning til videre forskning.

Resten af afhandlingen er et antal appendikser med udførlige detaljer for udregningen af exponentialfunktionen på quaternionske matricer samt udregningen af forskellige Fock matricer, samt et lille antal manuskripter og publicerede artikler.

# Part II

# Papers

# Summary of papers

## Paper I

In this paper, published in *Physical Review Letters*, **85**, 3105 – 3108 (2000), we present a study of correlation effects on parity violating effects in $H_2O_2$ and $H_2S_2$. In the paper we present four-component relativistic DHF, MP2, and CCSD(T) results of the matrix elements (see Eqs. (1.1) and (1.2) in Chapter 1)

$$\langle 0 | \varrho_A(\mathbf{r}) \gamma_5 | 0 \rangle \,, \tag{8.1}$$

needed to calculate the parity violating energy-difference as a function of the dihedral angle in $H_2O_2$ and $H_2S_2$. The correlated expectation values was calculated numerically as there is currently no analytic implementation of a four-component relativistic $e-p$ relaxed MP2 or CCSD(T) density matrix.

The conclusion was that correlation effects were small, in accordance with a prediction by Laerdahl and Schwerdtfeger [1], since the operator is very core-like (the operator is essentially a delta function a the nuclei).

## Paper II

In this paper, published in *Physical Review A*, **63**, 022505 (2001), we present a study of the hexadecapole coupling constant of $^{127}$I in Li$^{127}$I. The project was motivated by a recent publication by Cederberg *et al.* [2] claiming to have experimentally measured the hexadecapole coupling for $^{127}$I. The goal was to either confirm or reject their result. In the paper we review the theory for calculating the quadrupole and hexadecapole couplings constants, and present the formulae for the traceless electric field gradient, the electric field second derivative, and the electric field third derivative. The final value of the hexadecapole coupling constant calculated from self-consistent nuclear structure calculations and four-component relativistic Dirac-Hartree-Fock calculations is about three orders of magnitude smaller and of opposite

sign that the experimental value suggested by Cederberg *et al.* We speculate that their experimental value originates from the second-order quadropole ("pseudo-hexadecapole") interaction, and not from the hexadecapole coupling.

## Manustript I

In this manuscript we present the theory for analytical molecular gradients for Dirac-Hartree-Fock used for geometry optimizations. We also discuss the use of screening in the calculation of relativistic molecular gradients. As a preliminary applications we present a geometry optimizations on iodobenzene.

## Publications not included in this thesis

- V. Kellö, P. Pyykkö, A. J. Sadlej, P. Schwerdtfeger, J. Thyssen. The nuclear quadrupole moment of $^{91}$Zr from molecular data for ZrO and ZrS. *Chemical Physics Letters*, **318**, 222-231 (2000).

## In preparation

- J. Thyssen and H. J. Aa. Jensen: Relativistic four-component multiconfigurational self-consistent-field theory for molecules: Implementation.

## Bibliography

[1] J. K. Laerdahl and P. Schwerdtfeger, Phys. Rev. A **60**, 4439 (1999).

[2] J. Cederberg, D. Olson, A. Nelson, D. Laine, P. Zimmer, M. Welge, M. Feig, T. Höft, and N. London, J. Chem. Phys. **110**, 2431 (1999).

# Paper I

# Paper II

# Manuscript I

# Part III

# Appendices

# Appendix A

# Evaluation of Matrix Exponentials

In order to obtain the new orbitals in each macro iteration it is necesary to calculate

$$ {}^{Q}\mathbf{c}_{\text{new}} = {}^{Q}\mathbf{c}_{\text{old}} \exp\left(-{}^{Q}\boldsymbol{\kappa}\right), \tag{A.1} $$

where ${}^{Q}\boldsymbol{\kappa}$ is the anti-hermitian orbital rotation operator. For simplicity ${}^{Q}\boldsymbol{\kappa}$ is written as $\boldsymbol{\kappa}$ in the rest of this section.

The definition of the matrix exponential appearing in Eq. (A.1) is

$$ \exp\left(-\boldsymbol{\kappa}\right) = \sum_{n=0}^{\infty} \frac{1}{n!} \left(-\boldsymbol{\kappa}\right)^{n}. \tag{A.2} $$

There are many ways to to evaluate Eq. (A.1). Below we will give three different ways to do it.

1. The simplest is just to use the Taylor series to some order, for example a first order expansion:

$$ \exp\left(-\boldsymbol{\kappa}\right) \approx 1 - \boldsymbol{\kappa} \tag{A.3} $$

   However, $1 - \boldsymbol{\kappa}$ is not unitary, and it must be orthogonalized, *e.g.* by a symmetric orthogonalization. The resulting orbital rotation operator

$$ \mathbf{U} = \left(1 - \kappa\right) \mathbf{S}(\boldsymbol{\kappa})^{-\frac{1}{2}}, \tag{A.4} $$

   with $\mathbf{S}(\boldsymbol{\kappa}) = \left(1 - \boldsymbol{\kappa}\right)^{\dagger} \left(1 - \boldsymbol{\kappa}\right)$, is correct through second order as

$$ \mathbf{U} = 1 - \boldsymbol{\kappa} + \frac{1}{2}\boldsymbol{\kappa}^{2} + O(\boldsymbol{\kappa}^{3}) \tag{A.5} $$

where we have used

$$\begin{aligned} \mathbf{S}(\boldsymbol{\kappa}) &= (1-\boldsymbol{\kappa})^{\dagger}(1-\boldsymbol{\kappa}) \\ &= 1 + \frac{1}{2}\boldsymbol{\kappa}^2 + O(\boldsymbol{\kappa}^4). \end{aligned} \tag{A.6}$$

This procedure has two main advantages: (i) It works for quaternion matrices, and (ii) it does not involve any diagonalization procedure as the symmetric orthogonalization procedure can be formulated iteratively. This procedure is used in the SIRIUS MCSCF wave function module in DALTON [1].

2. If $\boldsymbol{\kappa}$ is a real or complex matrix the matrix exponential of Eq. (A.1) can be evaluated by as follows: The matrix

$$\boldsymbol{\Lambda} = -i\boldsymbol{\kappa} \tag{A.7}$$

is a Hermitian matrix[1], thus it can be diagonalized

$$\mathbf{U}^{\dagger}\boldsymbol{\Lambda}\mathbf{U} = \boldsymbol{\lambda}, \tag{A.8}$$

where $\boldsymbol{\lambda}$ is a real diagonal matrix. Hence,

$$\boldsymbol{\kappa} = i\boldsymbol{\Lambda} = i\mathbf{U}\boldsymbol{\lambda}\mathbf{U}^{\dagger}. \tag{A.9}$$

Using that $\mathbf{U}^{-1} = \mathbf{U}^{\dagger}$ and the identity

$$\exp\left(\mathbf{B}\mathbf{A}\mathbf{B}^{-1}\right) = \mathbf{B}\exp\left(\mathbf{A}\right)\mathbf{B}^{-1} \tag{A.10}$$

we get

$$\begin{aligned} \exp\left(\kappa\right) &= \exp\left(i\mathbf{U}\boldsymbol{\lambda}\mathbf{U}^{\dagger}\right) \\ &= \mathbf{U}\exp\left(i\boldsymbol{\lambda}\right)\mathbf{U}^{\dagger}. \end{aligned} \tag{A.11}$$

This method has the advantage that we evaluate the matrix exponential is evaluated analytically. However, this methods has two major drawbacks. First, it does not work for quaternion matrices. Second, it always involve complex algebra even if $\boldsymbol{\kappa}$ is real.

3. The most elegant way to evaluate Eq. (A.1) is to do something similar to Dalgaard and Jørgensen [2]. The matrix $-\boldsymbol{\kappa}^2$ is a Hermitian matrix, since

$$\begin{aligned} \left(-\boldsymbol{\kappa}^2\right)^{\dagger} &== -\boldsymbol{\kappa}^{\dagger}\boldsymbol{\kappa}^{\dagger} \\ &= -\boldsymbol{\kappa}^2, \end{aligned} \tag{A.12}$$

[1]Note that this is *not* true for a quaternion matrix, which is why this method cannot be used for such matrices.

where we have used that $\boldsymbol{\kappa}$ is anti-Hermitian. Since $-\boldsymbol{\kappa}^2$ is Hermitian there exists a matrix $\mathbf{V}$ that diagonalizes it

$$\mathbf{V}^\dagger \left(-\boldsymbol{\kappa}^2\right) \mathbf{V} = \boldsymbol{\delta}^2, \tag{A.13}$$

or

$$\mathbf{V}\boldsymbol{\delta}^2\mathbf{V}^\dagger = \left(-\boldsymbol{\kappa}^2\right), \tag{A.14}$$

where $\boldsymbol{\delta}^2$ is a real diagonal matrix. Using the definition of a matrix exponential, Eq. (A.2), we get

$$\begin{aligned}
\exp\left(-\boldsymbol{\kappa}\right) &= \sum_{n=0}^{\infty} \frac{1}{n!} \left(-\boldsymbol{\kappa}\right)^n \\
&= \sum_{n=0}^{\infty} \frac{1}{2n!} \left(-\boldsymbol{\kappa}\right)^{2n} - \sum_{n=0}^{\infty} \frac{1}{(2n+1)!} \left(-\boldsymbol{\kappa}\right)^{2n+1} \\
&= \mathbf{V} \sum_{n=0}^{\infty} \frac{1}{2n!} \boldsymbol{\delta}^{2n} \mathbf{V}^\dagger - \mathbf{V} \sum_{n=0}^{\infty} \frac{1}{(2n+1)!} \boldsymbol{\delta}^{2n+1} \boldsymbol{\delta}^{-1} \mathbf{V}^\dagger \kappa \\
&= \mathbf{V} \cos\left(\boldsymbol{\delta}\right) \mathbf{V}^\dagger - \mathbf{V} \sin\left(\boldsymbol{\delta}\right) \boldsymbol{\delta}^{-1} \mathbf{V}^\dagger \boldsymbol{\kappa}.
\end{aligned} \tag{A.15}$$

A potential problem arises if an eigenvalue is close to zero, since $\frac{\sin x}{x}$ will give zero divided by zero for $x = 0$. This is easily taken care of by using a second order Taylor expansion of $\frac{\sin x}{x}$ around zero

$$\frac{\sin x}{x} = 1 - \frac{x^2}{6} \tag{A.16}$$

for eigenvalues close to zero. The advantage of Eq. (A.15) is no approximations are involved and that it works for real, complex, and quaternion matrices (unlike the previous method). It is also important to note that no complex algebra is needed if $\boldsymbol{\kappa}$ is real. However, the method has the drawback that it requires one matrix diagonalization.

In the program method 3 is used (for no other reason than being the most mathematically elegant method), but method 1 has also been implemented for real matrices in order to facilitate exact comparisons with DALTON in the debugging phase.

# Bibliography

[1] T. Helgaker, H. J. A. Jensen, P. Jørgensen, J. Olsen, K. Ruud, H. Ågren, T. Andersen, K. L. Bak, V. Bakken, O. Christiansen, P. Dahle, E. K.

Dalskov, *et al.*, *DALTON, an electronic structure program, Release 1.0 (1997)*.

[2] E. Dalgaard and P. Jørgensen, J. Chem. Phys. **69**, 3833 (1978).

# Appendix B

# Quaternion MO integrals and Fock matrices

In this chapter we derive the formulae needed for the construction of the quaternion Fock matrices. We also discuss the double quaternion two-electron integrals and how to use them to construct auxiliary Fock matrices and one-index transformed auxilliary Fock matrices.

## B.1 ${}^{Q}\mathbf{F}^{C}$ and ${}^{Q}\mathbf{F}^{V}$

The "core" and "valence" Fock matrices $\mathbf{F}^{C}$ and $\mathbf{F}^{V}$[1] are defined by

$$\begin{aligned} F^{C}_{pq} &= h_{pq} + \sum_{i} \left(2\,(pq|ii) - (pi|iq) - (p\bar{i}|\bar{i}q)\right), \\ F^{V}_{pq} &= \frac{1}{2}\sum_{uv} D_{uv}\left((pq|uv) - (pv|uq)\right) + \frac{1}{2}\sum_{uv} D_{\bar{u}\bar{v}}\left((pq|\bar{u}\bar{v}) - (p\bar{v}|\bar{u}q)\right) \\ &\quad + \frac{1}{2}\sum_{uv} D_{u\bar{v}}\left((pq|u\bar{v}) - (p\bar{v}|uq)\right) + \frac{1}{2}\sum_{uv} D_{\bar{u}v}\left((pq|\bar{u}v) - (pv|\bar{u}q)\right), \end{aligned} \tag{B.1}$$

where $D_{uv}$ is the active part of the one-electron density matrix (Eq. (4.49)) and $(pq|rs)$ are molecular two-electron integrals. The ${}^{Q}\mathbf{F}^{C}$ and ${}^{Q}\mathbf{F}^{V}$ Fock matrices are also known from closed shell DHF and average-of-configuration open shell DHF (*e.g.*, see Chapter 3).

[1] The designation "core" ("inactive") and "valence" ("active") Fock matrices is somewhat arbitrary, since there might be core orbitals among the active ("valence") orbitals.

${}^{Q}\mathbf{F}^{C}$ and ${}^{Q}\mathbf{F}^{V}$ are used for the generalized Fock matrix with second index inactive

$$\begin{aligned} F_{pi} &= \sum_{r} \left(D_{ir} h_{pr} + D_{i\bar{r}} h_{p\bar{r}}\right) \\ &+ \sum_{rst} P_{ir,st} \left(pr|st\right) + \sum_{rst} P_{i\bar{r},st} \left(p\bar{r}|st\right) + \frac{1}{2} \sum_{rst} P_{i\bar{r},\bar{s}t} \left(p\bar{r}|\bar{s}t\right) \\ &+ \frac{1}{2} \sum_{rst} P_{i\bar{r},s\bar{t}} \left(p\bar{r}|s\bar{t}\right) + \frac{1}{2} \sum_{rst} P_{ir,\bar{s}t} \left(pr|\bar{s}t\right) + \frac{1}{2} \sum_{rst} P_{ir,s\bar{t}} \left(pr|s\bar{t}\right) \\ &= 2\left(F^{C}_{pi} + F^{V}_{pi}\right) \end{aligned} \tag{B.2}$$

The generalized Fock matrix is used for calculating orbital gradients and various sigma vectors (Sec. 4.7).

In the quaternion formalism $\mathbf{F}^{C}$ and $\mathbf{F}^{V}$ are defined by:

$$\begin{aligned} {}^{Q}F^{C}_{pq} &= F^{C}_{pq} + F^{C}_{p\bar{q}} \check{\jmath}, \\ {}^{Q}F^{V}_{pq} &= F^{V}_{pq} + F^{V}_{p\bar{q}} \check{\jmath}. \end{aligned} \tag{B.3}$$

The one-electron part of ${}^{Q}\mathbf{F}^{C}$ is just the quaternion one-electron Hamiltonian ${}^{Q}h_{pq} = h_{pq} + h_{p\bar{q}}\check{\jmath}$.

The two-electron part is, in fact, of the same type as $F^{V}$, which can be seen from:

$$\begin{aligned} F^{C}_{pq} &= h_{pq} + \frac{1}{2} \sum_{ij} D_{ij} \left((pq|ij) - (pj|iq)\right) + \frac{1}{2} \sum_{i\bar{\jmath}} D_{i\bar{\jmath}} \left((pq|i\bar{\jmath}) - (p\bar{\jmath}|iq)\right) \\ &+ \frac{1}{2} \sum_{ij} D_{i\bar{\jmath}} \left((pq|i\bar{\jmath}) - (p\bar{\jmath}|iq)\right) + \frac{1}{2} \sum_{ij} D_{\bar{\imath}j} \left((pq|\bar{\imath}j) - (pj|\bar{\imath}q)\right) \\ &= h_{pq} + \sum_{i} \left(2\,(pq|ii) - (pi|iq) - (p\bar{\imath}|\bar{\imath}q)\right), \end{aligned} \tag{B.4}$$

using $D_{ij} = 2\delta_{ij}$ and $(pq|ii) = (pq|\overline{ii})$.

Instead of constructing the matrices directly in MO basis, which require two-electron integrals with one general and three occupied indices[2], both ${}^{Q}\mathbf{F}^{V}$ and ${}^{Q}\mathbf{F}^{C}$ are constructed in AO basis by backtransforming the quaternion

[2]We only need the general-occupied block of $\mathbf{F}^{C}$ and $\mathbf{F}^{V}$, *i.e.* only $F^{C}_{pq}$ for $q$ occupied in Eq. (B.1), which only require integrals with one general and three occupied indices.

density matrices to AO-basis [1]

$$\begin{aligned}
{}^{Q}F^{C,AO}_{\mu\nu} &= {}^{Q}h_{\mu\nu} + \sum_{\kappa\lambda} D^{C,AO}_{\kappa\lambda;0}\left((\mu\nu|\kappa\lambda) - \frac{1}{2}(\mu\lambda|\kappa\nu)\right) \\
&\quad - \frac{1}{2}\sum_{\Lambda=1}^{3}\sum_{\kappa\lambda} e_\Lambda D^{C,AO}_{\kappa\lambda;\Lambda}(\mu\lambda|\kappa\nu) \\
{}^{Q}F^{V,AO}_{\mu\nu} &= \sum_{\kappa\lambda} D^{V,AO}_{\kappa\lambda;0}\left((\mu\nu|\kappa\lambda) - \frac{1}{2}(\mu\lambda|\kappa\nu)\right) \\
&\quad - \frac{1}{2}\sum_{\Lambda=1}^{3}\sum_{\kappa\lambda} e_\Lambda D^{V,AO}_{\kappa\lambda;\Lambda}(\mu\lambda|\kappa\nu)
\end{aligned} \tag{B.5}$$

where ${}^{Q}\mathbf{D}^{C,AO}$ and ${}^{Q}\mathbf{D}^{V,AO}$ are the backtransformed inactive and active AO density matrices, respectively. $e_\Lambda$ ($\Lambda = 0, \ldots, 3$) are the quaternion units 1, $\check{i}$, $\check{j}$, and $\check{k}$, respectively. Note that for the imaginary parts of ${}^{Q}\mathbf{F}^{C,AO}$ and ${}^{Q}\mathbf{F}^{V,AO}$ only the exchange part contributes: the Coulomb part is zero as $\mathbf{D}^{AO}_{\Lambda}$ are anti-symmetric matrices for $\Lambda = 1, \ldots, 3$.

The matrices form Eq. (B.5) are standard Fock matrices from closed shell Hartree-Fock and can be constructed by any non-relativistic integral generator [1].

## B.2 One index transformed Fock matrices

For the orbital part of the orbital sigma vectors, Eq. (4.38), we need Fock matrices from one-index transformed integrals:

$$\tilde{F}^{C}_{pq} = \tilde{h}_{pq} + \sum_{i}\left(2\widetilde{(pq|ii)} - \widetilde{(pi|iq)} - \widetilde{(p\bar{\imath}|\bar{\imath}q)}\right), \tag{B.6}$$

where

$$\tilde{h}_{pq} = \sum_{r}\left((b_{pr}h_{rq} - h_{pr}b_{rq}) + (b_{p\bar{r}}h_{\bar{r}q} - h_{p\bar{r}}b_{\bar{r}q})\right) \tag{B.7}$$

and

$$\begin{aligned}
\widetilde{(pq|rs)} &= (\widetilde{pq}|rs) + (pq|\widetilde{rs}) \\
&= \sum_{t}\left(b_{pt}(tq|rs) - (pt|rs)b_{tq} + b_{p\bar{t}}(\bar{t}q|rs) - (p\bar{t}|rs)b_{\bar{t}q}\right) \\
&\quad + \sum_{t}\left(b_{rt}(pq|ts) - (pq|rt)b_{ts} + b_{r\bar{t}}(pq|\bar{t}s) - (pq|r\bar{t})b_{\bar{t}s}\right).
\end{aligned} \tag{B.8}$$

Eq. (B.6) can now be rewritten as

$$\begin{aligned}\tilde{F}^C_{pq} = \tilde{h}_{pq} &+ \sum_i \left(2\left(\widetilde{pq}|ii\right) - \left(\tilde{p}i|i\tilde{q}\right) - \left(\tilde{p}\bar{\imath}|\bar{\imath}\tilde{q}\right)\right) \\ &+ \sum_i \left(2\left(pq|\widetilde{ii}\right) - \left(p\tilde{i}|\tilde{i}q\right) - \left(p\tilde{i}|\tilde{i}q\right)\right).\end{aligned} \tag{B.9}$$

The first line of Eq. (B.9) is just the one-index transform of $F^C_{pq}$:

$$\sum_r \left(\left(b_{pr}F^C_{rq} - F^C_{pr}b_{rq}\right) + \left(b_{p\bar{r}}F^C_{\bar{r}q} - F^C_{p\bar{r}}b_{\bar{r}q}\right)\right), \tag{B.10}$$

whereas the second line can be expanded to:

$$\begin{aligned}&\sum_{ir} b_{ir}\left((pq|ri) - (pi|rq)\right) + \sum_{ir} b_{\bar{\imath}r}\left((pq|r\bar{\imath}) - (p\bar{\imath}|rq)\right) \\ &+ \sum_{ir} b_{i\bar{r}}\left((pq|\bar{r}i) - (pi|\bar{r}q)\right) + \sum_{ir} b_{\bar{\imath}\bar{r}}\left((pq|\bar{r}\bar{\imath}) - (p\bar{\imath}|\bar{r}q)\right) \\ &+ \sum_{ir} -b_{ri}\left((pq|ir) - (pr|iq)\right) + \sum_{ir} -b_{r\bar{\imath}}\left((pq|\bar{\imath}r) - (pr|\bar{\imath}q)\right) \\ &+ \sum_{ir} -b_{\bar{r}i}\left((pq|i\bar{r}) - (p\bar{r}|iq)\right) + \sum_{ir} -b_{\bar{r}\bar{\imath}}\left((pq|\bar{\imath}\bar{r}) - (p\bar{r}|\bar{\imath}q)\right).\end{aligned} \tag{B.11}$$

Defining a new matrix

$$\begin{aligned}A_{pq} = &\sum_{ir} b_{ir}\left((pq|ri) - (pi|rq)\right) + \sum_{ir} b_{\bar{\imath}r}\left((pq|r\bar{\imath}) - (p\bar{\imath}|rq)\right) \\ &+ \sum_{ir} b_{i\bar{r}}\left((pq|\bar{r}i) - (pi|\bar{r}q)\right) + \sum_{ir} b_{\bar{\imath}\bar{r}}\left((pq|\bar{r}\bar{\imath}) - (p\bar{\imath}|\bar{r}q)\right),\end{aligned} \tag{B.12}$$

and using that the trial vector is anti-Hermitian ($b_{ri} = -b^*_{ir}$) we can rewrite Eq. (B.11) to

$$A_{pq} + \left(A_{qp}\right)^*, \tag{B.13}$$

which is the Hermitian part of $\mathbf{A}$, which is a standard Fock matrix constructed using a modified density matrix $D_{ri} = b_{ir}$ — or equivalently: calculating the Fock matrix using only the Hermitian part of the density matrix $D_{ri}$.

The quaternion $\tilde{\mathbf{F}}^C$ is easily obtained after some trivial algebra

$$\begin{aligned}{}^Q\tilde{F}^C_{pq} &\equiv \tilde{F}^C_{pq} + \tilde{F}^C_{p\bar{q}}\check{\jmath} \\ &= \sum_r \left({}^Q b_{pr}\ {}^Q F^C_{rq} - {}^Q F^C_{pr}\ {}^Q b_{rq}\right) + \mathrm{Hp}\left\{{}^Q A_{pq}\right\},\end{aligned} \tag{B.14}$$

where Hp takes out the Hermitian part of a matrix and ${}^{Q}A_{pq}$ is a quaternion Fock matrix constructed using a quaternion density matrix ${}^{Q}D_{ri} = {}^{Q}b_{ir}$.

Similarly, one obtains the quaternion $\mathbf{F}^V$ matrix as

$$\begin{aligned} {}^{Q}\tilde{F}^V_{pq} &\equiv \tilde{F}^V_{pq} + \tilde{F}^V_{p\bar{q}}\check{\jmath} \\ &= \sum_r \left( {}^{Q}b_{pr}\ {}^{Q}F^V_{rq} - {}^{Q}F^V_{pr}\ {}^{Q}b_{rq} \right) + \mathrm{Hp}\left\{ {}^{Q}B_{pq} \right\}, \end{aligned} \tag{B.15}$$

where we have defined another Fock matrix

$$\begin{aligned} B_{pq} = &\sum_{uvr} D^V_{uv} b_{ur} \left( (pq|rv) - (pv|rq) \right) + \sum_{uvr} D^V_{\bar{u}v} b_{\bar{u}r} \left( (pq|r\bar{v}) - (p\bar{v}|rq) \right) \\ &+ \sum_{uvr} D^V_{u\bar{v}} b_{u\bar{r}} \left( (pq|\bar{r}v) - (pv|\bar{r}q) \right) + \sum_{uvr} D^V_{\bar{u}\bar{v}} b_{\bar{u}\bar{r}} \left( (pq|\bar{r}\bar{v}) - (p\bar{v}|\bar{r}q) \right). \end{aligned} \tag{B.16}$$

Again, this is a standard Fock matrix, this time constructed using a density matrix $D_{rv} = \sum_u D^V_{uv} b_{ur} = ((D^V)^T b)_{vr}$ — or in the quaternion formalism: a standard quaternion Fock matrix constructed using a quaternion density matrix ${}^{Q}D_{rv} = \left( \left( {}^{Q}D^V \right)^T {}^{Q}b \right)_{vr}$.

## B.3 Two-electron integrals

For orbital indices $p$, $q$, $r$, and $s$ there are 16 integrals arising from all possible combinations of barred and unbarred indices:

$$\begin{array}{cccc} (pq|rs), & (pq|\bar{r}s), & (pq|r\bar{s}), & (pq|\bar{r}\bar{s}), \\ (\bar{p}q|rs), & (\bar{p}q|\bar{r}s), & (\bar{p}q|r\bar{s}), & (\bar{p}q|\bar{r}\bar{s}), \\ (p\bar{q}|rs), & (p\bar{q}|\bar{r}s), & (p\bar{q}|r\bar{s}), & (p\bar{q}|\bar{r}\bar{s}), \\ (\bar{p}\bar{q}|rs), & (\bar{p}\bar{q}|\bar{r}s), & (\bar{p}\bar{q}|r\bar{s}), & (\bar{p}\bar{q}|\bar{r}\bar{s}). \end{array} \tag{B.17}$$

With a spin-free Hamiltonian (*e.g.*, a non-relativistic Hamiltonian) it is possible to reduce the number of integrals in two ways. First, $p$ and $\bar{p}$ are pure spin functions: for a given orbital $p$ then $p$ is pure $\beta$ spin and $\bar{p}$ pure $\alpha$ spin or vice versa. Many integrals vanish as the $\alpha$ and $\beta$ spin functions are orthogonal. Furthermore, all the non-zero integrals are all related, which leaves us with only one unique integral. Second, it is possible to reduce the number of integrals further by exploring the fact the the orbitals can be made real, hence for example $(pq|rs) = (qp|rs)$ etc. Thus, it is only necesary to store integrals with $p \geq q$, $r \geq s$, and, by using particle interchange symmetry, compound index $(pq) \geq (rs)$.

However, in the relativistic case neither the former nor the latter reduction is possible. It is possible, however, to do obtain reductions analogous to above. First, using time-reversal symmetry and that $(pq|rs) = (qp|sr)^*$, we can establish the following relations:

$$\begin{array}{ll} (pq|rs) = (\bar{p}\bar{q}|\bar{r}\bar{s})^*, & (pq|\bar{r}\bar{s}) = (\bar{p}\bar{q}|rs)^*, \\ (p\bar{q}|r\bar{s}) = (\bar{p}q|\bar{r}s)^*, & (p\bar{q}|\bar{r}s) = (\bar{p}q|r\bar{s})^*, \\ (pq|\bar{r}s) = -(\bar{p}\bar{q}|r\bar{s})^*, & (pq|r\bar{s}) = -(\bar{p}\bar{q}|\bar{r}s)^*, \\ (\bar{p}q|rs) = -(p\bar{q}|\bar{r}\bar{s})^*, & (p\bar{q}|rs) = -(\bar{p}q|\bar{r}\bar{s})^*, \end{array} \tag{B.18}$$

which reduce the number of integrals by a factor of 2. Second, we can save an additional factor of two using that $(pq|rs) = (qp|sr)^*$, allowing us to only save integrals with $r \geq s$.

We can, in fact, get away with saving only six of the integrals above, since $(pq|rs) = (qp|\bar{r}\bar{s})^*$ and $(pq|r\bar{s}) = -(qp|\bar{r}s)^*$, leaving us with the following integrals which we put in a $4 \times 3$ matrix:

$$\begin{bmatrix} (pq|rs)_{1,1} & (pq|rs)_{1,2} & (pq|rs)_{1,3} \\ (pq|rs)_{2,1} & (pq|rs)_{2,2} & (pq|rs)_{2,3} \\ (pq|rs)_{3,1} & (pq|rs)_{3,2} & (pq|rs)_{3,3} \\ (pq|rs)_{4,1} & (pq|rs)_{4,2} & (pq|rs)_{4,3} \end{bmatrix} = \begin{bmatrix} \Re((pq|rs)) & \Re((p\bar{q}|r\bar{s})) & \Re((\bar{p}q|\bar{r}s)) \\ \Im((pq|rs)) & \Im((p\bar{q}|r\bar{s})) & \Im((\bar{p}q|\bar{r}s)) \\ \Re((pq|r\bar{s})) & \Re((p\bar{q}|rs)) & \Re((\bar{p}q|rs)) \\ \Im((pq|r\bar{s})) & \Im((p\bar{q}|rs)) & \Im((\bar{p}q|rs)) \end{bmatrix} \tag{B.19}$$

For real points groups ($D_{2h}$, $C_{2v}$ in $D_{2h}$ and subgroups) only the first row is non-zero. For complex point groups ($C_2$, $D_2$, and $C_{2h}$ the first two rows of integrals are non-zero. For quarternion groups all four rows of integrals are generally non-zero. We call this the `(NZ,3)` format, since the dimensions of the matrix is `NZ` $\times$ 3, where `NZ` is 1, 2, or 4 for real, complex, or quaternion point groups, respectively.

A charge distribution can be written in quaternion form:

$$^{Q}(pq) = \Re(pq) + \Im(pq)\check{\imath} + \Re(p\bar{q})\check{\jmath} + \Im(p\bar{q})\check{k}. \tag{B.20}$$

The two-electron integrals, which are integrals over two charge distributions, can be written in a double-quaternion (rather, in a two-dimension quaternion

vector space) format:

$$\begin{aligned}
{}^{Q_1Q_2}(pq|rs) &= \left({}^{Q_1}(pq)\middle|{}^{Q_2}(rs)\right) \\
&= (\Re(pq)|\Re(rs)) + (\Im(pq)|\Re(rs))\,\check{\imath}_1 \\
&+ (\Re(p\bar{q})|\Re(rs))\,\check{\jmath}_1 + (\Im(p\bar{q})|\Re(rs))\,\check{k}_1 \\
&+ (\Re(pq)|\Im(rs))\,\check{\imath}_2 + (\Im(pq)|\Im(rs))\,\check{\imath}_1\check{\imath}_2 \\
&+ (\Re(p\bar{q})|\Im(rs))\,\check{\jmath}_1\check{\imath}_2 + (\Im(p\bar{q})|\Im(rs))\,\check{k}_1\check{\imath}_2 \\
&+ (\Re(pq)|\Re(r\bar{s}))\,\check{\jmath}_2 + (\Im(pq)|\Re(r\bar{s}))\,\check{\imath}_1\check{\jmath}_2 \\
&+ (\Re(p\bar{q})|\Re(r\bar{s}))\,\check{\jmath}_1\check{\jmath}_2 + (\Im(p\bar{q})|\Re(r\bar{s}))\,\check{k}_1\check{\jmath}_2 \\
&+ (\Re(pq)|\Im(r\bar{s}))\,\check{k}_2 + (\Im(pq)|\Im(r\bar{s}))\,\check{\imath}_1\check{k}_2 \\
&+ (\Re(p\bar{q})|\Im(r\bar{s}))\,\check{\jmath}_1\check{k}_2 + (\Im(p\bar{q})|\Im(r\bar{s}))\,\check{k}_1\check{k}_2.
\end{aligned} \tag{B.21}$$

Note that we have one real part and 15 imaginary parts, where the imaginary parts of a specific electron anti-commute, e.g. $\check{\imath}_1\check{\jmath}_1 = -\check{\jmath}_1\check{\imath}_1$, and the imaginary parts of electron 1 and electron 2 commute, e.g. $\check{\imath}_1\check{\jmath}_2 = \check{\jmath}_2\check{\imath}_1$. All sixteen integrals are best visualized in a $4 \times 4$ matrix:

$$\begin{bmatrix}
(\Re(pq)|\Re(rs)) & (\Re(pq)|\Im(rs)) & (\Re(pq)|\Re(r\bar{s})) & (\Re(pq)|\Im(r\bar{s})) \\
(\Im(pq)|\Re(rs)) & (\Im(pq)|\Im(rs)) & (\Im(pq)|\Re(r\bar{s})) & (\Im(pq)|\Im(r\bar{s})) \\
(\Re(p\bar{q})|\Re(rs)) & (\Re(p\bar{q})|\Im(rs)) & (\Re(p\bar{q})|\Re(r\bar{s})) & (\Re(p\bar{q})|\Im(r\bar{s})) \\
(\Im(p\bar{q})|\Re(rs)) & (\Im(p\bar{q})|\Im(rs)) & (\Im(p\bar{q})|\Re(r\bar{s})) & (\Im(p\bar{q})|\Im(r\bar{s}))
\end{bmatrix} \tag{B.22}$$

For real point groups ($D_{2h}$, $C_{2v}$ in $D_{2h}$ and subgroups) we only need the diagonal of the matrix:

$$\begin{bmatrix}
(\Re(pq)|\Re(rs)) & 0 & 0 & 0 \\
0 & (\Im(pq)|\Im(rs)) & 0 & 0 \\
0 & 0 & (\Re(p\bar{q})|\Re(r\bar{s})) & 0 \\
0 & 0 & 0 & (\Im(p\bar{q})|\Im(r\bar{s}))
\end{bmatrix}, \tag{B.23}$$

for complex point groups ($C_2$, $D_2$, and $C_{2h}$) we only need the $2 \times 2$ diagonal blocks:

$$\begin{bmatrix}
(\Re(pq)|\Re(rs)) & (\Re(pq)|\Im(rs)) & 0 & 0 \\
(\Im(pq)|\Re(rs)) & (\Im(pq)|\Im(rs)) & 0 & 0 \\
0 & 0 & (\Re(p\bar{q})|\Re(r\bar{s})) & (\Re(p\bar{q})|\Im(r\bar{s})) \\
0 & 0 & (\Im(p\bar{q})|\Re(r\bar{s})) & (\Im(p\bar{q})|\Im(r\bar{s}))
\end{bmatrix}, \tag{B.24}$$

whereas we for quaternion groups ($C_i$ and $C_1$) need the full $4 \times 4$ matrix (Eq. (B.22)).

All 6 integrals in Eq. (B.19) can be written from the double quaternion integrals in Eq. (B.22):

$$\begin{aligned}
(pq|rs) &= [(\Re(pq)|\Re(rs)) - (\Im(pq)|\Im(rs))] \\
&\quad + i\,[(\Re(pq)|\Im(rs)) + (\Im(pq)|\Re(rs))] \\
(p\bar{q}|r\bar{s}) &= [(\Re(p\bar{q})|\Re(r\bar{s})) - (\Im(p\bar{q})|\Im(r\bar{s}))] \\
&\quad + i\,[(\Re(p\bar{q})|\Im(r\bar{s})) + (\Im(p\bar{q})|\Re(r\bar{s}))] \\
(\bar{p}q|r\bar{s}) &= [-(\Re(p\bar{q})|\Re(r\bar{s})) - (\Im(p\bar{q})|\Im(r\bar{s}))] \\
&\quad + i\,[+(\Re(p\bar{q})|\Im(r\bar{s})) - (\Im(p\bar{q})|\Re(r\bar{s}))] \\
(pq|r\bar{s}) &= [(\Re(pq)|\Re(r\bar{s})) - (\Im(pq)|\Im(r\bar{s}))] \\
&\quad + i\,[(\Re(pq)|\Im(r\bar{s})) + (\Im(pq)|\Re(r\bar{s}))] \\
(p\bar{q}|rs) &= [(\Re(p\bar{q})|\Re(rs)) - (\Im(p\bar{q})|\Im(rs))] \\
&\quad + i\,[+(\Re(p\bar{q})|\Im(rs)) + (\Im(p\bar{q})|\Re(rs))] \\
(\bar{p}q|rs) &= [-(\Re(p\bar{q})|\Re(rs)) - (\Im(p\bar{q})|\Im(rs))] \\
&\quad + i\,[-(\Re(p\bar{q})|\Im(rs)) + (\Im(p\bar{q})|\Re(rs))]
\end{aligned} \tag{B.25}$$

For example, $(pq|rs)$ can be written as

$$\begin{aligned}
(pq|rs) &= (\Re(pq) + i\Im(pq) \mid \Re(rs) + i\Im(rs)) \\
&= [(\Re(pq)|\Re(rs)) - (\Im(pq)|\Im(rs))] \\
&\quad + i\,[(\Re(pq)|\Im(rs)) + (\Im(pq)|\Re(rs))]
\end{aligned} \tag{B.26}$$

and $(\bar{p}q|rs)$ as

$$\begin{aligned}
(\bar{p}q|rs) &= -(\bar{q}p|rs) = -(p\bar{q}|sr)^* \\
&= -(\Re(p\bar{q}) + i\Im(p\bar{q}) \mid \Re(sr) + i\Im(sr))^* \\
&= [-(\Re(p\bar{q})|\Re(sr)) + (\Im(p\bar{q})|\Im(sr))] \\
&\quad - i\,[-(\Re(p\bar{q})|\Im(sr)) - (\Im(p\bar{q})|\Re(sr))] \\
&= [-(\Re(p\bar{q})|\Re(rs)) - (\Im(p\bar{q})|\Im(rs))] \\
&\quad + i\,[-(\Re(p\bar{q})|\Im(rs)) + (\Im(p\bar{q})|\Re(rs))]\,,
\end{aligned} \tag{B.27}$$

where we in the last equation have used the following relations for the charge distributions $rs$ and $sr$:

$$\begin{aligned}
\Re(rs) &= \Re(sr), \\
\Im(rs) &= -\Im(sr).
\end{aligned} \tag{B.28}$$

From this we see that $(pq|rs)$ and $(\bar{p}q|rs)$ can be generated from the double quaternion integrals (Eq. (B.22)). The remaining four integrals can be treated analogous.

## B.4 The two-electron density matrix $P$

For the wave function optimization we only need the $P^{++}$ density matrix:

$$P^{++}_{pq,rs} = \left\langle L \middle| \hat{x}^{++}_{pq,rs} \middle| R \right\rangle . \tag{B.29}$$

We use the two-electron density matrix $P$ in the `(NZ,3)` format derived for two-electron integrals above (Eq. (B.19)). This is essentially the same as storing it in spinor basis. We do not store it in the double-quaternion format, Eq. (B.21). One of the big advantages of the double-quaternion format is the permutation relations, for example:

$$\begin{aligned} \Re(pq) &= \Re(qp), \\ \Re(p\bar{q}) &= -\Re(q\bar{p}), \end{aligned} \tag{B.30}$$

allowing us to use a triangular index $(rs)$ in $(pq|rs)$, because integrals $(\Re(pq)|\Re(rs)) = (\Re(pq)|\Re(sr))$. However, in general,

$$P_{\Re(pq),\Re(rs)} \neq P_{\Re(pq),\Re(sr)}, \tag{B.31}$$

since $P_{pq,rs} \neq P_{pq,sr}$. So in order to use the double-quaternion format for density matrices we would have to use full indices for both electron 1 and electron 2. The storage requirements would be $4n_z n^4_{act}$ for the double-quaternion format whereas it is $\frac{3}{2}n_z n^4_{act} + O(n^3_{act})$ for the `(NZ,3)` format. On the other hand one may expect simplifications in the formulae for the auxiliary Fock matrix (the topic of the following section) using the double-quaterion format for integrals and density matrix, but, in fact, we have found none.

## B.5 The auxiliary Fock matrix ${}^{Q}\mathbf{F}^{Q}$

$\mathbf{F}^{Q}$ is defined in Eq. (4.52) (for simplicity we leave out the ++'s on the density matrices):

$$\begin{aligned}
F^{Q}_{pq} &= \sum_{vxy} (pv|xy)\, P_{qv,xy} + (p\bar{v}|xy)\, P_{q\bar{v},xy} \\
&\quad + \frac{1}{2}(p\bar{v}|\bar{x}y)\, P_{q\bar{v},\bar{x}y} + \frac{1}{2}(p\bar{v}|x\bar{y})\, P_{q\bar{v},x\bar{y}} \\
&\quad + \frac{1}{2}(pv|\bar{x}y)\, P_{qv,\bar{x}y} + \frac{1}{2}(pv|x\bar{y})\, P_{qv,x\bar{y}} \\
F^{Q}_{p\bar{q}} &= \sum_{vxy} (pv|xy)\, P_{\bar{q}v,xy} + (p\bar{v}|xy)\, P_{\bar{q}\bar{v},xy} \\
&\quad + \frac{1}{2}(p\bar{v}|\bar{x}y)\, P_{\bar{q}\bar{v},\bar{x}y} + \frac{1}{2}(p\bar{v}|x\bar{y})\, P_{\bar{q}\bar{v},x\bar{y}} \\
&\quad + \frac{1}{2}(pv|\bar{x}y)\, P_{\bar{q}v,\bar{x}y} + \frac{1}{2}(pv|x\bar{y})\, P_{\bar{q}v,x\bar{y}}.
\end{aligned} \tag{B.32}$$

The quaternion auxiliary Fock matrix, ${}^{Q}\mathbf{F}^{Q}$, is defined as

$${}^{Q}F^{Q}_{pq} = F^{Q}_{pq} + F^{Q}_{p\bar{q}}\check{j}, \tag{B.33}$$

*i.e.*

$$\begin{aligned}
{}^{Q}F^{Q}_{pq;0} &= \Re(F^{Q}_{pq}), \\
{}^{Q}F^{Q}_{pq;1} &= \Im(F^{Q}_{pq}), \\
{}^{Q}F^{Q}_{pq;2} &= \Re(F^{Q}_{p\bar{q}}), \\
{}^{Q}F^{Q}_{pq;3} &= \Im(F^{Q}_{p\bar{q}}).
\end{aligned} \tag{B.34}$$

Expanding the right hand sides of Eq. (B.34) inserting the integrals and

density matrices in the `(NZ,3)` format we get:

$$
\begin{aligned}
{}^{Q}F^{Q}_{pq;0} = \sum_{vxy} & \\
& (pv|xy)_{1,1}\, P_{qv,xy;1,1} - (pv|xy)_{2,1}\, P_{qv,xy;2,1} \\
& + \frac{1}{2}\,(pv|xy)_{3,1}\, P_{qv,xy;3,1} - \frac{1}{2}\,(pv|xy)_{4,1}\, P_{qv,xy;4,1} \\
& + \frac{1}{2}\,(pv|xy)_{1,2}\, P_{qv,xy;1,2} - \frac{1}{2}\,(pv|xy)_{2,2}\, P_{qv,xy;2,2} \\
& + (pv|xy)_{3,2}\, P_{qv,xy;3,2} - (pv|xy)_{4,2}\, P_{qv,xy;4,2} \\
& + \frac{1}{2}\,(pv|xy)_{1,3}\, P_{qv,xy;1,3} - \frac{1}{2}\,(pv|xy)_{2,3}\, P_{qv,xy;2,3} \\
& + \frac{1}{2}\,(vp|xy)_{3,1}\, P_{vq,xy;3,1} - \frac{1}{2}\,(vp|xy)_{4,1}\, P_{vq,xy;4,1},
\end{aligned}
\tag{B.35}
$$

$$
\begin{aligned}
{}^{Q}F^{Q}_{pq;1} = \sum_{vxy} & \\
& (pv|xy)_{1,1}\, P_{qv,xy;2,1} + (pv|xy)_{2,1}\, P_{qv,xy;1,1} \\
& + \frac{1}{2}\,(pv|xy)_{3,1}\, P_{qv,xy;4,1} + \frac{1}{2}\,(pv|xy)_{4,1}\, P_{qv,xy;3,1} \\
& + \frac{1}{2}\,(pv|xy)_{1,2}\, P_{qv,xy;2,2} + \frac{1}{2}\,(pv|xy)_{2,2}\, P_{qv,xy;1,2} \\
& + (pv|xy)_{3,2}\, P_{qv,xy;4,2} + (pv|xy)_{4,2}\, P_{qv,xy;3,2} \\
& - \frac{1}{2}\,(pv|xy)_{1,3}\, P_{qv,xy;2,3} - \frac{1}{2}\,(pv|xy)_{2,3}\, P_{qv,xy;1,3} \\
& - \frac{1}{2}\,(vp|xy)_{3,1}\, P_{vq,xy;4,1} - \frac{1}{2}\,(vp|xy)_{4,1}\, P_{vq,xy;3,1},
\end{aligned}
\tag{B.36}
$$

$$
\begin{aligned}
{}^{Q}F^{Q}_{pq;2} = \sum_{vxy} & \\
& (pv|xy)_{1,1}\, P_{qv,xy;3,3} - (pv|xy)_{2,1}\, P_{qv,xy;4,3} \\
& + (pv|xy)_{3,2}\, P_{vq,xy;1,1} - (pv|xy)_{4,2}\, P_{vq,xy;2,1} \\
& - \frac{1}{2}\,(pv|xy)_{1,3}\, P_{qv,xy;3,1} + \frac{1}{2}\,(pv|xy)_{2,3}\, P_{qv,xy;4,1} \\
& + \frac{1}{2}\,(pv|xy)_{1,2}\, P_{vq,xy;3,1} - (pv|xy)_{2,2}\, P_{vq,xy;4,1} \\
& - \frac{1}{2}\,(vp|xy)_{3,1}\, P_{qv,xy;1,2} + \frac{1}{2}\,(vp|xy)_{4,1}\, P_{qv,xy;2,2} \\
& + \frac{1}{2}\,(pv|xy)_{3,1}\, P_{qv,xy;1,3} - \frac{1}{2}\,(pv|xy)_{4,1}\, P_{qv,xy;2,3},
\end{aligned}
\tag{B.37}
$$

and

$$
\begin{aligned}
{}^{Q}F^{Q}_{pq;3} = \sum_{vxy} & \\
& (pv|xy)_{1,1}\, P_{qv,xy;4,3} + (pv|xy)_{2,1}\, P_{qv,xy;3,3} \\
& + (pv|xy)_{3,2}\, P_{vq,xy;2,1} + (pv|xy)_{4,2}\, P_{vq,xy;1,1} \\
& + \frac{1}{2}\,(pv|xy)_{1,3}\, P_{qv,xy;4,1} + \frac{1}{2}\,(pv|xy)_{2,3}\, P_{qv,xy;3,1} \\
& + \frac{1}{2}\,(pv|xy)_{1,2}\, P_{vq,xy;4,1} + (pv|xy)_{2,2}\, P_{vq,xy;3,1} \\
& + \frac{1}{2}\,(vp|xy)_{3,1}\, P_{qv,xy;2,2} + \frac{1}{2}\,(vp|xy)_{4,1}\, P_{qv,xy;1,2} \\
& + \frac{1}{2}\,(pv|xy)_{3,1}\, P_{qv,xy;2,3} + \frac{1}{2}\,(pv|xy)_{4,1}\, P_{qv,xy;1,3}.
\end{aligned}
\tag{B.38}
$$

The sum $\sum_{vxy}$ is a full summation over all active orbitals. However, it is possible to restrict the full $xy$ summation to a triangular $x \geq y$ summation. This will give a lower operation count. To use a triangular sum we need the following relations, relating $(pv|xy)_{i,j}$ to $(pv|yx)_{i,j}$ and $P_{qv,xy;i,j}$ to $P_{qv,yx;i,j}$:

$$
\begin{aligned}
(pv|yx)_{1,1} &= (vp|xy)_{1,1}\,, \\
(pv|yx)_{2,1} &= -\,(vp|xy)_{2,1}\,, \\
(pv|yx)_{3,1} &= -\,(pv|xy)_{3,1}\,, \\
(pv|yx)_{4,1} &= -\,(pv|xy)_{4,1}\,, \\
(pv|yx)_{1,2} &= -\,(pv|xy)_{1,2}\,, \\
(pv|yx)_{2,2} &= -\,(pv|xy)_{2,2}\,, \\
(pv|yx)_{3,2} &= (vp|xy)_{3,3}\,, \\
(pv|yx)_{4,2} &= -\,(vp|xy)_{4,3}\,, \\
(pv|yx)_{1,3} &= -\,(pv|xy)_{1,3}\,, \\
(pv|yx)_{2,3} &= -\,(pv|xy)_{2,3}\,, \\
(pv|yx)_{3,3} &= (vp|xy)_{3,2}\,, \\
(pv|yx)_{4,3} &= -\,(vp|xy)_{4,2}\,,
\end{aligned}
\tag{B.39}
$$

and identical formulae for the density matrix elements.

We can now write the final formulae used in the actual implementation

$$
\begin{aligned}
{}^{Q}F^{Q}_{pq;0} = & \\
& + \sum_{x \geq y} \sum_{v} (pv|xy)_{1,1} P_{qv,xy;1,1} + \sum_{x>y} \sum_{v} (vp|xy)_{1,1} P_{vq,xy;1,1} \\
& - \sum_{x \geq y} \sum_{v} (pv|xy)_{2,1} P_{qv,xy;2,1} - \sum_{x>y} \sum_{v} (vp|xy)_{2,1} P_{vq,xy;2,1} \\
& + \sum_{x>y} \sum_{v} (pv|xy)_{3,1} P_{qv,xy;3,1} \\
& - \sum_{x>y} \sum_{v} (pv|xy)_{4,1} P_{qv,xy;4,1} \\
& + \sum_{x>y} \sum_{v} (pv|xy)_{1,2} P_{qv,xy;1,2} \\
& - \sum_{x>y} \sum_{v} (pv|xy)_{2,2} P_{qv,xy;2,2} \\
& + \sum_{x \geq y} \sum_{v} (pv|xy)_{3,2} P_{qv,xy;3,2} + \sum_{x>y} \sum_{v} (vp|xy)_{3,3} P_{vq,xy;3,3} \\
& - \sum_{x \geq y} \sum_{v} (pv|xy)_{4,2} P_{qv,xy;4,2} - \sum_{x>y} \sum_{v} (vp|xy)_{4,3} P_{vq,xy;4,3} \\
& + \sum_{x>y} \sum_{v} (pv|xy)_{1,3} P_{qv,xy;1,3} \\
& - \sum_{x>y} \sum_{v} (pv|xy)_{2,3} P_{qv,xy;2,3} \\
& + \sum_{x>y} \sum_{v} (vp|xy)_{3,1} P_{vq,xy;3,1} \\
& - \sum_{x>y} \sum_{v} (vp|xy)_{4,1} P_{vq,xy;4,1},
\end{aligned}
\tag{B.40}
$$

$$
\begin{aligned}
{}^{Q}F^{Q}_{pq;1} = & \\
& + \sum_{x \geq y} \sum_{v} (pv|xy)_{1,1} P_{qv,xy;2,1} - \sum_{x > y} \sum_{v} (vp|xy)_{1,1} P_{vq,xy;2,1} \\
& + \sum_{x \geq y} \sum_{v} (pv|xy)_{2,1} P_{qv,xy;1,1} - \sum_{x > y} \sum_{v} (vp|xy)_{2,1} P_{vq,xy;1,1} \\
& + \sum_{x > y} \sum_{v} (pv|xy)_{3,1} P_{qv,xy;4,1} \\
& + \sum_{x > y} \sum_{v} (pv|xy)_{4,1} P_{qv,xy;3,1} \\
& + \sum_{x > y} \sum_{v} (pv|xy)_{1,2} P_{qv,xy;2,2} \\
& + \sum_{x > y} \sum_{v} (pv|xy)_{2,2} P_{qv,xy;1,2} \\
& + \sum_{x \geq y} \sum_{v} (pv|xy)_{3,2} P_{qv,xy;4,2} - \sum_{x > y} \sum_{v} (vp|xy)_{3,3} P_{vq,xy;4,3} \\
& + \sum_{x \geq y} \sum_{v} (pv|xy)_{4,2} P_{qv,xy;3,2} - \sum_{x > y} \sum_{v} (vp|xy)_{4,3} P_{vq,xy;3,3} \\
& - \sum_{x > y} \sum_{v} (pv|xy)_{1,3} P_{qv,xy;2,3} \\
& - \sum_{x > y} \sum_{v} (pv|xy)_{2,3} P_{qv,xy;1,3} \\
& + \sum_{x > y} \sum_{v} (vp|xy)_{3,1} P_{vq,xy;4,1} \\
& + \sum_{x > y} \sum_{v} (vp|xy)_{4,1} P_{vq,xy;3,1},
\end{aligned}
\tag{B.41}
$$

$$
\begin{aligned}
{}^{Q}F^{Q}_{pq;2} = & \\
& + \sum_{x \geq y} \sum_{v} (pv|xy)_{1,1} \, P_{qv,xy;3,3} + \sum_{x > y} \sum_{v} (vp|xy)_{1,1} \, P_{vq,xy;3,2} \\
& - \sum_{x \geq y} \sum_{v} (pv|xy)_{2,1} \, P_{qv,xy;4,3} - \sum_{x > y} \sum_{v} (vp|xy)_{2,1} \, P_{vq,xy;4,2} \\
& + \sum_{x \geq y} \sum_{v} (pv|xy)_{3,2} \, P_{vq,xy;1,1} + \sum_{x > y} \sum_{v} (vp|xy)_{3,3} \, P_{qv,xy;1,1} \\
& - \sum_{x \geq y} \sum_{v} (pv|xy)_{4,2} \, P_{vq,xy;2,1} - \sum_{x > y} \sum_{v} (vp|xy)_{4,3} \, P_{qv,xy;2,1} \\
& - \sum_{x > y} \sum_{v} (pv|xy)_{1,3} \, P_{qv,xy;3,1} \\
& + \sum_{x > y} \sum_{v} (pv|xy)_{2,3} \, P_{qv,xy;4,1} \\
& + \sum_{x > y} \sum_{v} (pv|xy)_{1,2} \, P_{vq,xy;3,1} \\
& - \sum_{x > y} \sum_{v} (pv|xy)_{2,2} \, P_{vq,xy;4,1} \\
& - \sum_{x > y} \sum_{v} (vp|xy)_{3,1} \, P_{qv,xy;1,2} \\
& + \sum_{x > y} \sum_{v} (vp|xy)_{4,1} \, P_{qv,xy;2,2} \\
& + \sum_{x > y} \sum_{v} (pv|xy)_{3,1} \, P_{qv,xy;1,3} \\
& - \sum_{x > y} \sum_{v} (pv|xy)_{4,1} \, P_{qv,xy;2,3},
\end{aligned}
\tag{B.42}
$$

and

$$
\begin{aligned}
{}^{Q}F^{Q}_{pq;3} = & \\
& + \sum_{x\geq y}\sum_{v} (pv|xy)_{1,1}\, P_{qv,xy;4,3} - \sum_{x>y}\sum_{v} (vp|xy)_{1,1}\, P_{vq,xy;4,2} \\
& + \sum_{x\geq y}\sum_{v} (pv|xy)_{2,1}\, P_{qv,xy;3,3} - \sum_{x>y}\sum_{v} (vp|xy)_{2,1}\, P_{vq,xy;3,2} \\
& + \sum_{x\geq y}\sum_{v} (pv|xy)_{3,2}\, P_{vq,xy;2,1} - \sum_{x>y}\sum_{v} (vp|xy)_{3,3}\, P_{qv,xy;2,1} \\
& + \sum_{x\geq y}\sum_{v} (pv|xy)_{4,2}\, P_{vq,xy;1,1} - \sum_{x>y}\sum_{v} (vp|xy)_{4,3}\, P_{qv,xy;1,1} \\
& + \sum_{x>y}\sum_{v} (pv|xy)_{1,3}\, P_{qv,xy;4,1} \\
& + \sum_{x>y}\sum_{v} (pv|xy)_{2,3}\, P_{qv,xy;3,1} \\
& + \sum_{x>y}\sum_{v} (pv|xy)_{1,2}\, P_{vq,xy;4,1} \\
& + \sum_{x>y}\sum_{v} (pv|xy)_{2,2}\, P_{vq,xy;3,1} \\
& + \sum_{x>y}\sum_{v} (vp|xy)_{3,1}\, P_{qv,xy;2,2} \\
& + \sum_{x>y}\sum_{v} (vp|xy)_{4,1}\, P_{qv,xy;1,2} \\
& + \sum_{x>y}\sum_{v} (pv|xy)_{3,1}\, P_{qv,xy;2,3} \\
& + \sum_{x>y}\sum_{v} (pv|xy)_{4,1}\, P_{qv,xy;1,3},
\end{aligned}
\tag{B.43}
$$

Note that all the $\sum_v$ terms are, in fact, matrix multiplications, for example:

$$
\sum_{v} (pv|xy)_{1,1}\, P_{qv,xy;1,1} = \left( (\cdot\cdot|xy)_{1,1}\, (P_{\cdot\cdot,xy;1,1})^{T} \right)_{pq}. \tag{B.44}
$$

The algorithm for the construction of ${}^{Q}\mathbf{F}^{Q}$ can now be written as:

1. Loop over integral distributions $(\cdot\cdot|xy)$ with $x \geq y$ in the integral file
   (a) If $(xy)$ is an active-active distribution then
      i. Read integrals in double-quaternion format.

ii. Transform integrals to `(NZ,3)` format.

iii. Add terms to quaternion ${}^{Q}\mathbf{F}^{Q}$ matrix (Eqs. (B.41)-(B.43))

## B.6 The auxiliary Fock matrix with transition density matrix

The formulae for the auxiliary Fock, ${}^{Q}\check{\mathbf{F}}^{Q}$, constructed using the symmetrized two-electron transition density matrix $\check{\mathbf{P}}$ is completely analogous to the formulae for the normal ${}^{Q}\mathbf{F}^{Q}$ (Eqs. (B.41) – (B.43)), except that the transition density matrix $\check{\mathbf{P}}$ is used instead.

## B.7 The auxiliary Fock matrix with one-index transformed integrals

The formulae for the ${}^{Q}F^{Q}$ with one-index transformed integrals ${}^{Q}\tilde{\mathbf{F}}^{Q}$ is analogous to the normal ${}^{Q}F^{Q}$ (Eqs. (B.41)) (B.43)) in the previous section, except that the normal two-electron integrals are replaced with one-index transformed two-electron integrals, *i.e.* we have terms like:

$$\sum_{vxy} \widetilde{(pv|xy)}_{1,1} P_{qv,xy;1,1}, \tag{B.45}$$

which can be rewritten to

$$\sum_{vxy} (\widetilde{pv}|xy)_{1,1}\, P_{qv,xy;1,1}, + \sum_{vxy} (pv|\widetilde{xy})_{1,1}\, P_{qv,xy;1,1}. \tag{B.46}$$

The first term is just like a normal ${}^{Q}\mathbf{F}^{Q}$ matrix (*i.e.*, a number of "matrix multiply"-like terms), *i.e.* can use Eqs. (B.40) – (B.43) by simply replacing the integrals $(pv|xy)$ with $pv$ one-index transformed integrals $(\widetilde{pv}|xy)$. The second term:

$$\sum_{vxy} (pv|\widetilde{xy})_{1,1}\, P_{qv,xy;1,1} = \sum_{v} \sum_{xy} (\widetilde{xy}|pv)_{1,1}\, P_{xy,qv;1,1}, \tag{B.47}$$

is a "dot product"-like term:

$$\sum_{v} \sum_{xy} (\widetilde{xy}|pv)_{1,1}\, P_{xy,qv;1,1}, = \sum_{v} \left( (\widetilde{\cdot\cdot}|pv)_{1,1}\, ; P_{\cdot\cdot,qv;1,1}, \right), \tag{B.48}$$

where $(a;b)$ is the dot product between two vectors.

It is easiest to calculate the one-index transform of the two-electron integrals from the double quaternion format. We want to calculate

$$^{Q_1Q_2}(\widetilde{pq}|rs) = \left(^{Q_1}(\widetilde{pq})\middle|^{Q_2}(rs)\right) \tag{B.49}$$

which is just a usual quaternion one-index transform (like the first terms of Eq. (B.14) and Eq. (B.15)):

$$\left(^{Q_1}(\widetilde{pq})\middle|^{Q_2}(rs)\right) = \sum_r {}^{Q_1}b_{pr}\left(^{Q_1}(rq)\middle|^{Q_2}(rs)\right) - \left(^{Q_1}(pr)\middle|^{Q_2}(rs)\right){}^{Q_1}b_{rq}. \tag{B.50}$$

The algorithm for the construction of $^{Q}\tilde{\mathbf{F}}^{Q}$ and $^{Q}\check{\mathbf{F}}^{Q}$ can now be written as:

1. Loop over integral distributions $(\cdot\cdot|xy)$ with $x \geq y$ in the integral file
   (a) If $(xy)$ is an active-active distribution then
      i. Read integrals $(pq|xy)$ in double-quaternion format.
      ii. Transform integrals to `(NZ,3)` format.
      iii. Add "matrix multiply"-like terms to the quaternion $^{Q}\hat{\mathbf{F}}^{Q}$ matrix (Eqs. (B.41)-(B.43)).
      iv. Loop over 1, $\check{\imath}_2$, $\check{\jmath}_2$, $\check{k}_2$
         A. One-index transform electron 1 yielding integrals $(\widetilde{pq}|xy)$
      v. Transform one-index transformed integrals to `(NZ,3)` format.
      vi. Add "matrix multiply"-like terms to quaternion $^{Q}\tilde{\mathbf{F}}^{Q}$ matrix (Eqs. (B.41)-(B.43))
   (b) If $(xy) = (pv)$ is an general-active distribution then (the active-active distributions are only needed for GAS/RAS wave functions)
      i. Read integrals $(rs|pv)$ in double quaternion format.
      ii. Loop over 1, $\check{\imath}_2$, $\check{\jmath}_2$, $\check{k}_2$
         A. One-index transform electron 1 yielding integrals $(\widetilde{rs}|pv)$
      iii. Transform one-index transformed integrals to `(NZ,3)` format.
      iv. Add "dot product"-like terms to quaternion $^{Q}\tilde{\mathbf{F}}^{Q}$ matrix (Eq. (B.48))
   (c) else if $(xy) = (vp)$ in an active-general distribution then
      i. ... the same as for $(xy)$ general-active.

# Bibliography

[1] T. Saue and H. J. Aa.. Jensen, J. Chem. Phys. **111**, 6211 (1999).